ÇUKUROVA UNIVERSITY
INSTITUTE OF NATURAL AND APPLIED SCIENCES

MSc THESIS

Eylem ZEYDAN

ANALYTICAL INVESTIGATION OF PARAMETERS AFFECTING STIFFNESS OF HELICAL SPRINGS OF ARBITRARY SHAPES UNDER COMPRESSION

DEPARTMENT OF MECHANICAL ENGINEERING

ADANA, June 2006

ÇUKUROVA ÜNİVERSİTESİ
FEN BİLİMLERİ ENSTİTÜSÜ

ANALYTICAL INVESTIGATION OF PARAMETERS
AFFECTING STIFFNESS OF HELICAL SPRINGS
OF ARBITRARY SHAPES UNDER COMPRESSION

Eylem ZEYDAN

YÜKSEK LİSANS TEZİ

MAKİNA MÜHENDİSLİĞİ ANABİLİM DALI

Bu Tez 19/06/2006 Tarihinde Aşağıdaki Jüri Üyeleri Tarafından Oybirliği/Oyçokluğu İle Kabul Edilmiştir.

İmza:	İmza:	İmza:
Prof. Dr. Vebil YILDIRIM	Prof. Dr. Naki TÜTÜNCÜ	Yrd. Doç. Dr. H. Murat ARSLAN
DANIŞMAN	ÜYE	ÜYE

Bu Tez Enstitümüz Makina Mühendisliği Anabilim Dalında Hazırlanmıştır.
Kod No:

Prof. Dr. Aziz ERTUNÇ
Enstitü Müdürü

ABSTRACT

MSc THESIS

ANALYTICAL INVESTIGATION OF PARAMETERS AFFECTING STIFFNESS OF HELICAL SPRINGS OF ARBITRARY SHAPES UNDER COMPRESSION

Eylem ZEYDAN

DEPARTMENT OF MECHANICAL ENGINEERING
INSTITUTE OF NATURAL AND APPLIED SCIENCES
UNIVERSITY OF ÇUKUROVA

Supervisor : Prof. Dr. Vebil YILDIRIM
Year: 2006, Pages: 112
Jury : Prof. Dr. Vebil YILDIRIM
: Prof. Dr. Naki TÜTÜNCÜ
: Assist. Prof. Dr. H. Murat ARSLAN

The present study deals with the determination of the vertical tip deflection of the most commonly used cylindrical and noncylindrical (barrel, conical, hyperboloidal types) helical compression springs subjected to an axial concentrated force acting along the helix axis and springs having doubly symmetric cross-sections such as solid circle, square, rectangle, ellipse, and hollow circle etc. By using Castigliano's first theorem, closed-form solutions for the vertical tip deflection of helical springs with arbitrary shaped and large pitch angles are obtained by considering the whole effect of the stress resultants such as axial and shearing forces, bending and torsional moments. The analytical formulas presented in the present study may be used for springs made of both isotropic and composite (transversely isotropic) materials. Thus, the designers will be free to design more appropriate and more accurate springs by using those generalized formulas presented in this study.

Key Words: Helical springs, Castigliano's theorem, Spring constant

ÖZ

YÜKSEK LİSANS TEZİ

BASMAYA MARUZ GELİŞİGÜZEL ŞEKİLLİ HELİSEL YAYLARIN RİJİDLİĞİNİ ETKİLEYEN PARAMETRELERİN ANALİTİK OLARAK İNCELENMESİ

Eylem ZEYDAN

ÇUKUROVA ÜNİVERSİTESİ
FEN BİLİMLERİ ENSTİTÜSÜ
MAKİNA MÜHENDİSLİĞİ ANABİLİM DALI

Supervisor : Prof. Dr. Vebil YILDIRIM
Yıl: 2006, Sayfa : 112
Jury : Prof. Dr. Vebil YILDIRIM
: Prof. Dr. Naki TÜTÜNCÜ
: Yrd. Doç. Dr. H. Murat ARSLAN

Bu çalışma uygulamada sıkça kullanılan, helis ekseni boyunca etkiyen tekil kuvvete maruz silindirik ve silindirik olmayan (fıçı, konik, hiperboloidal tip), dolu daire, kare, dikdörtgen, elips ve halka kesit gibi çift simetri eksenine sahip helisel bası yaylarında meydana gelen düşey doğrultudaki uç yer değiştirmenin belirlenmesi konusu ile ilgilidir. Castiliano'nun birinci teoremi yardımıyla, eksenel ve kayma kuvvetleri, eğilme ve burulma momentleri gibi tüm gerilme bileşkelerinin etkisi dikkate alınarak, büyük helis yükselme açısına sahip helisel yayların düşey yer değiştirmesi için kapalı formdaki çözümler elde edilmiştir. Bu çalışmada sunulan formüller izotropik ve kompozit (enine izotropik) malzemeden yapılmış yaylar için kullanılabilmektedir. Bu çalışmada geliştirilen formüller yardımı ile tasarımcılar uygun ve hassas yay tasarımında daha özgür olacaklardır.

Anahtar Kelimeler: Helisel yaylar, Castigliano teoremi, Yay sabiti.

ACKNOWLEDGEMENTS

I am grateful to my supervisor Prof. Dr. Vebil YILDIRIM for helping me patiently throughout the preparation of this thesis.

I would like to thank to Prof. Dr. Naki TÜTÜNCÜ for introducing me to the subject of the Strength of the Materials.

I want to thank my friend research assistants Ertaç HÜRDOĞAN, Arif ÖZBEK, Uğur EŞME, Hasan SERİN, and Ahmet FERTELLİ. I also want to thank all staff of the Mechanical Engineering Laboratory.

I would also like to special thanks to my family for their encouragements and endless support.

CONTENT PAGE

LIST of TABLES **PAGES**

LIST of FIGURES **PAGES**

NOMENCLATURE

A	Undeformed area of the cross-section
C	Spring index
C_t	Axial rigidity
C_n, C_b	Shearing rigidities
C, S	Stiffness and compliance tensors, respectively
$d\ (=2r)$	Diameter of the wire
D	The mean coil diameter $(=2R)$
D_t	Torsional rigidity
D_n, D_b	Bending rigidities
ds	Infinitesimal arch length of the helix
E_1, E_2, E_3	Young's moduli in 1, 2, and 3 directions, respectively
G_{ij}	Shear modulus of orthotropic material
f_{T_t}	Tip deflection due to the axial force
$f_{T_{bt}}$	Tip deflection due to the shearing force
f_{M_t}	Tip deflection due to the torsional moment
$f_{M_{bt}}$	Tip deflection due to the bending moment
f_{Tot}	Total tip deflection
h	The step for unit angle
H	Helix pitch
i, j, k	Cartesian unit vectors
I_n, I_b ,	Moments of inertia about n and b axes
I_0	Polar moment of inertia
I	Unit matrix
J_0, J_b	Torsional moment of inertia of the section
k, K	Spring constant
k', k_b, k_n	Shear coefficient factor (=6/5 for rectangle)
L, L_a	Active length of the spring
n	Number of active turns

N, T_t	Axial force
P	External single vertical force acting along cylinder axis
$\vec{P}, \vec{p}$	Concentrated and distributed force acting on a helix element
Q	Reduced stiffness matrix for rods
R	Centerline radius of the helix *(=D/2)*
t, n, b	Frenet unit vectors
T, M	Resultant force and moment vectors, respectively
u, v, w	Displacements along x,y,z axes
u_i	Strain energy density
U_i	Strain energy
U, Ω	Displacement and rotation vectors, respectively
V	Volume
α	Helix pitch angle
Δw	Vertical tip deflection
λ	Lame's constant
$\vec{\gamma}, \vec{\omega}$	Relative unit extension vector and relative unit rotation vector on a point on the wire axis.
δ_{ij}	Kronecker delta
σ_i, e_i	Stress components and engineering strain components, respectively
ρ	Mass density
ν_{ij}	Poisson's ratio for transverse strain in the *j*-direction when stressed in the *I*-direction
τ_b	Shearing stress induced by torsion moment
τ_k	Shearing stress induced by shearing force
θ	Horizontal angular displacement

Subscripts

t, n, b	Frenet components of a vector quantity

Superscripts

T	Transpose of a matrix
-1	Inverse of a matrix

1. INTRODUCTION

When an elastic function is required, designers often use springs which are classified as compression springs, extension springs, torsion springs, specialty springs, assembly springs and wire forms.

It is commonly known that the helical springs are fundamental elements of machines. Helical springs can be found in basic mechanisms where their sizing is not critical and can also be found in high-level mechanisms such as cars, hand prostheses and satellites. In such mechanisms, spring design has to be reliable and well controlled as poor spring behavior would lead to major damage.

Helical springs generally work under dynamic conditions and under take different tasks. They are also referred to as coil springs. Coil springs come in many forms but there are three common classes; Compression springs, extension/tension springs and torsion springs (Figure 1.1).

(a) (b) (c)

Figure 1.1. Types of helical springs a) compression b) tension c) torsion

Regardless of which is used, coil springs must be designed to satisfy four operating requirements: Energy, Space, Environment and Service.

Energy is the first consideration in coil spring design because a spring is by definition a device for storing energy. Energy is a function of load and deflection.

Space is defined by the operating envelope, the area in which the coil springs will operate. In the case of a compression spring, this might be the hole into which the spring fits, the rod over which it operates.

Compression helical springs are springs with an open-coil configuration designed to store energy or to resist a force applied along the axis of the coil. When you put a load on the compression spring, making it shorter, it pushes back against the load and tries to get back to its original length. The most common form of compression spring is a straight cylindrical coil spring with the ends squared (closed). The end coils may also be ground to improve squareness and reduce buckling.

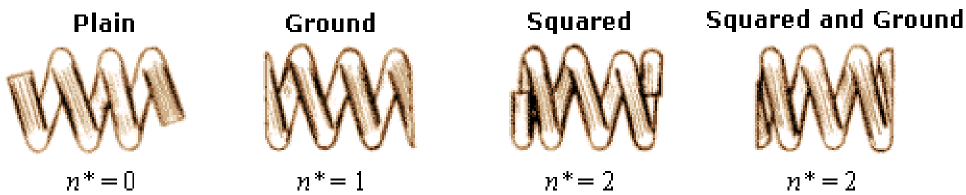

Figure 1.2. The ends of the compression helical springs (http://www.efunda.com/designstandards/springs/spring_design.cfm)

The number of active coils is equal to the total number of coils minus the number of end coils $n*$ that do not help carry the load. The value for $n*$ depends on the ends of the spring (Figure 1.2).

Compression springs are commonly wound with uniform spacing between the coils however variable coil spacing can be used to achieve improved performance against buckling and surging. A compression spring with variable pitch assures a spectrum of frequency response as opposed to the single resonant frequency in a compression spring with constant pitch.

Compression springs are also manufactured in conical, barrel or hourglass (hyperboloidal) configurations (Figure 1.3). These forms of compression springs allow for reduced solid height.

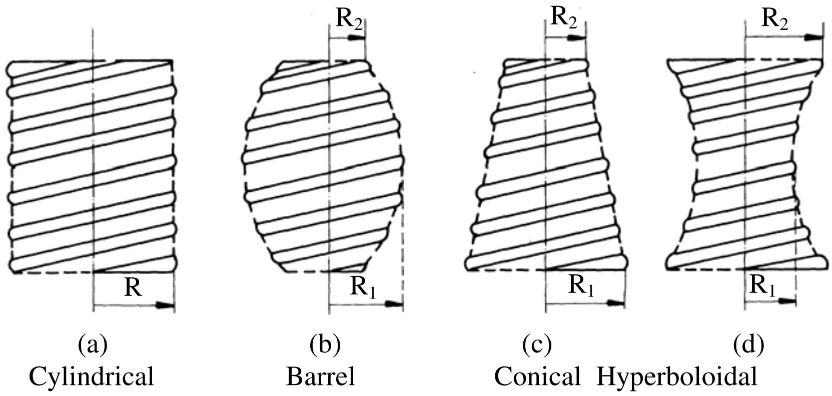

Figure 1.3. Types of helical compression springs

The extension/tension spring is similar to the compression spring however it requires special ends to permit application of the load. A tension spring can be wound with initial pre-load so that it deforms only after the load reaches a certain minimum value. The ends of tension springs assume many forms but they are all potential sources of weakness not present in compression springs. Extension springs are found in garage door assemblies, vise-grip pliers, and carburetors. They are attached at both ends, and when the things they are attached to move apart, the spring tries to bring them together again.

Helical torsion spring is similar to the helical tension spring in requiring specially formed ends to transmit the load. Torsion springs can be found on clipboards, underneath swing-down tailgates, and, again, in car engines. The ends of torsion springs are attached to other things, and when those things rotate around the center of the spring, the spring tries to push them back to their original position.

Rigorous duties usually call for compression rather than tension and torsion helical springs. The basic geometrical parameters of a helical compression spring are shown in Figure (1.4). Close-coiled requires a small helix pitch angle, say $\alpha \leq 5^{o}...12^{o}$. The ratio of mean coil diameter to wire diameter is known as the spring index, *C=D/d.* Low indices result in difficulty with spring manufacture and in stress concentrations induced by curvature. Springs in the range $5 \leq C \leq 10$ are preferred, while indices less than 3 are generally impracticable.

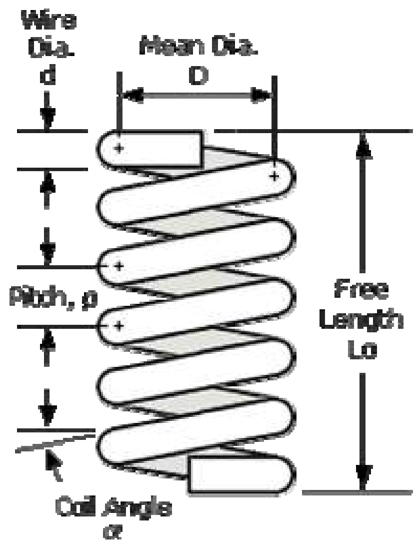

Figure 1.4. Helical spring geometry
(http://www.engineerstoolbox.com/doc/etb/mod/stat1/spring/spring_help.html)

Various wire diameters are obtainable, most frequently used decade is

. . . 0.8 0.9 1.0 1.12 1.25 1.4 1.6 1.8 2 2.24 2.5 2.8 3.15 3.55 4 4.5 5 5.6 6.3 7.1 8 9 10 11.2 12.5 . . . mm

The performance of a spring is characterized by the relationship between the load applied to it and the deflection $(F - \Delta)$.

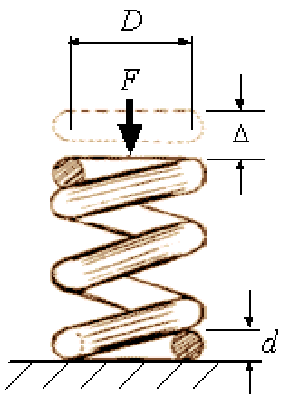

Figure 1.5. Helical spring subjected to an axial load.
(http://www.efunda.com/designstandards/springs/spring_design.cfm)

The F-$\varDelta$ characteristic is approximately linear provided the spring is close-coiled and the material elastic, that is Hooke's law is typically assumed to hold, $F = k\Delta$. The slope of the characteristic, k, is known as “the stiffness of the spring” (spring 'constant', or 'rate', or 'scale' or 'gradient') and is determined by the spring geometry and modulus of rigidity, G.

Active coils (n) are the number of coils which actually deform when the spring is loaded, as opposed to the inactive turns at each end which are in contact with the spring seat or base.

The spring constant k for a compression spring that exerts a force F when deformed to the length L_{def} is

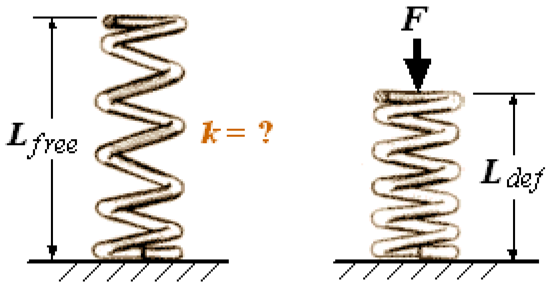

Figure 1.6. Deformed compression helical spring
(http://www.efunda.com/designstandards/springs/calc_comp_k.cfm)

The spring constant k is found by inverting Hooke's Law

$$k = \left| \frac{F}{L_{free} - L_{def}} \right| \tag{1.1}$$

The spring constant can be expanded as a function of the material properties of the spring as follows

$$k = \frac{F}{\Delta} = \frac{Gd^4}{8D^3n} = \frac{Gd}{8C^3n} = \frac{\pi Gd^4}{8D^2L_a} = \frac{Gd^4}{64nR^3} \tag{1.2}$$

where L_a is the active wire length, $L_a = \pi Dn$. The useful range for C is about *4* to *12*, with an optimum value of approximately *9*. The wire diameter, d, should conform to a standard size if at all possible. Considering the formula given above, there are three basic principles in spring design:

- The heavier the wire, the stronger the spring.
- The smaller the coil, the stronger the spring.
- The more active coils, the less load you will have to apply in order to get it to move a certain distance.

Based on these general principles, you know what to do to change the properties of a spring you already have. For instance, if you want to make the spring a little stronger than stock, you can a) go to a slightly heavier wire and keep the dimensions and coil count the same, b) decrease the diameter of the spring, keeping the wire size and coil count the same, or c) decrease the number of active coils, keeping the wire size and spring diameter the same. Naturally, you can also go to a stronger material to achieve the same result. Equation (1.2.) is valid for

- Small pitch angles
- Circular cross-sections
- Just taking into consideration the effect of torsional moment.
- Isotropic material with Poisson's ratio of *0.3*.
- Cylinder surface with constant radius.
- Constant curvatures.

Helical springs of square or rectangular bar section are sometimes used for cases where a large amount of energy must be stored within a given space. The formulas are based on the assumption of a true square or rectangular shape and will generally be sufficiently accurate for practical calculations.

In general, when bar stock of rectangular section is coiled to a helical form, a key-stone or trapezoidal shape of cross section finally results, and this tends to reduce the space efficiency and energy storage capacity.

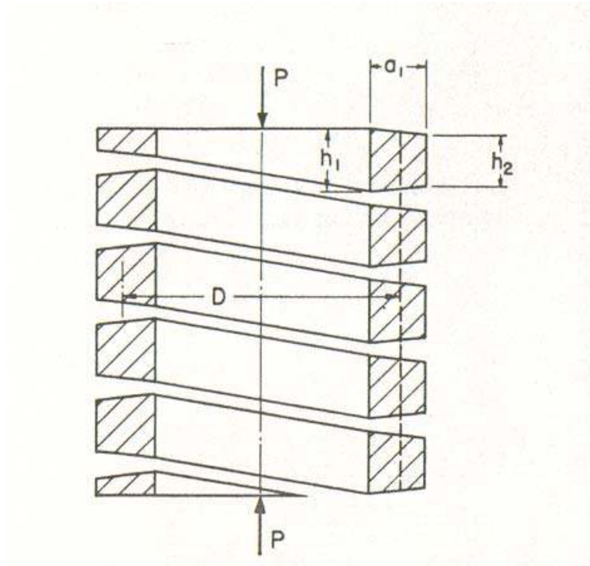

Figure 1.7. Helical spring of square wire axially loaded (The wire becomes somewhat trapezoidal during the cooling operation) (Wahl, 1963)

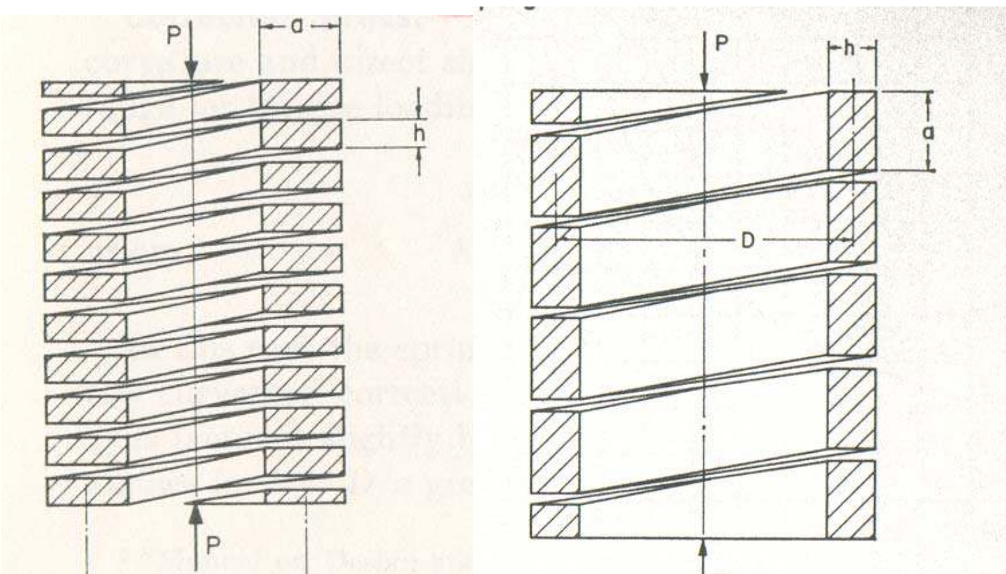

(a) (b)

Figure 1.8. a) Helical spring of rectangular wire, coiled flat-wise,
b) Helical spring with long side of bar parallel to axis (Wahl, 1963)

In contrast to round-wire helical compression or tension springs where curvature effects can be neglected in calculating deflections, such effects are particularly important in rectangular-wire springs coiled flat-wise (Figure 1.8). In such cases neglecting curvature may result in errors of *15* percent or more. Such effects may be taken into account using chart in Figure 1.9. 10-6.

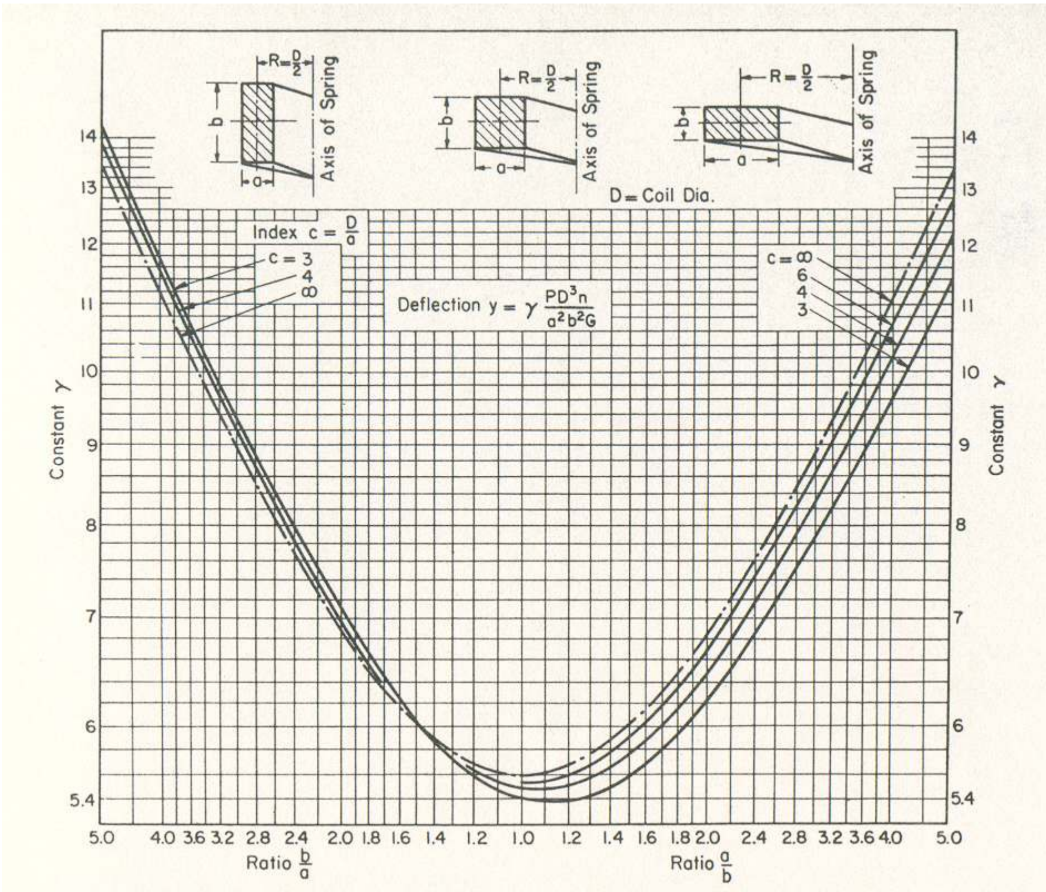

Figure 1.9. Curves for finding deflection factor γ for calculating rectangular-bar springs (Wahl, 1963)

Particularly if the spring is coiled flat-wise (Figure 1.8a), it is clear that a larger amount of material may be provided within a given outside diameter and compressed length than if a circular section were used. Consequently, other things being equal, more energy may be stored within a given space for such a design than would be the case if a circular bar section were used. Although the rectangular bar section theoretically does not have as favorable an elastic stress distribution as does the round bar section, for static loading or loads repeated only a few times this disadvantage is of no particular importance, since local yielding of the highest stressed portions can occur without appreciably affecting the performance of the spring or the capacity for storing energy. However, where fatigue or repeated loading of the spring is present, this non-uniformity of stress distribution will be disadvantage. A further disadvantage is the fact that the quality of material used is generally not as good as would be the case where round wire is used; also, the rectangular-bar material may be difficult to produce.

Springs with rectangular cross sections having the long side of the section parallel to the axis (Figure 1.8b) are sometimes used in the design of precision scales in order to obtain a more nearly linear load-deflection characteristic. The best results are obtained by making the ratio *a/h=3* and *D/h=20* for small deflections. Where large deflections are involved, the analysis shows that a more nearly linear load-deflection diagram is found for $\frac{b}{h} \cong 2$

The amount of upsetting due to cooling of a rectangular or square wire section can be obtained from the following formula (Wahl, 1963)

$$h_1 = h\{1 + \frac{k(D_0 - D_i)}{D_0 + D_i}\} \qquad (1.3)$$

where D_0 is the outside diameter of the spring, D_i is the inside diameter of the spring, h is the original thickness, h_1 is the upset thickness, and $k=0.3$ for cold-wound springs, $k=0.4$ for hot-wound springs and annealed materials.

In helical compression spring design with square section, $\tau^{'}$ represents the corrected stress, which includes effects of curvature and direct shear and which should be used to calculate stress range for fatigue loading and $K^{'}$ is the curvature correction factor.

$$K' = 1 + \frac{1.2}{c} + \frac{0.56}{c^2} + \frac{0.5}{c^3} \tag{1.4a}$$

$$\tau' = K'\tau = (1 + \frac{1.2}{c} + \frac{0.56}{c^2} + \frac{0.5}{c^3})\frac{2.4PD}{a^3} \tag{1.4b}$$

where the spring index is defined by (Wahl,1963)

$$c = \frac{D}{a} \quad (\text{or } c = \frac{D}{a_1}) \tag{1.5}$$

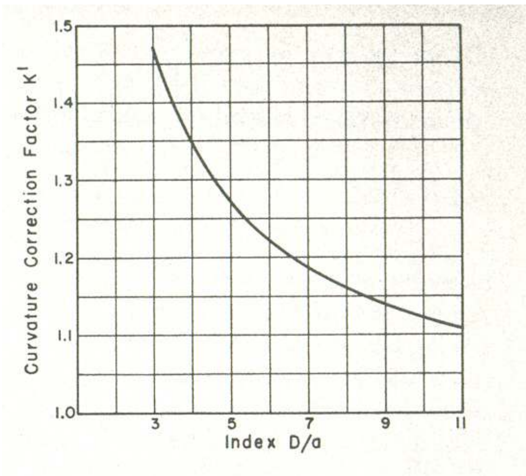

Figure 1.10. Curvature correction factor for square sections (Wahl, 1963)

As seen from Figure (1.10), K' is slightly below the factor *K* for round wire and applies for $c = \frac{D}{a} > 3$.

The deflection δ for a square-bar helical spring is given by Wahl (1963)

$$\delta = \frac{5.59PD^3n}{Ga^4} \tag{1.6}$$

where *G* is the modulus of rigidity and *n* is the number of active turns. This formula is theoretically around *2* to *4* per cent in error for springs with indexes between *3* and *4*, but for most practical cases it is accurate enough (Wahl, 1963).

$$\text{Spring rate} = \frac{P}{\delta} = \frac{Ga^4}{5.59D^3 n} \tag{1.7}$$

As stated above, helical compression springs are open-coiled springs having helix pitch angles greater than $\alpha > 10^o$. In this case, the effects of all the stress resultants at the centroid of the cross-section should be considered, namely axial and shearing forces, bending and torsional moments.

As far as known, the analytical deflection expressions where variable curvatures, different types of helical spring, different types of cross-sections, different materials, and large pitch angles are considered do not exist in the available literature.

The present study deals with the most commonly used helical compression springs having doubled symmetric such as solid circle, square, rectangle, and ellipse, and hollow circle etc., cross-sections. By using Castigliano's theorem, it is expected to find closed-form solutions for the vertical tip deflection of helical springs with arbitrary shaped and large pitch angles. As it is well known, the stiffness of the spring is closely related with the tip deflection. From equation (1.7) the spring constant can be easily determined by multiplying the reciprocal of the deflection and the force applied.

Thus, the designers will be free to design suitable and most accurate springs by using more generalized formulas presented in the present study.

2. PREVIOUS STUDIES

Wahl (1963) presented a book, which is assumed to be an authoritative work on spring design, emphasizing the widely used isotropic helical compression and extension springs. This book is considered by many spring makers as the "bible" of spring design. This book also covers helical torsion springs, ring springs, coned-disk springs, torsion bar springs, power springs, volute springs and other types.

Compression spring design considerations are numerous. The problem of spring design is often resolved using tables and charts containing certain pre-selected specifications and objectives. Spring design takes considerable time due to trial and error method. Along with the development in computers, some commercial software programs based on existing analytical and empirical equations together with some design charts are presented for designers. The main commercial software available to designers is stated as “Compression Spring Software” from IST, “FED1” from Hexagon and “Advanced Spring Design” from SMI. They use standard calculations.

Existing analytical formulas used in the spring design for computation of vertical displacements due to the static load are generally valid for small helix pitch angles ($\alpha \leq 10^{o}$), relatively large spring indices (D/d≥ 10), circular/square cross-sections and right cylinders.

In general, the effects of the axial force and bending moment are not considered in the spring design. For springs with circular sections and large pitch angles, Timoshenko (1984) presented a formula by taking into consideration the whole effects of the shearing force, bending and torsional moment except the axial force.

As it is well known, one way to obtain springs having different rigidities under the constant load for a given volume is to wrap the wire on different cylindrical surfaces by keeping other geometrical and material properties constant.

Although dynamic behaviour of isotropic and composite cylindrical and non-cylindrical helical springs are almost widely studied recently (Yıldırım, 1999a-b, Yıldırım and Sancaktar, 2000; Yıldırım, 2001a-b; Yıldırım, 2002; Yıldırım, 2004), there is not enough contribution on the determination of the vertical tip deflection of those springs.

Haktanır (1992) studied numerically on the variation of the spring constants with respect to the spring index, helix pitch angle and the ratio of R_{min}/R_{max} of the isotropic conical helical springs with the help of the complementary functions method. The effects of axial and shear deformations and bending moment are considered in this work.

Haktanır (1994) worked out the static behaviour of isotropic cylindrical and non-cylindrical helical springs (barrel, hyperboloidal and conical types) subjected to a concentrated axial force acting along the cylinder axis. She presented analytical formulas for the vertical tip deflection of those springs by considering the whole effects of the stress resultants, large helix pitch angles and different types of cross sections with the help of the Castigliano's first theorem.

The present study is a continuation of Haktanır (1994)'s work to study the determination of the vertical tip deflection of springs made of orthotropic materials. Thus the stiffness of the spring is determined by using this deflection.

3. MATERIAL AND METHOD

3.1. Calculations of Stress and Deformation for Cylindrical Helical Springs with Small Pitch Angles

3.1.1. Stress Calculations

Consider a helical spring with a pitch angle α loaded axially with a force P shown in Figure 3.1. In this figure the mean coil diameter and the wire diameter are symbolized by D and d respectively. The vertical distance between two coils called pitch, H, is defined by

$$\tan\alpha = \frac{H}{2\pi R} = \frac{2\pi h}{2\pi R} = \frac{h}{R} \tag{3.1}$$

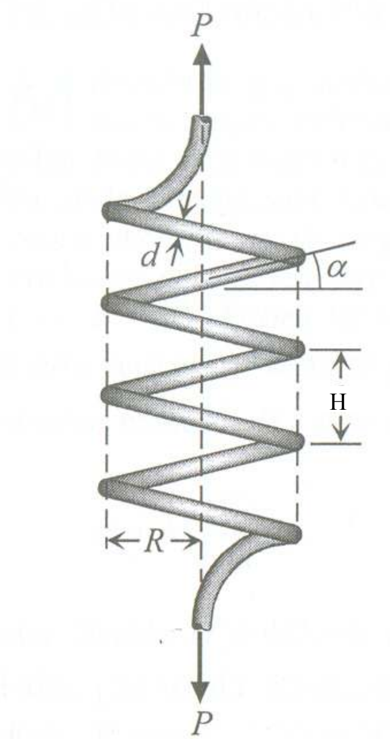

Figure 3.1 Axially loaded helical spring (Omurtag, 2005)

If the spring is cut by two perpendicular planes passing through the cylinder axis, than the equivalent force-couple system at sections of wire due to the axial load is shown in Figure 3.2.

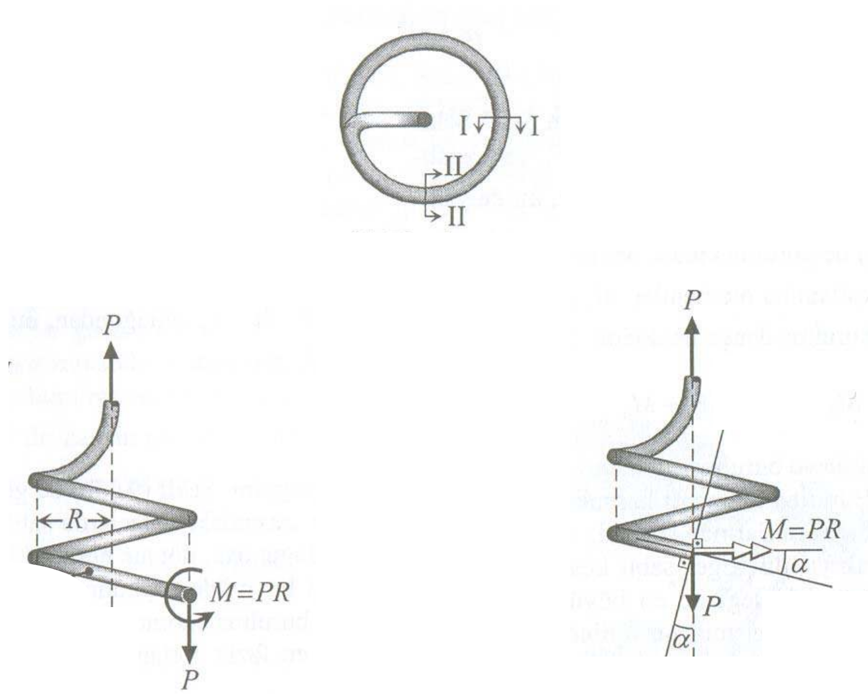

a) Section I-I b) Section II-II

Figure 3.2 Equivalent force couple system at sections I-I and II-II (Omurtag, 2005)

The sections shown in Figure 3.2 are not true cross-sections. Those sections make an angle α with the true cross section of the wire. Thus, that force and couple acting on those sections are not considered as true shearing force and true torsional moment. The components of the equivalent force-couple system along the coordinate axes attached to the centroid of the sections are

$$N = P\sin\alpha \tag{3.2a}$$

$$T = P\cos\alpha \tag{3.2b}$$

$$M_b = PR\sin\alpha \tag{3.2c}$$

$$M_t = PR\cos\alpha \tag{3.2d}$$

where N is the axial force, T is the shearing force, M_b is the bending moment and M_t is he torsional moment.

Under the assumption that pitch angle is small, than the effect of the axial force and bending moment becomes zero, $Sin\alpha \cong 0$ and $Cos\alpha \cong 1$. Mainly stress resultants are being torsional moment and shearing force at cross-section of the wire (Figure 3.3)

$$N \cong 0 \tag{3.3a}$$

$$M_b \cong 0 \tag{3.3b}$$

$$T \cong P \tag{3.3c}$$

$$M_t \cong PR \tag{3.3d}$$

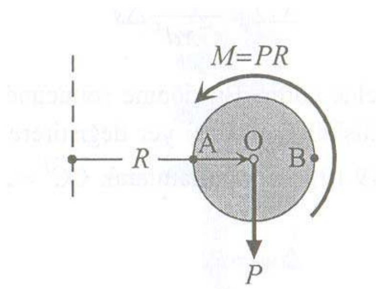

Figure 3.3 Mainly stress resultants at the cross section of the wire (Omurtag, 2005)

Both the shearing force and the torsional moment cause just the shearing stresses at the section. Denoting the shear correction factor (*k*-factor) by *k'*, which appears as a coefficient in the expression for the transverse shear stress resultant, to consider the shear deformation effects with a good approximation as a result of non-uniform distribution of the shear stresses over the cross-section of the beam, shearing stresses induced by shearing moment is computed by (Omurtag, 2005)

$$\tau_k = \frac{T}{k'A} = \frac{4}{3}\frac{T}{A} = \frac{4}{3}\frac{P}{\frac{\pi d^2}{4}} = \frac{16P}{3\pi d^2} \tag{3.4}$$

and due to the torsional moment is as follows

$$\tau_b = \frac{M_b(\frac{d}{2})}{I_o} = \frac{PR(\frac{d}{2})}{\frac{\pi d^4}{32}} = \frac{16PR}{\pi d^3} \tag{3.5}$$

where A is the cross-sectional area of the circular cross-section, I_o is the polar moment of inertia of that section, and *k'* is the shear correction factor.

By using the superposition principle, the total shearing stress at points A and B on the cross-section is determined by (İnan, 1967; Kayan, 1987; Omurtag, 2005)

$$\tau_{\substack{max\\min}} = \frac{16P}{3\pi d^2} \pm \frac{16PR}{\pi d^3} = \frac{16PR}{\pi d^3}(\frac{d}{3R} \pm 1) \tag{3.6}$$

The first term in equation (3.6) represents the contribution of the shearing force. The stress distribution over the cross section is shown in Figure (3.4). It is concluded from the figure that, the critical point on the section is actually point A. That is, the maximum shear stress in a helical spring occurs on the inner face of the spring coils.

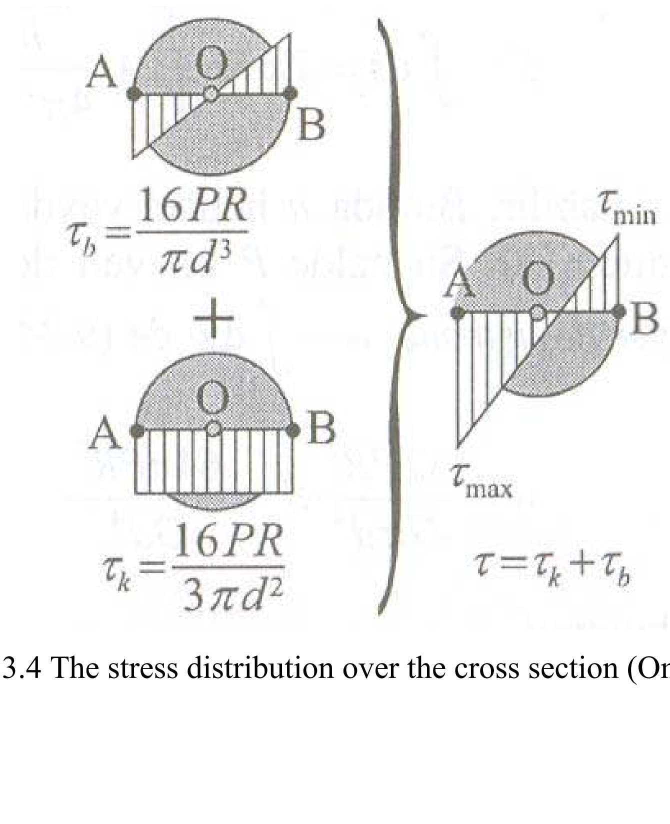

Figure 3.4 The stress distribution over the cross section (Omurtag, 2005)

The ratio of mean coil diameter to wire diameter is known as the “spring index”.

$$C = \frac{D}{d} \tag{3.7}$$

Low indices result in difficulty with spring manufacture and in stress concentrations induced by curvature. Springs in the range *5 ≤ C ≤ 10* are preferred, while indices less than 3 are generally impracticable. The optimum value of the spring index is taken as *C=9* in practice.

If we consider just helical springs with large spring indices then equation (3.6) becomes

$$\tau_{\max} \cong \frac{16PR}{\pi d^3} = \frac{8PD}{\pi d^3} = \frac{8PC}{\pi d^2} \leq \tau_{safety} \tag{3.8}$$

Wahl (1963) proposed the following equation with a correction factor called with his name, *K*, to consider the whole effect of both shearing force and torsional moment.

$$\tau_{\max} \cong K\frac{16PR}{\pi d^3} = K\frac{8PD}{\pi d^3} = K\frac{8PC}{\pi d^2} \leq \tau_{safety} \tag{3.9}$$

where Wahl factor is defined as a function of the spring index.

$$K = \frac{4C-1}{4C-4} + \frac{0.615}{C} \tag{3.10}$$

Variation of the Wahl factor, which accounts for shear stress resulting from spring curvature, with the spring index is shown in Figure (3.5). Since the stress calculation is out of the scope of the present study, the knowledge given above is almost sufficient to understand the behavior of the spring subjected to the axial force.

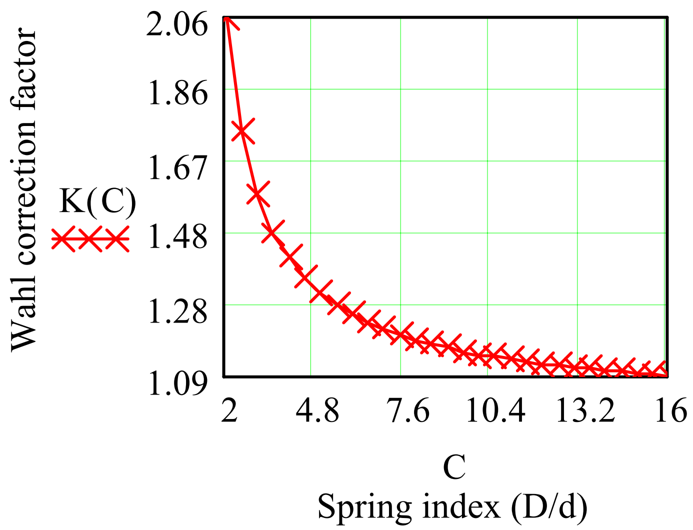

Figure 3.5 Variation of the Wahl factor with the spring index

3.1.2. Deformation Calculations

The performance of a spring is characterized by the relationship between the load applied to it and the deflection $(P - w)$ (Figure 3.6). The $(P - w)$ characteristic is approximately linear provided the spring is close-coiled and the material elastic, that is Hooke's law is typically assumed to hold $P = kw$. The slope of the characteristic, k, is known as “the stiffness of the spring” or “spring constant”, or “spring rate”, or “spring scale” or “spring gradient”, and is determined by the spring geometry and spring material.

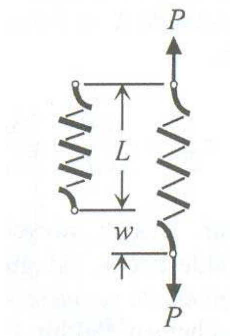

Figure 3.6 Axial deformation of the spring subjected to the an axial force (Omurtag, 2005)

Let's consider a small spring arc element Δs with an opening angle, $\Delta\theta$ (Figure 3.7).

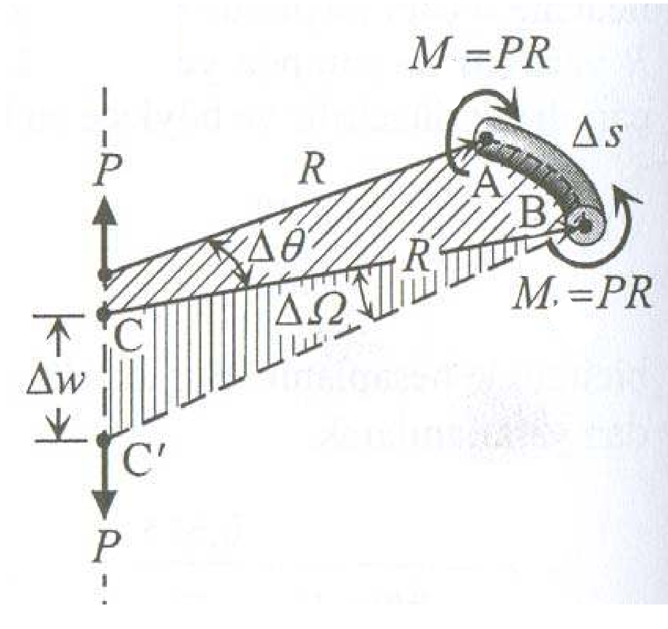

Figure 3.7 Deflection of a small spring arc element (Omurtag, 2005)

Relative rotation between two sections, $\Delta\Omega$, is defined by

$$\Delta\Omega = \omega\Delta s = \frac{M_t}{GJ_0}\Delta s \tag{3.11}$$

where G is the shear modulus of the wire material, ω is the unit relative torsional rotation about helix axis, and J_0 is the torsional moment of the inertia of the wire section. Torsional moment of inertia takes different values with respect to the section types (Table 3.1).

Table 3.1 Formulas for finding the torsional moment of inertia (İnan, 1967)

Circular section	$J_0 = I_0$
Ellipse section	$J_0 = \dfrac{\pi a^3 b^3}{a^2 + b^2}$
Equilateral triangle section	$J_0 = \dfrac{\sqrt{3}}{80} a^4$
Square section	$J_0 = 0.141 a^4$
General solid section	$J_0 \cong \dfrac{A^4}{40 I_0} \cong 0.025 \dfrac{A^4}{I_0}$

For circular sections, since the torsional moment of inertia and the polar moment of inertia are equal to each other.

$$I_0 = \frac{\pi d^4}{32} = \frac{\pi r^4}{2} \tag{3.12}$$

Equation (3.11) may be rewritten in the following form.

$$\Delta\Omega = \omega \Delta s = \frac{M_t}{G I_0} \Delta s = \frac{32 P R}{G \pi d^4} \Delta s \tag{3.13}$$

From the Figure (3.6),

$$\Delta w = R\Delta\Omega = \frac{32PR^2}{G\pi d^4}\Delta s \tag{3.14}$$

The above means that the vertical displacement along the cylinder axis is proportional to the length of the spring.

For closed coil springs having small pitch angles, the total active length of the wire is defined by

$$L = 2\pi\, nc = 2\pi\, Rn\sqrt{1+\tan^2\alpha} = 2\pi\, Rn\sqrt{1+\frac{H^2}{4\pi^2R^2}} \cong 2\pi\, Rn = \pi Dn \tag{3.15}$$

where n is the total number of active coils and

$$h = R\tan\alpha$$
$$H = 2\pi\, h$$
$$c^2 = R^2 + h^2 = R^2(1+\tan^2\alpha) = R^2(1+\frac{h^2}{R^2}) = R^2(1+\frac{H^2}{4\pi^2R^2}) \tag{3.16}$$

Active coils are the number of coils which actually deform when the spring is loaded, as opposed to the inactive turns at each end which are in contact with the spring seat or base.

Substituting equation (3.15) into equation (3.14) yields the following.

$$w = \frac{64nPR^3}{Gd^4} \tag{3.17}$$

The spring constant can be evaluated in different form as follows

$$k = \frac{P}{w} = \frac{Gd^4}{8D^3n} = \frac{Gd}{8C^3n} = \frac{\pi\, Gd^4}{8D^2L} = \frac{Gd^4}{64nR^3} \tag{3.18}$$

For conical springs shown in Figure (3.8) the radius of the cylinder along the wire axis is variable.

$$R = R(\theta) = R_1 + \frac{(R_2 - R_1)}{2\pi n}\theta \tag{3.19}$$

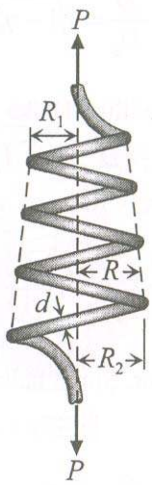

Figure 3.8 Conical helical spring (Omurtag, 2005)

For closed coiled springs, the infinitesimal arc length becomes $ds \cong Rd\theta$ and total axial deflection is obtained by using equation (3.14), $\Delta w = R\Delta\Omega = \dfrac{32PR^2}{G\pi d^4}\Delta s$

$$w = \frac{32P}{G\pi d^4}\int_0^{2\pi n} R^3 d\theta = \frac{16nP(R_1^2 + R_2^2)(R_1 + R_2)}{Gd^4} \tag{3.20}$$

$$f(\theta, r1, r2, n) := r1 + (r2 - r1)\cdot\frac{\theta}{2\cdot\pi\cdot n}$$

$$w := \int_0^{2\cdot\pi\cdot n} (f(\theta, r1, r2, n))^3\, d\theta$$

$$ww := w \text{ simplify } \rightarrow \frac{1}{2}\cdot\left(r1^3 + r2\cdot r1^2 + r2^2\cdot r1 + r2^3\right)\cdot\pi\cdot n$$

$$www := ww \text{ factor } \rightarrow \frac{1}{2}\cdot(r2 + r1)\cdot\left(r1^2 + r2^2\right)\cdot\pi\cdot n$$

3.2. Elastic Strain Energy

For the elastic deformation of an isotropic body, the strain energy, U_i, is defined by the following

$$U_i = \int_V u_i dV$$

(3.21)

where u_i is the strain-energy density and V is the volume of the body.

$$u_i = \frac{dU}{dV} \tag{3.22}$$

3.2.1. Generalized Hooke's Law

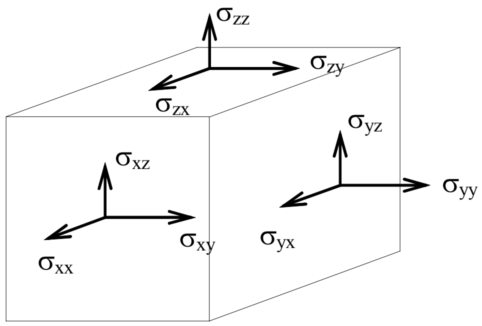

Figure 3.9 Normal and shear stresses on surfaces of a cube element

The generalized Hooke's law for a homogeneous anisotropic material under the most general stress condition is (Figure 3.9)

$$\sigma_{ij} = C_{ijkl}\varepsilon_{kl}$$

(3.23)

or

$$\varepsilon_{ij} = S_{ijkl}\sigma_{kl} \tag{3.24}$$

where ε_{ii} is the normal strain, σ_{ii} is the normal stress, $\sigma_{ij} = \tau_{ij}$ is the shear stress, and $\varepsilon_{ij} = (1/2)\gamma_{ij}$ is the shear stain. For a linear elastic material, C_{ijkl} is the element of the material stiffness tensor and S_{ijkl} is the element of the material compliance tensor. Those tensors are inverses of each other. For isotropic material those constitutive equations becomes

$$\varepsilon_x = +\frac{\sigma_x}{E} - \frac{\nu\sigma_y}{E} - \frac{\nu\sigma_z}{E} \tag{3.25a}$$

$$\varepsilon_y = -\frac{\nu\sigma_x}{E} + \frac{\sigma_y}{E} - \frac{\nu\sigma_z}{E} \tag{3.25b}$$

$$\varepsilon_z = -\frac{\nu\sigma_x}{E} - \frac{\nu\sigma_y}{E} + \frac{\sigma_z}{E} \tag{3.25c}$$

$$\gamma_{xy} = \frac{\tau_{xy}}{G} \tag{3.25d}$$

$$\gamma_{xz} = \frac{\tau_{xz}}{G} \tag{3.25e}$$

$$\gamma_{yz} = \frac{\tau_{yz}}{G} \tag{3.25f}$$

where E is the Young's modulus of the material, G is the shear modulus. The Poisson's ratio of the linear elastic material is represented by ν. The three independent material constants of an isotropic material are related by

$$\frac{1+\nu}{E} = \frac{1}{2G} \tag{3.26}$$

A compact form of equation (3.25) as follows

$$\varepsilon_{ij} = \frac{1+\nu}{E}\sigma_{ij} - \frac{\nu}{E}\delta_{ij}\sigma_{kk} \tag{3.27}$$

or

$$\sigma_{ij} = \lambda e\delta_{ij} + 2G\varepsilon_{ij}$$
(3.28)

where δ_{ij} is the Kronecker delta ($\delta_{ii} = 1$ and $\delta_{ij} = 0$), and

$$e = \varepsilon_{kk} = \frac{\partial u}{\partial x} + \frac{\partial v}{\partial y} + \frac{\partial w}{\partial z} = di\vec{v}\vec{U} = \frac{1-2\nu}{E}(\sigma_1 + \sigma_2 + \sigma_3) \tag{3.29}$$

and, Lame constant is given by

$$\lambda = \frac{E\nu}{(1+\nu)(1-2\nu)} \tag{3.30}$$

3.2.2. Strain Energy Density For A General State of Stress

For 3-D anisotropic body, the strain energy density may be expressed by six stress relations as follows

$$u_i = \frac{1}{2}\sigma_{ij}\varepsilon_{ij} = \frac{1}{2}C_{ijkl}\varepsilon_{ij}\varepsilon_{kl} = \frac{1}{2}S_{ijkl}\sigma_{ij}\sigma_{kl} \tag{3.31}$$

or

$$u_i = \frac{1}{2}(\sigma_x\varepsilon_x + \sigma_y\varepsilon_y + \sigma_z\varepsilon_z + \tau_{xy}\gamma_{xy} + \tau_{xz}\gamma_{xz} + \tau_{yz}\gamma_{yz}) \tag{3.32}$$

Using the stress-strain equations in (3.25), the strain energy density may be written in terms of just stresses for isotropic materials

$$u_i = \frac{1}{2E}\left\{(\sigma_x^2 + \sigma_y^2 + \sigma_z^2) - 2\nu(\sigma_x\sigma_y + \sigma_x\sigma_z + \sigma_y\sigma_z)\right\} + \frac{1}{2G}\left\{\tau_{xy}^2 + \tau_{xz}^2 + \tau_{yz}^2\right\} \tag{3.33}$$

If the principal axes *(1,2,3)* at a given point are used as coordinate axes, the shearing stresses become zero and the above equation reduces to

$$u_i = \frac{1}{2E}\left\{(\sigma_1^2 + \sigma_2^2 + \sigma_3^2) - 2\nu(\sigma_1\sigma_2 + \sigma_1\sigma_3 + \sigma_2\sigma_3)\right\} \tag{3.34}$$

And finally, the strain energy density may be written in terms of just strains for isotropic material as follows

$$u_i = \frac{1}{2}\lambda e^2 + G(\varepsilon_x^2 + \varepsilon_y^2 + \varepsilon_z^2) + \frac{G}{2}(\gamma_{xy}^2 + \gamma_{xz}^2 + \gamma_{yz}^2) \tag{3.35}$$

For in cases where just principal strains exist, $\gamma = 0$,

$$u_i = \frac{1}{2}\lambda e^2 + G(\varepsilon_1^2 + \varepsilon_2^2 + \varepsilon_3^2) \tag{3.36}$$

3.3. Computation of Work for Spatial Bars

3.3.1. Work Done by External Loads

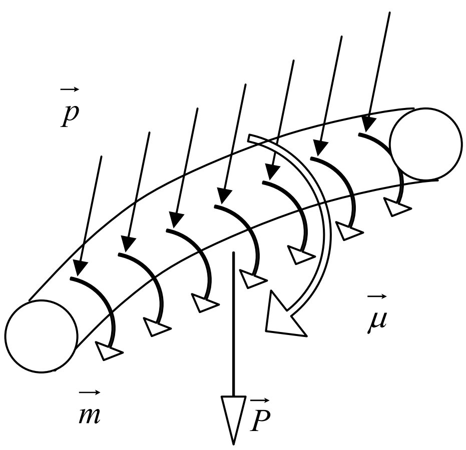

Figure 3.10 External concentrated and distributed loads acting on *ds* element

Consider an infinitesimal arc element, *ds*, and external force and couples acting on it (Figure 3.10). Let $\vec{P}$ be concentrated force, $\vec{p}$ be distributed force, $\vec{\mu}$ be concentrated couple, and $\vec{m}$ be distributed couple acting on the element. The scalar components of those vector quantities along (*x,y,z*) axes are

$$\vec{p} = p_x \vec{i} + p_y \vec{j} + p_z \vec{k} \tag{3.37a}$$

$$\vec{P} = P_x \vec{i} + P_y \vec{j} + P_z \vec{k} \tag{3.37b}$$

$$\vec{m} = m_x \vec{i} + m_y \vec{j} + m_z \vec{k} \tag{3.37c}$$

$$\vec{\mu} = \mu_x \vec{i} + \mu_y \vec{j} + \mu_z \vec{k} \tag{3.37d}$$

Assume that the external loads acting on the element are slowly increased from zero to the final value.

Let $\vec{U}$ be the displacement vector of a point on the bar axis and $\vec{\Omega}$ be the rotation of the section. Those vectors may be expressed as follows in rectangular coordinates

$$\vec{U} = U_x \vec{i} + U_y \vec{j} + U_z \vec{k} \tag{3.38a}$$

$$\vec{\Omega} = \Omega_x \vec{i} + \Omega_y \vec{j} + \Omega_z \vec{k} \tag{3.38b}$$

As it is well known, the work done by a force is defined by a scalar product (dot product) of the force and displacement vectors.

$$
\begin{aligned}
U_d &= \frac{1}{2}\int_A^B (\vec{p}\bullet\vec{U}+\vec{m}\bullet\vec{\Omega})ds+\frac{1}{2}\sum(\vec{P}\bullet\vec{U}+\vec{\mu}\bullet\vec{\Omega}) \\
&= \frac{1}{2}\int_A^B (p_xU_x+p_yU_y+p_zU_z+m_x\Omega_x+m_y\Omega_y+m_z\Omega_z)ds \\
&+\frac{1}{2}\sum(P_xU_x+P_yU_y+P_zU_z+\mu_x\Omega_x+\mu_y\Omega_y+\mu_z\Omega_z)
\end{aligned}
\tag{3.39}
$$

3.3.2. Work Done by Internal Forces

It is common to use the Frenet unit vectors, *($\vec{t},\vec{n},\vec{b}$= tangential, normal and binormal unit vectors)* to determine the stress resultants.

Let $\vec{T}$ be the internal force vector, $\vec{M}$ be the internal couple vector attached at centroid of the section. Let $\vec{\gamma}$ be the relative unit extension vector and $\vec{\omega}$ be the relative unit rotation vector on a point on the bar axis. Frenet components of the vectors stated above are

$$\vec{M} = M_t\vec{t}+M_n\vec{n}+M_b\vec{b} \tag{3.40a}$$

$$\vec{T} = T_t\vec{t}+T_n\vec{n}+T_b\vec{b} \tag{3.40b}$$

$$\vec{\gamma} = \gamma_t\vec{t}+\gamma_n\vec{n}+\gamma_b\vec{b} \tag{3.40c}$$

$$\vec{\omega} = \omega_t\vec{t}+\omega_n\vec{n}+\omega_b\vec{b} \tag{3.40d}$$

From the constitutive relations for isotropic materials the followings may be written

$$\gamma_t=\frac{T_t}{C_t};\qquad \gamma_n=\frac{T_n}{C_n};\qquad \gamma_b=\frac{T_b}{C_b} \tag{3.41a}$$

$$\omega_t=\frac{M_t}{D_t};\qquad \omega_n=\frac{M_n}{D_n};\qquad \omega_b=\frac{M_b}{D_b} \tag{3.41b}$$

where T_t is the axial force; T_n and T_b are shearing forces; M_t is the torsional moment; M_n and M_b are the bending moments; C_t is the axial rigidity; C_n and C_b are the shearing rigidities; D_t is the torsional rigidity; and finally D_n and D_b are bending rigidities

.

$$C_t = EA; \qquad C_n = \frac{GA}{k_n}; \quad C_b = \frac{GA}{k_b} \tag{3.42a}$$

$$D_t = GJ_b; \quad D_n = EI_n; \quad D_b = EI_b \tag{3.42b}$$

where J_b is the torsional moment of inertia (see the Table 3.1), I_n and I_b are the of inertia of the section, k_n and k_b are shear correction factors of the section.

Timoshenko's beam theory (*TBT)* accounts both the shear and rotatory inertia effects based upon the first order shear deformation theory which offers the simple and acceptable solutions. The numerical value of the *k*-factor which was originally proposed by Timoshenko depends upon generally both the Poisson's ratio of the material and the shape of the cross-section. For rectangular sections, Timoshenko (1921, 1922) offers the *k*-factor dependent on just Poisson's ratio as follows by solving *2-D* elasticity bending problem

$$k_{Timoshenko}(\upsilon) = k_1 = k_2 = \frac{5 + 5\upsilon}{6 + 5\upsilon} \tag{3.43}$$

and Cowper (1966) recommended the following *k*-factor which depends upon Poisson's ratio for the 3-D integral solution of the elasticity problem

$$k_{Cowper}(\upsilon) = k_1 = k_2 = \frac{10 + 10\upsilon}{12 + 11\upsilon} \tag{3.44}$$

Here some *k*- factors:

- ✓ $k_n = k_b = 1.2$ (for rectangle)
- ✓ $k_n = k_b = 1.1$ (for solid circle) (Cowper, 1966)

- ✓ $k_n = k_b = 1.61$ (for hollow circle with $\dfrac{d_{inner}}{d_{outer}} = 0.5$) (Cowper, 1966)
- ✓ $k_n = k_b = 2$ (for thin hollow circle) (İnan, 1967)

The work done by internal forces are computed by the following integrals.

$$\begin{aligned} U_i &= \frac{1}{2}\int_A^B (\vec{T} \bullet \vec{\gamma} + \vec{M} \bullet \vec{\omega}) ds \\ &= \frac{1}{2}\int_A^B (T_t\gamma_t + T_n\gamma_n + T_b\gamma_b + M_t\omega_t + M_n\omega_n + M_b\omega_b) ds \\ &= \frac{1}{2}\int_A^B \left(\frac{T_t^2}{C_t} + \frac{T_n^2}{C_n} + \frac{T_b^2}{C_b} + \frac{M_t^2}{D_t} + \frac{M_n^2}{D_n} + \frac{M_b^2}{D_b}\right) ds \\ &= \frac{1}{2}\int_A^B (C_{tt}\gamma_t^2 + C_n\gamma_n^2 + C_b\gamma_b^2 + D_t\omega_t^2 + D_n\omega_n^2 + D_b\omega_b^2) ds \end{aligned} \tag{3.45}$$

3.4. Determination of Deflection by Castigliano's Theorem

According to the conservation of the energy the work done by external forces is equal to the work done by internal forces.

$$U_i = U_d \tag{3.46}$$

In order to determine the deflection under a single load (concentrated force or couple) applied to a structure consisting of several component parts, it may be necessary to integrate the strain energy density over the various parts of the structure. This procedure simplifies the solution of many impact loading problems.

The strain energy of the structure subjected to several loads cannot be determined by computing the work of each load as if it were applied independently to the structure. If it were possible to compute the strain energy of the structure in this manner, only one equation would be available to determine deflections corresponding to the various loads.

Castigliano's theorem based on the concept of strain energy is used to determine the deflection or slope at a given point of a structure, even when that structure is subjected simultaneously to several concentrated loads, distributed loads, or couples.

If an elastic structure is subjected to n loads P *(or M)*, the deflection x_j of the point of application of P_j, measured along the line of action of P_j, may be expressed as the partial derivative of the strain energy of the structure with respect to the P_j.

$$x_j = \frac{\partial U_i}{\partial P_j} \tag{3.47a}$$

$$\theta_j = \frac{\partial U_i}{\partial M_j} \tag{3.47b}$$

Equation (3.47) is called Castigliano's first theorem that is valid for linear elastic structures. Castigliano's second theorem, which is used for both linear and nonlinear elastic structures, is determined as follows

$$P_j = \frac{\partial U_i}{\partial x_j} \tag{3.48a}$$

$$M_j = \frac{\partial U_i}{\partial \theta_j} \tag{3.48b}$$

For example, for the truss consisting of n uniform members of length L_i, cross sectional area A_i, and the internal force F_i, the strain energy of the truss

$$U_i = \sum_{i=1}^{n} \frac{F_i^2 L_i}{2 A_i E} \tag{3.49}$$

The deflection x_j of the point of application of the load P_j is obtained by differentiating with respect to P_j each term of sum.

$$x_j = \frac{\partial U_i}{\partial P_j} = \sum_{i=1}^{n} \frac{F_i L_i}{A_i E} \frac{\partial F_i}{\partial P_j} \tag{3.50}$$

In this study we will use just Castigliano's first theorem. In summary, the deflection x_j of a structure at the point of application of a load P_j may be determined by computing the partial derivative $\frac{\partial U}{\partial P_j}$ of the strain energy U of the structure. The total strain energy is obtained by integrating or summing over the structure the strain energy of each element of the structure. From equation (3.45), for spatial bars of length L, the following may be written.

$$U_i = \frac{1}{2}\int_0^L \left(\frac{T_t^2}{C_t} + \frac{T_n^2}{C_n} + \frac{T_b^2}{C_b} + \frac{M_t^2}{D_t} + \frac{M_n^2}{D_n} + \frac{M_b^2}{D_b}\right) ds \tag{3.51}$$

Substituting equation (3.51) into the first equation (3.47) gives

$$x_j = \frac{1}{2}\frac{\partial}{\partial P_j}\int_0^L \left(\frac{T_t^2}{C_t} + \frac{T_n^2}{C_n} + \frac{T_b^2}{C_b} + \frac{M_t^2}{D_t} + \frac{M_n^2}{D_n} + \frac{M_b^2}{D_b}\right) ds \tag{3.52}$$

By interchanging the integral and derivative operators we have

$$x_j = \int_0^L \left\{ \frac{T_t}{C_t}.\frac{\partial T_t}{\partial P_j} + \frac{T_n}{C_n}.\frac{\partial T_n}{\partial P_j} + \frac{T_b}{C_b}.\frac{\partial T_b}{\partial P_j} + \frac{M_t}{D_t}.\frac{\partial M_t}{\partial P_j} + \frac{M_n}{D_n}.\frac{\partial M_n}{\partial P_j} + \frac{M_b}{D_b}.\frac{\partial M_b}{\partial P_j} \right\} ds \tag{3.53}$$

So, the calculation of the deflection is simplified by carrying out the differentiation before the integration.

Castigliano's theorem is used for determination of deflections and slopes at various points of a given structure. The theorem may be used for both statically determinate and statically indeterminate structures. The use of dummy loads enables us to include points where no actual load is applied.

3.5. Application of Castigliano's Theorem to the Determination of Deflection of Helical Springs

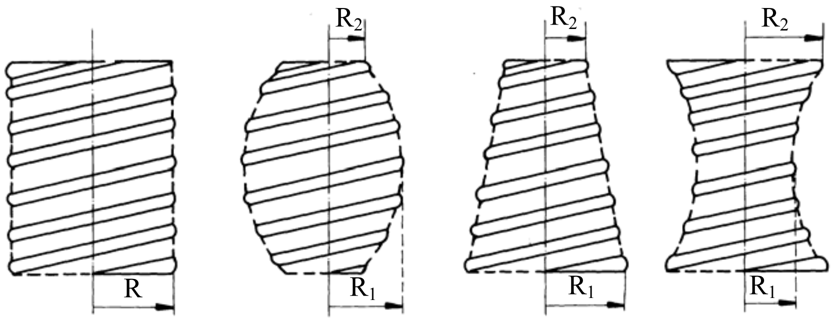

Figure 3.11 Types of helical compression springs

Considering Figure 3.11, the radius of the cylinder at any point on the rod axis can be defined for conical springs as follows

$$R(\theta) = R_1 + \frac{(R_2 - R_1)}{2\pi n}\theta \tag{3.54}$$

and for barrel and hyperboloidal type helical springs as

$$R(\theta) = R_1 + (R_2 - R_1)(1 - \frac{\theta}{\pi n})^2 \tag{3.55}$$

where n and θ represent the number of active coils and angular displacement respectively, and $0 \le \theta \le 2\pi n$. For helical springs subjected to a single vertical force, non-zero stress resultants at the cross-section are defined by

$$T_t = -P\sin\alpha \qquad ; \qquad T_b = -P\cos\alpha \tag{3.56a}$$

$$M_t = PR(\theta)\cos\alpha \qquad ; \qquad M_b = -PR(\theta)\sin\alpha \tag{3.56b}$$

where T_t is the axial force, T_n is the shearing force, M_b is the bending moment and M_t is the torsional moment (Figure 3.12).

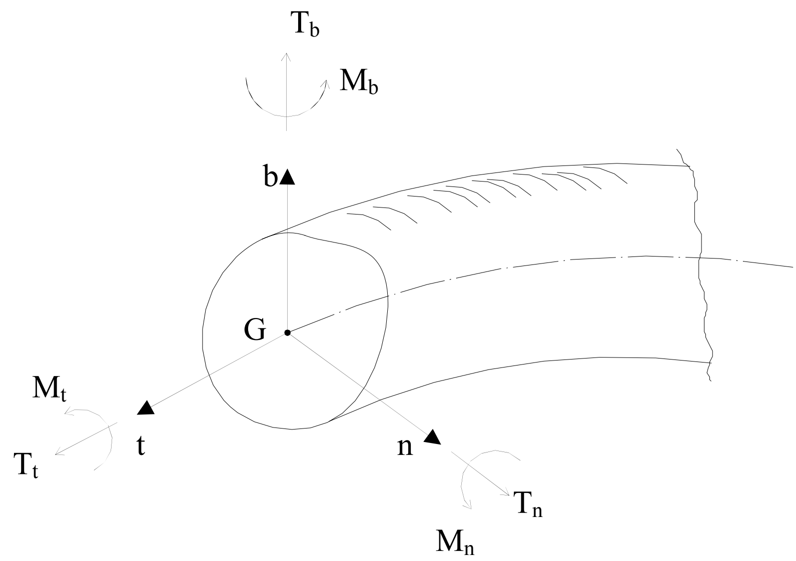

Figure 3.12 Stress resultants in Frenet coordinates (***t,n,b***)

The first derivative of the stress resultants with respect to the external single force are

$$\frac{\partial T_t}{\partial P} = -\sin\alpha \tag{3.57a}$$

$$\frac{\partial T_b}{\partial P} = -\cos\alpha \tag{3.57b}$$

$$\frac{\partial M_b}{\partial P} = -R(\theta)\sin\alpha \tag{3.57c}$$

$$\frac{\partial M_t}{\partial P} = -R(\theta)\sin\alpha \tag{3.57d}$$

Considering the non-zero stress resultants and denoting the total vertical deflection at the end of the spring by f_{Total}, equation (3.53) becomes

$$f_{Total} = \int_0^L \left\{ \frac{T_t}{C_t}.\frac{\partial T_t}{\partial P} + \frac{T_b}{C_b}.\frac{\partial T_b}{\partial P} + \frac{M_t}{D_t}.\frac{\partial M_t}{\partial P} + \frac{M_b}{D_b}.\frac{\partial M_b}{\partial P} \right\} ds \tag{3.58}$$

where C_t is the axial rigidity; C_b is the shearing rigidity; D_t is the torsional rigidity; and finally D_b is the bending rigidity.

The infinitesimal arc length of the spring may be written in terms of θ ($0 \le \theta \le 2\pi n$) and the helix pitch angle, α.

$$ds = cd\theta = R(\alpha)\sqrt{1+\tan^2\alpha}.d\theta = \frac{R(\theta)}{\cos\alpha}d\theta \tag{3.59}$$

Equation (3.58) may be rewritten as follows

$$f_{Total} = \frac{1}{\cos\alpha}\int_0^{2\pi n} \left\{ \frac{T_t}{C_t}.\frac{\partial T_t}{\partial P} + \frac{T_b}{C_b}.\frac{\partial T_b}{\partial P} + \frac{M_t}{D_t}.\frac{\partial M_t}{\partial P} + \frac{M_b}{D_b}.\frac{\partial M_b}{\partial P} \right\} R(\theta)d\theta \tag{3.60}$$

or

$$f_{Total} = f_{T_t} + f_{T_b} + f_{M_b} + f_{M_t} \tag{3.61}$$

where f_{T_t}, f_{T_b}, f_{M_b} and f_{M_t} represent the contribution of each stress resultant to the total vertical deflection. Substituting equation (3.57) into equation (3.60) yields the followings

$$f_{T_t} = \frac{P.\sin\alpha.\tan\alpha}{C_t}\int_0^{2\pi n} R(\theta)d\theta \tag{3.62a}$$

$$f_{T_b} = \frac{P.\cos\alpha}{C_b}\int_0^{2\pi n} R(\theta)d\theta \tag{3.62b}$$

$$f_{M_b} = \frac{P.\sin\alpha.\tan\alpha}{D_b}\int_0^{2\pi n} (R(\theta))^3 d\theta \tag{3.62c}$$

$$f_{M_t} = \frac{P.\cos\alpha}{D_t}\int_0^{2\pi n} (R(\theta))^3 d\theta \tag{3.62d}$$

Equations (3.62) comprise the effect of the helix pitch angle and variation of the helix axis. They are also valid for the general cross sections having two symmetry axes. Finally they can be used for both isotropic and transversely isotropic materials. Evaluation of the integrals in equation (3.62) is given in Table (3.2).

$$f(\theta, r1, r2, n) := r1 + (r2 - r1)\cdot\left(1 - \frac{\theta}{\pi\cdot n}\right)^2$$

$$w := \int_0^{2\cdot\pi\cdot n} (f(\theta, r1, r2, n))^3\, d\theta$$

$$w \rightarrow \frac{2}{7}\cdot r2^3\cdot\pi\cdot n + \frac{12}{35}\cdot\pi\cdot n\cdot r2^2\cdot r1 + \frac{16}{35}\cdot\pi\cdot n\cdot r2\cdot r1^2 + \frac{32}{35}\cdot\pi\cdot n\cdot r1^3$$

$$ww := w \text{ simplify } \rightarrow \frac{2}{7}\cdot r2^3\cdot\pi\cdot n + \frac{12}{35}\cdot\pi\cdot n\cdot r2^2\cdot r1 + \frac{16}{35}\cdot\pi\cdot n\cdot r2\cdot r1^2 + \frac{32}{35}\cdot\pi\cdot n\cdot r1^3$$

$$www := ww \text{ factor } \rightarrow \frac{2}{35}\cdot\pi\cdot n\cdot\left(5\cdot r2^3 + 6\cdot r2^2\cdot r1 + 8\cdot r2\cdot r1^2 + 16\cdot r1^3\right)$$

Table 3.2 Evaluation of the integrals in equation (3.62)

	$\int_0^{2\pi n} R(\theta)d\theta$	$\int_0^{2\pi n} (R(\theta))^3 d\theta$
Cylindrical	$2\pi nR$	$2\pi nR^3$
Conical	$\pi n(R_1 + R_2)$	$\frac{1}{2}\pi n(R_1 + R_2)(R_1^2 + R_2^2)$
Barrel and Hyperboloidal	$\frac{2}{3}\pi n(2R_1 + R_2)$	$\frac{2}{35}\pi n(5R_2^3 + 6R_2^2R_1 + 8R_2R_1^2 + 16R_1^3)$

3.5.1. For Isotropic Materials

As it is known, isotropic materials are defined by just three material properties as follows. Two of them may be determined independently.

$$G = \frac{E}{2(1+\nu)} \tag{3.63}$$

where G is called the modulus of rigidity or shear modulus, E is Young's modulus and ν is Poisson's ratio. These three quantities are independent from the orientation of coordinate axes attached at the centroid of the cross section.

The axial, the shearing, the torsional and the bending rigidities for an isotropic material can be defined as follows

$$C_t = EA = 2(1+\nu)GA \tag{3.64a}$$

$$C_b = \frac{GA}{k_b} \tag{3.64b}$$

$$D_t = GJ_b \tag{3.64c}$$

$$D_b = EI_b = 2(1+\nu)GI_b \tag{3.64d}$$

where k_b represents the shear correction factor, J_b denotes the torsional moment of inertia, I_b represents the second moment of inertia of the section with respect to the binormal axis, and A is the undeformed cross sectional area.

3.5.2. For Transversely Isotropic Materials

For a three-dimensional body, the stress-strain relationship, σ - ε, is assumed to be in the following form:

$$\{\sigma_1, \sigma_2, \sigma_3, \tau_{23}, \tau_{31}, \tau_{12}\}^T = \boldsymbol{C}\{\varepsilon_1, \varepsilon_2, \varepsilon_3, \gamma_{23}, \gamma_{31}, \gamma_{12}\}^T \tag{3.65}$$

The elements of the compliance matrix, $\boldsymbol{S}=\boldsymbol{C}^{-1}$, for an orthotropic material are given in terms of engineering constants.

$$\boldsymbol{S} = \begin{bmatrix} S_{11} & S_{12} & S_{13} & 0 & 0 & 0 \\ S_{12} & S_{22} & S_{23} & 0 & 0 & 0 \\ S_{13} & S_{23} & S_{33} & 0 & 0 & 0 \\ 0 & 0 & 0 & S_{44} & 0 & 0 \\ 0 & 0 & 0 & 0 & S_{55} & 0 \\ 0 & 0 & 0 & 0 & 0 & S_{66} \end{bmatrix} \tag{3.66}$$

where (Jones, 1975)

$$S_{11} = \frac{1}{E_1} \tag{3.67a}$$

$$S_{22} = \frac{1}{E_2} \tag{3.67b}$$

$$S_{33} = \frac{1}{E_3} \tag{3.67c}$$

$$S_{12} = -\frac{\nu_{12}}{E_1} = -\frac{\nu_{21}}{E_2} \tag{3.67d}$$

$$S_{13} = -\frac{\nu_{13}}{E_1} = -\frac{\nu_{31}}{E_3} \tag{3.67e}$$

$$S_{23} = -\frac{\nu_{23}}{E_2} = -\frac{\nu_{32}}{E_3} \tag{3.67f}$$

$$S_{44} = \frac{1}{G_{23}} \tag{3.67g}$$

$$S_{55} = \frac{1}{G_{13}} \tag{3.67h}$$

$$S_{66} = \frac{1}{G_{12}} \tag{3.67i}$$

The elements of the stiffness matrix, ***C***, for an orthotropic material are given in terms of engineering constants or elements of the compliance matrix.

$$\boldsymbol{C} = S^{-1} = \begin{bmatrix} C_{11} & C_{12} & C_{13} & 0 & 0 & 0 \\ C_{12} & C_{22} & C_{23} & 0 & 0 & 0 \\ C_{13} & C_{23} & C_{33} & 0 & 0 & 0 \\ 0 & 0 & 0 & C_{44} & 0 & 0 \\ 0 & 0 & 0 & 0 & C_{55} & 0 \\ 0 & 0 & 0 & 0 & 0 & C_{66} \end{bmatrix} \tag{3.68}$$

where (Jones, 1975)

$$C_{11} = \frac{S_{22}S_{33} - S_{23}^2}{S} = \frac{1 - \nu_{23}\nu_{32}}{E_2 E_3 \Delta} \tag{3.69a}$$

$$C_{22} = \frac{S_{11}S_{33} - S_{13}^2}{S} = \frac{1 - \nu_{13}\nu_{31}}{E_1 E_3 \Delta} \tag{3.69b}$$

$$C_{33} = \frac{S_{11}S_{22} - S_{12}^2}{S} = \frac{1 - \nu_{12}\nu_{21}}{E_1 E_2 \Delta} \tag{3.69c}$$

$$C_{12} = \frac{S_{13}S_{23} - S_{12}S_{33}}{S} = \frac{\nu_{21} + \nu_{31}\nu_{23}}{E_2 E_3 \Delta} = \frac{\nu_{12} + \nu_{32}\nu_{13}}{E_1 E_3 \Delta} \tag{3.69d}$$

$$C_{13} = \frac{S_{12}S_{23} - S_{13}S_{22}}{S} = \frac{\nu_{31} + \nu_{21}\nu_{32}}{E_2 E_3 \Delta} = \frac{\nu_{13} + \nu_{12}\nu_{23}}{E_1 E_2 \Delta} \tag{3.69e}$$

$$C_{23} = \frac{S_{11}S_{13} - S_{23}S_{11}}{S} = \frac{\nu_{32} + \nu_{12}\nu_{31}}{E_1 E_3 \Delta} = \frac{\nu_{23} + \nu_{21}\nu_{13}}{E_1 E_2 \Delta} \tag{3.69f}$$

$$S = S_{11}S_{22}S_{33} - S_{11}S_{23}^2 - S_{22}S_{13}^2 - S_{33}S_{12}^2 + 2S_{12}S_{23}S_{13} \tag{3.69g}$$

$$\Delta = \frac{1 - \nu_{12}\nu_{21} - \nu_{23}\nu_{32} - \nu_{31}\nu_{13} - 2\nu_{21}\nu_{32}\nu_{13}}{E_1 E_2 E_3} \tag{3.69h}$$

$$C_{44} = \frac{1}{S_{44}} = G_{23} \tag{3.69i}$$

$$C_{55} = \frac{1}{S_{55}} = G_{31} \tag{3.69j}$$

$$C_{66} = \frac{1}{S_{66}} = G_{12} \tag{3.69k}$$

The following relations exist in the definition of the elements given above (Jones, 1975; Tsai and Hahn, 1980).

$$\nu_{ij} = -\frac{\varepsilon_j}{\varepsilon_i} \tag{3.70a}$$

$$\frac{\nu_{ij}}{E_i} = \frac{\nu_{ji}}{E_j} \tag{3.70b}$$

From the equation (3.65), the reduced stiffness matrix for rods, $\boldsymbol{Q}$, is in the form of

$$\{\sigma_1, \tau_{12}, \tau_{13}\}^T = \boldsymbol{Q}\{\varepsilon_1, \gamma_{12}, \gamma_{31}\}^T \tag{3.71}$$

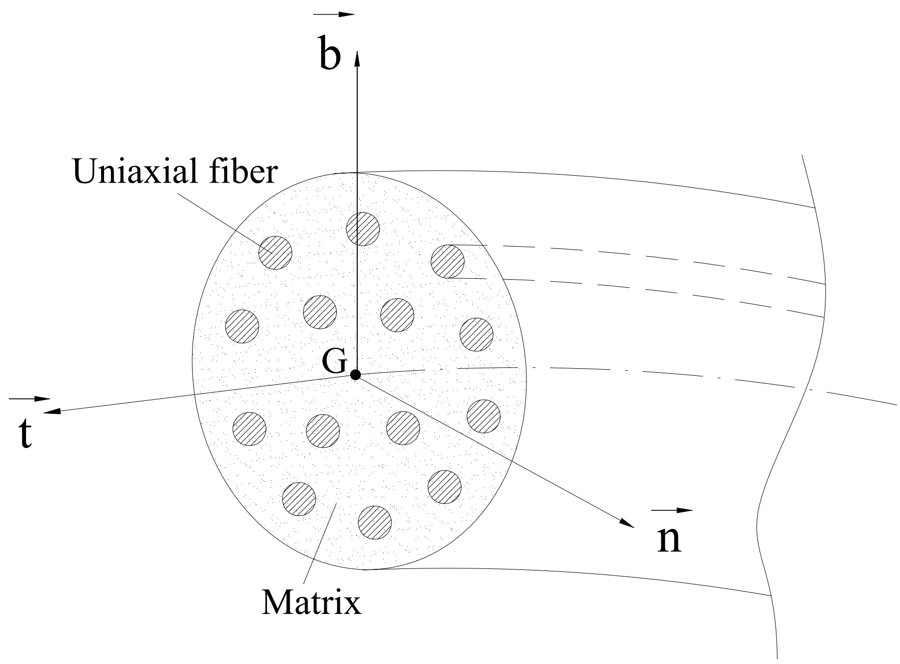

Figure 3.13 Unidirectional fibers along the helix axis.

For unidirectional fibers and transversely isotropic material, the reduced stiffness matrix becomes diagonal (Yıldırım, 1999)

$$\boldsymbol{Q} = \begin{bmatrix} Q_{11} & 0 & 0 \\ 0 & Q_{22} & 0 \\ 0 & 0 & Q_{33} \end{bmatrix} \tag{3.72}$$

where

$$Q_{11} = C_{11} + (C_{12}S_{12} + C_{13}S_{13}) / S_{11} \tag{3.73a}$$

$$Q_{22} = C_{66} \tag{3.73b}$$

$$Q_{33} = C_{55} \tag{3.73c}$$

As seen from equation (3.73), the elements of the reduced stiffness matrix, are achieved in terms of the elements of general three dimensional stiffness and compliance matrices, ***C*** and ***S***, respectively. In Equations (3.65)-(3.73), (***1,2,3***)axes are coincide with Frenet unit vectors (***t,n,b***) (Figure 3.13).

The axial, the shearing, the torsional and the bending rigidities for a transversely isotropic material can be defined as follows

$$C_t = Q_{11}A \tag{3.74a}$$

$$C_b = Q_{33}A \tag{3.74b}$$

$$D_b = Q_{11}I_b \tag{3.74c}$$

$$D_t = Q_{33}I_b + Q_{22}I_n \tag{3.74d}$$

Since $Q_{33} = Q_{22}$ for transversely isotropic material, the above can be generalized as

$$C_t = Q_{11}A \tag{3.75a}$$

$$C_b = \frac{Q_{22} A}{k_b} \tag{3.75b}$$

$$D_b = Q_{11} I_b \tag{3.75c}$$

$$D_t = Q_{22} (I_b + I_n) = Q_{22} I_0 = Q_{22} J_b \tag{3.75d}$$

where A is the undeformed cross-sectional area of the cross-section, I_n and I_b are the inertia moments about the normal and binormal axes, I_0 is the polar moment of inertia for circular sections. As stated before the torsional moment of inertia is defined for general closed sections having two symmetry axes by

$$J_b \cong \frac{1}{40} A^4 (I_n + I_b) \tag{3.76}$$

4. RESULTS AND DISCUSSION

In this study the following assumptions are used for obtaining the analytical expressions for isotropic and composite helical springs of arbitrary shapes

- ✓ The helix pitch angle is assumed to be constant along the helix.
- ✓ The centroid of the cross section and the shear center coincide.
- ✓ The material is homogeneous and linear.
- ✓ Warping and pre-twisting of the cross-section are neglected.
- ✓ (***n,b***) axes are principal inertia moment axes.
- ✓ The first order shear deformation theory called Timoshenko beam theory is used. That is shear deformations are considered in the formulation.
- ✓ Deformations are assumed to be infinitesimal.

4.1. Analytical Expressions for the Tip Deflection of the Spring

Analytical expressions given below may be used for

- ✓ All sections having double symmetry property.
- ✓ Isotropic and composite springs of unidirectional fibers.
- ✓ Both small and large constant helix pitch angles.

The axial, the shearing, the torsional and the bending rigidities for a transversely isotropic material can be defined as follows ($E=Q_{11}$ *and* $G=Q_{22}$)

$$C_t = EA = Q_{11}A$$

$$C_b = \frac{GA}{k_b} = \frac{Q_{22}A}{k_b}$$

$$D_t = GJ_b = Q_{22}J_b$$

$$D_b = EI_b = Q_{11}I_b \tag{4.1}$$

4.1.1. Cylindrical Helical Springs

$$f_{T_b} = \frac{2Pn\pi R\cos\alpha}{C_b} \tag{4.2a}$$

$$f_{T_t} = \frac{2Pn\pi R\sin\alpha\tan\alpha}{C_t} \tag{4.2b}$$

$$f_{M_b} = \frac{2Pn\pi R^3\sin\alpha\tan\alpha}{D_b} \tag{4.2c}$$

$$f_{M_t} = \frac{2Pn\pi R^3\cos\alpha}{D_t} \tag{4.2d}$$

4.1.2. Conical Helical Springs (*R_1=R_{max}*)

$$f_{T_b} = \frac{Pn\pi(R_1+R_2)\cos\alpha}{C_b} \tag{4.3a}$$

$$f_{T_t} = \frac{Pn\pi(R_1+R_2)\sin\alpha\tan\alpha}{C_t} \tag{4.3b}$$

$$f_{M_b} = \frac{Pn\pi(R_1^3+R_1^2R_2+R_1R_2^2+R_2^3)\sin\alpha\tan\alpha}{2D_b} \tag{4.3c}$$

$$f_{M_t} = \frac{Pn\pi(R_1^3+R_1^2R_2+R_1R_2^2+R_2^3)\cos\alpha}{2D_t} \tag{4.3d}$$

4.1.3. Barrel (R_1=R_{max}) and Hyperboloidal (R_2=R_{max}) Helical Springs

$$f_{T_b} = \frac{2Pn\pi(2R_1 + R_2)\cos\alpha}{3C_b} \tag{4.4a}$$

$$f_{T_t} = \frac{2Pn\pi(2R_1 + R_2)\sin\alpha\tan\alpha}{3C_t} \tag{4.4b}$$

$$f_{M_b} = \frac{2Pn\pi(16R_1^3 + 8R_1^2R_2 + 6R_1R_2^2 + 5R_2^3)\sin\alpha\tan\alpha}{35D_b} \tag{4.4c}$$

$$f_{M_t} = \frac{2Pn\pi(16R_1^3 + 8R_1^2R_2 + 6R_1R_2^2 + 5R_2^3)\cos\alpha}{35D_t} \tag{4.4d}$$

Equations (4.2-4.4) coincide with the formulas for vertical tip deflection given by Haktanır (1994).

The percent contribution of each stress resultant is defined by the division of each deflection due to related stress resultant by the total tip deflection.

4.2. Numerical Results for Isotropic Springs Having Circular Sections

Let reconsider equations (3.62) to study the variation of integrals with respect to the ratio (R_{min}/R_{max}) (See Appendix A).

$$f_{T_t} = \frac{P.n.\sin\alpha.\tan\alpha}{C_t}\int_0^{2\pi} R(\theta)d\theta = \frac{Pn\sin\alpha\tan\alpha}{C_t}(Integral\,1) \tag{4.5a}$$

$$f_{T_b} = \frac{P.n.\cos\alpha}{C_b}\int_0^{2\pi} R(\theta)d\theta = \frac{Pn\cos\alpha}{C_b}(Integral\,1) \tag{4.5b}$$

$$f_{M_b} = \frac{P.n.\sin\alpha.\tan\alpha}{D_b}\int_0^{2\pi} (R(\theta))^3 d\theta = \frac{Pn\sin\alpha\tan\alpha}{D_b}(Integral\,2) \tag{4.5c}$$

$$f_{M_t} = \frac{P.n.\cos\alpha}{D_t}\int_0^{2\pi} (R(\theta))^3 d\theta = \frac{Pn\cos\alpha}{D_t}(Integral\,2) \tag{4.5d}$$

As seen from the above equations tip deflection is proportional to the quantities (*Integral* 1) and (*Integral* 2) for the same spring. If the other properties are kept constant, the percent variation of those integrals with the ratio (R_{min}/R_{max}) will be in the form of in Figure (4.1). In this figure the maximum radius of the cylinder is taken as unity. $R_{min}/R_{max}=1$ corresponds to the cylindrical helical spring.

Increasing the ratio of R_{min}/R_{max} increases the numerical value of those integrals. This means that the tip deflection increases since the total length of the wire increases. The cylindrical helical spring has the maximum wire length. The deflection is given as hyperboloidal, conical, barrel, and cylindrical in ascending order. Stated in another words, among the springs having the same value of D_{max}, hyperboloidal type is stronger one.

For non-cylindrical helical springs the spring index is defined as

$$C = \frac{D_{\max}}{d} = \frac{2R_{\max}}{d} \tag{4.6}$$

The geometric and material properties of the spring considered in this section are as follows (İnan, 1967):

$$k_b = 1.1\,(circular)$$
$$k_b = 1.2\,(square)$$
$$G = 800000\ kg_f / cm^2$$
$$P = 150\ kg_f$$
$$n = 18$$
$$\nu = 0.3$$
$$d = 1.85 = const$$

$$R_{\max} = \frac{Cd}{2}$$
$$C = 3,4,..15$$
$$\frac{R_{\min}}{R_{\max}} = 0.1 - 0.9$$
$$\alpha = 10^o - 40^o$$
$$I_b = \frac{\pi\, r^4}{4} = \frac{\pi d^4}{64}(circular)$$
$$J_b = I_0 = \frac{\pi\, r^4}{2} = \frac{\pi d^4}{32}(circular)$$

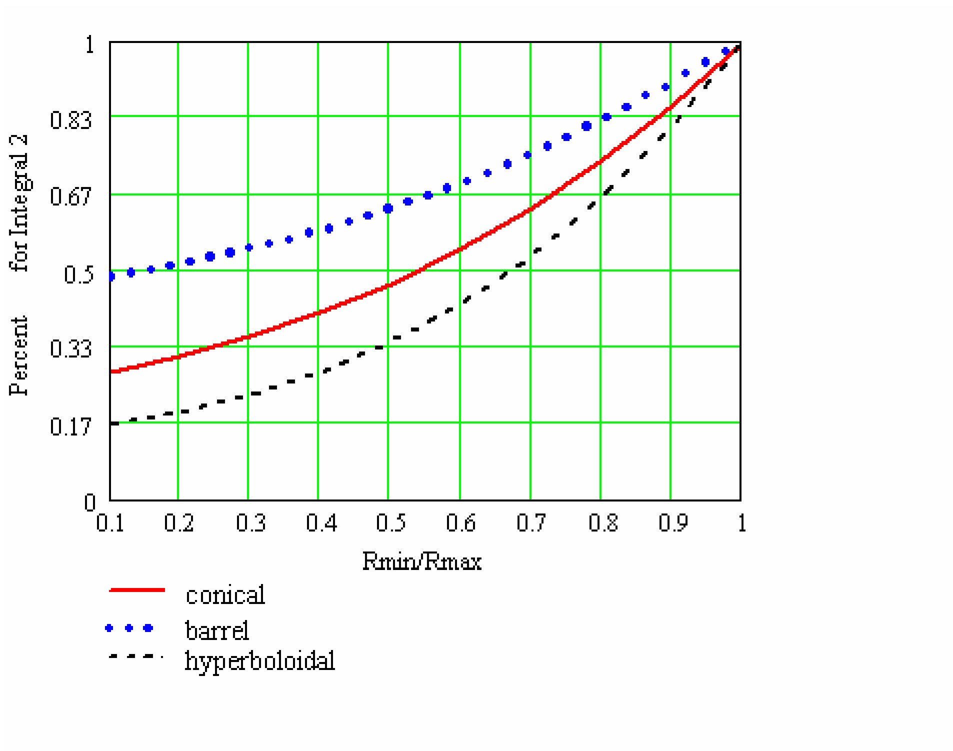

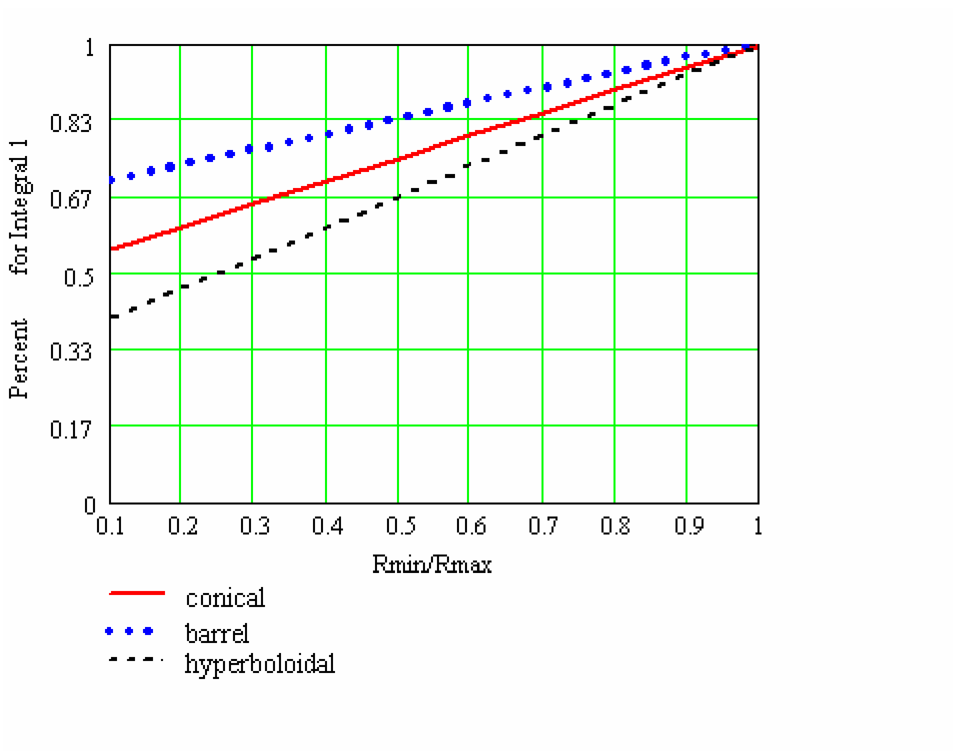

Figure 4.1. Percent variations of the integrals in equation (3.62) with respect to (R_{min}/R_{max})

4.2.1. Cylindrical Helical Springs

The percent effect of the stress resultants on the tip deflection of the cylindrical helical compression spring is shown in Figures (4.2) and (4.3) (See Appendix B). From those figures the followings may be written.

The effect of the axial force on the tip deflection (Figure 4.2):

- ✓ Increasing the helix angle results an apparent increase in the percent contribution of the axial force on the tip deflection of the spring.
- ✓ Increasing the spring index decreases the percent contribution of the axial force on the tip deflection of the cylindrical helical spring.
- ✓ For small spring indices *($C=3$)* and large helix pitch angles *($\alpha=40^o$)*, the effect of the axial force on the tip deflection is about 1%.

The effect of the shearing force on the tip deflection (Figure 4.2):

- ✓ Increasing the helix angle results a decrease in the percent contribution of the shearing force on the tip deflection of the spring.
- ✓ Increasing the spring index decreases the percent contribution of the shearing force on the tip deflection of the cylindrical helical spring.
- ✓ For small spring indices *($C=3$)* and small helix pitch angles *($\alpha=10^o$)*, the effect of the shearing force on the tip deflection is less than 6%.

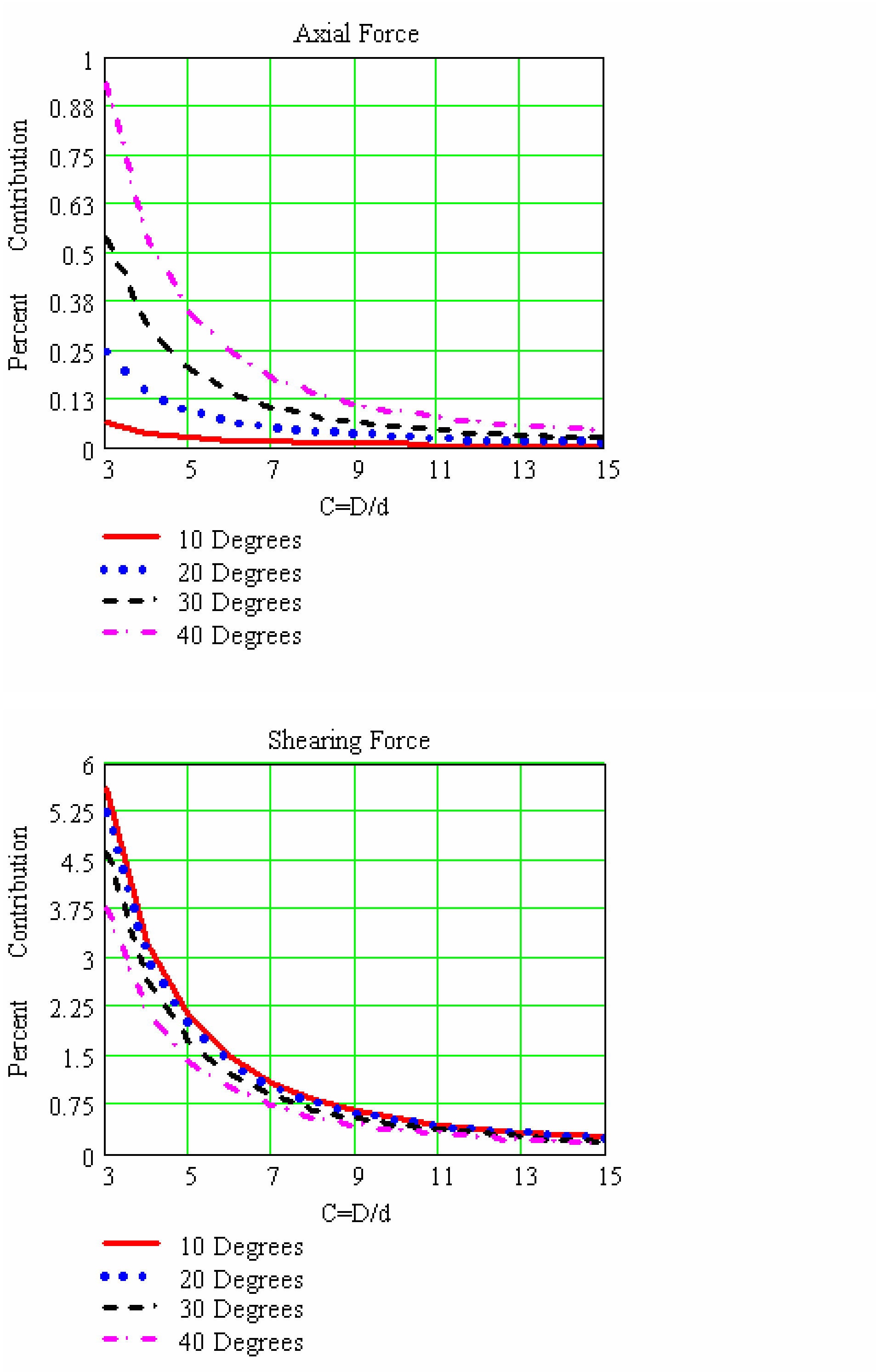

Figure 4.2. Percent contributions of axial and shearing forces on the total deflection of cylindrical isotropic spring

The effect of the bending moment on the tip deflection (Figure 4.3):

- ✓ Increasing the helix angle results a visible increase in the percent contribution of the bending moment on the tip deflection of the spring.
- ✓ Increasing the spring index increases very little by little the percent contribution of the bending moment on the tip deflection of the cylindrical helical spring. It may be concluded that the value of the spring index almost does not affect the numerical value of the tip deflection for $C \geq 5$.
- ✓ For large helix pitch angles *(α=40^o)*, the effect of the bending moment on the tip deflection is about 35%. For α=*10^o* this value is about 2-2.5%.

The effect of the torsional moment on the tip deflection (Figure 4.3):

- ✓ Increasing the helix angle results a noticeable decrease in the percent contribution of the torsional moment on the tip deflection of the spring.
- ✓ Increasing the spring index increases very slightly the percent contribution of the torsional moment on the tip deflection of the cylindrical helical spring. It may be concluded that the value of the spring index almost the same for $C \geq 10$.
- ✓ For small helix pitch angles *(α=10^o)*, the effect of the bending moment on the tip deflection is about 97.5%. For α=*40^o* this value is about 65%.

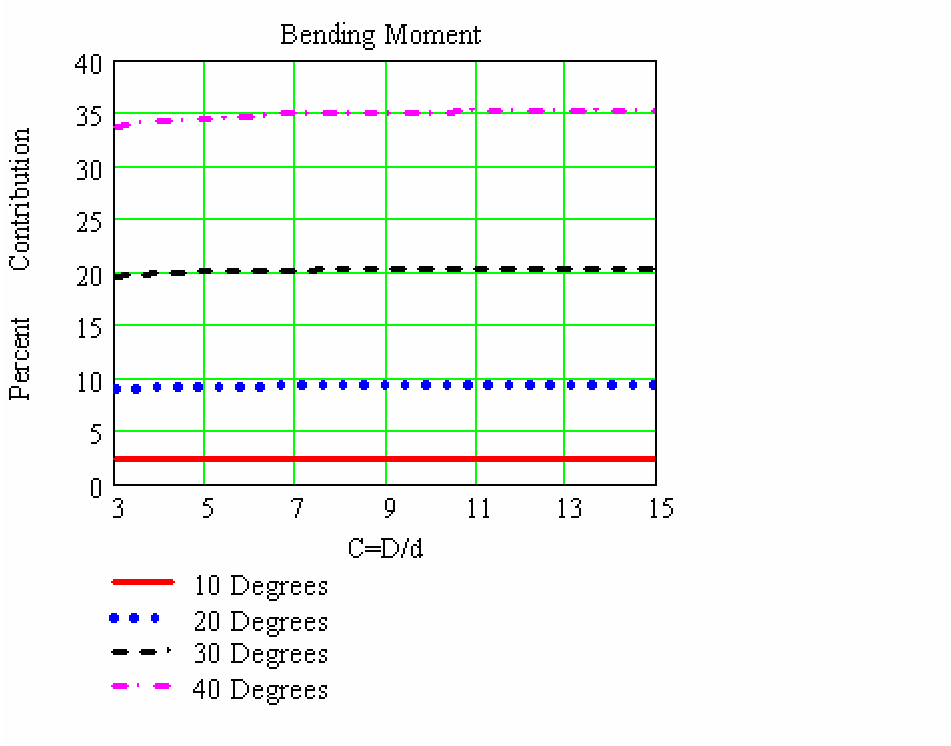

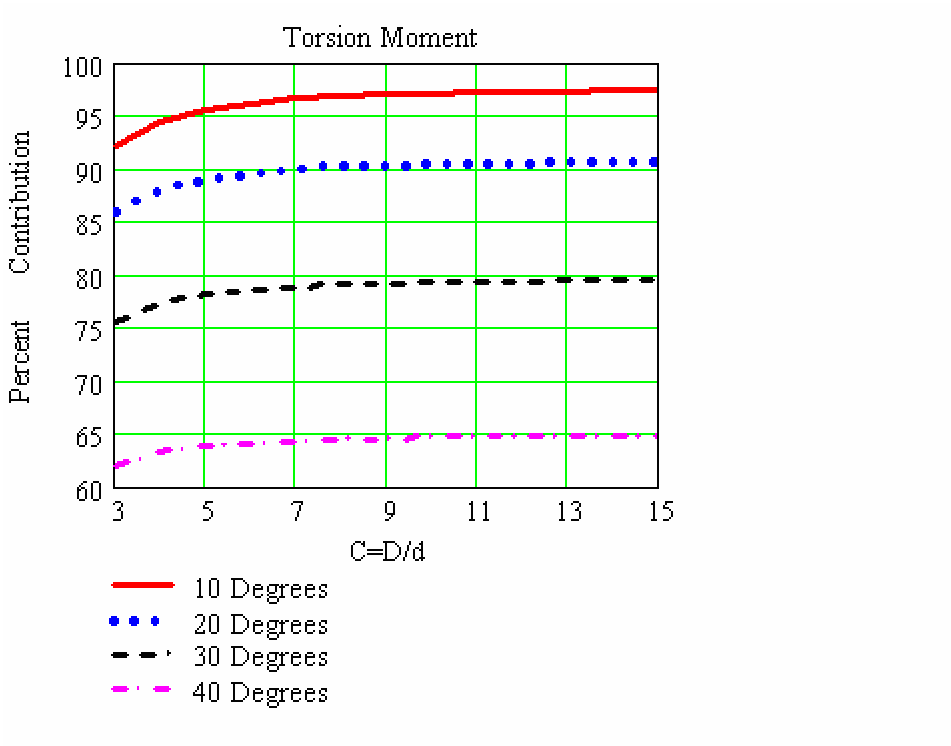

Figure 4.3. Percent contributions of bending and torsional moments on the total deflection of cylindrical isotropic spring

4.2.2. Conical Helical Springs

The percent effect of the stress resultants on the tip deflection of the conical helical compression spring is shown in Figures (4.4-4.7). From those figures the followings may be drawn (See also Appendix C).

The effect of the axial force on the tip deflection (Figure 4.4):

- ✓ Increasing the helix angle results an apparent increase in the percent contribution of the axial force on the tip deflection of the conical spring.
- ✓ Increasing the spring index decreases the percent contribution of the axial force on the tip deflection of the conical spring.
- ✓ Increasing the ratio R_{min}/R_{max} decreases those effects.
- ✓ For small spring indices *(C=3)*, for small ratio R_{min}/R_{max} and large helix pitch angles $(\alpha=40^o)$, the effect of the axial force on the tip deflection is about 1.8% while this value is almost 1% for cylindrical helical springs.
- ✓ The percent contribution of the axial force acting on the conical springs is greater than the cylindrical ones.

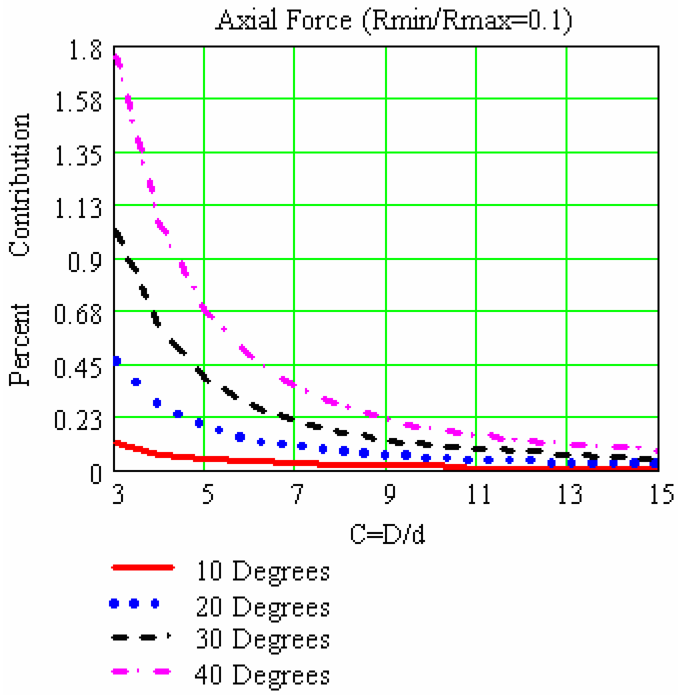

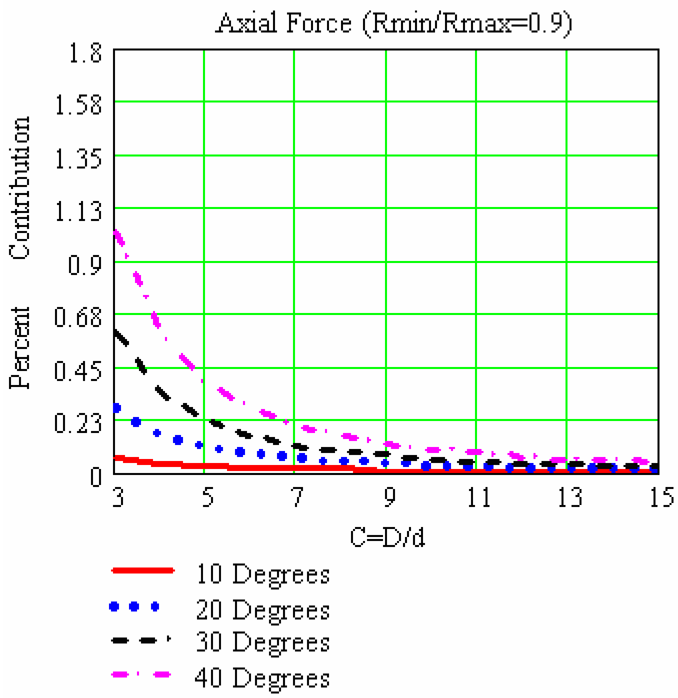

Figure 4.4. Percent contribution of axial force on the total deflection of conical isotropic spring

The effect of the shearing force on the tip deflection (Figure 4.5):

- ✓ Increasing the helix angle results a decrease in the percent contribution of the shearing force on the tip deflection of the conical spring.
- ✓ Increasing the spring index decreases the percent contribution of the shearing force on the tip deflection of the conical spring. For $C \geq 10$ the percent contribution is less than 1%.
- ✓ Increasing the ratio R_{min}/R_{max} decreases those effects.
- ✓ For small spring indices *(C=3),* for small ratio R_{min}/R_{max} and small helix pitch angles $(\alpha=10^o)$, the effect of the shearing force on the tip deflection is less than 11% while this value is almost 6% for cylindrical helical springs.

The effect of the bending moment on the tip deflection (Figure 4.6):

- ✓ Increasing the helix angle results a visible increase in the percent contribution of the bending moment on the tip deflection of the conical spring.
- ✓ Increasing the spring index increases very slowly the percent contribution of the bending moment on the tip deflection of the conical helical spring. It may be concluded that the value of the spring index almost does not affect the numerical value of the tip deflection for $C \geq 7$.
- ✓ Increasing the ratio R_{min}/R_{max} increases very slightly those effects especially for small helix indices.
- ✓ For large helix pitch angles $(\alpha=40^o)$, for large ratio R_{min}/R_{max} the effect of the bending moment on the tip deflection is about 35%. For $\alpha=10^o$ this value is about 2-2.5%.
- ✓ In general the effect of the bending moment on the tip deflection is not very changed with the types of helices for $C \geq 7$.

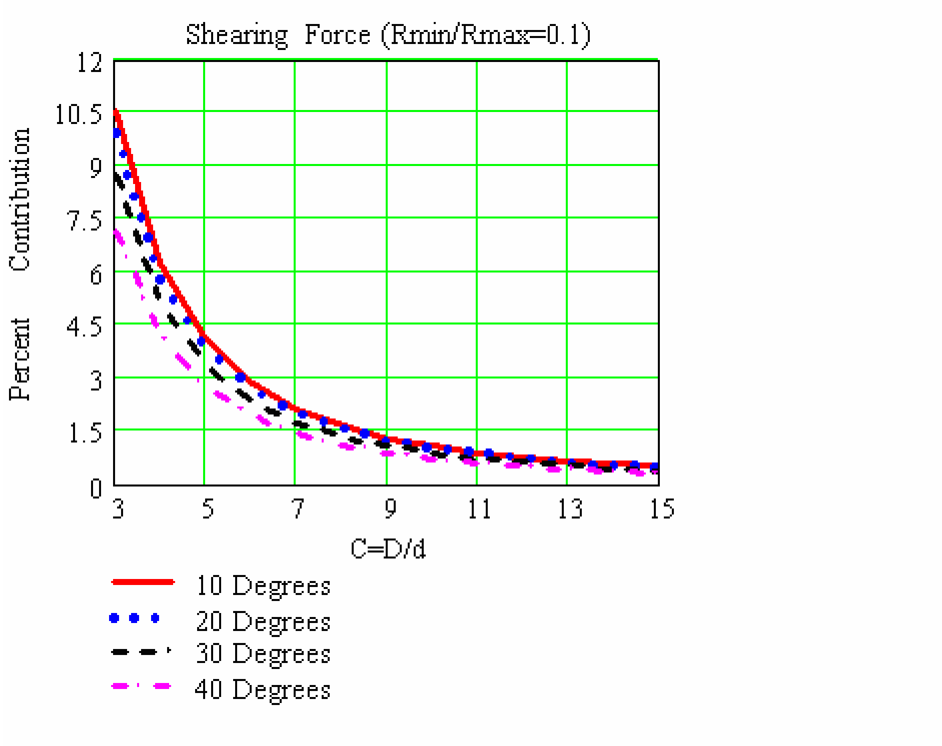

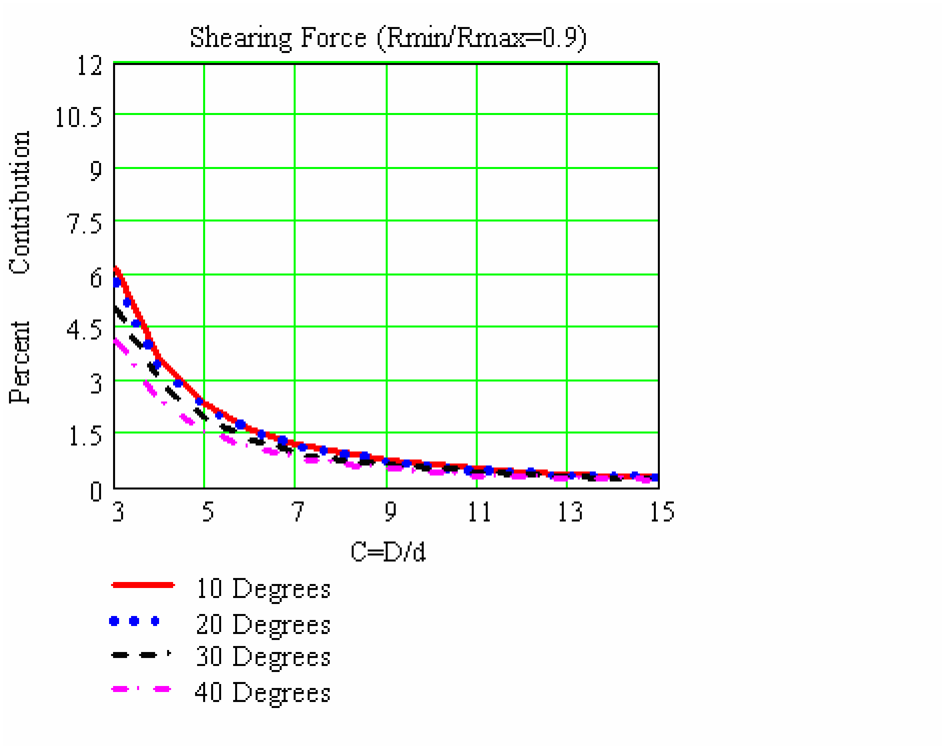

Figure 4.5. Percent contribution of shearing force on the total deflection of conical isotropic spring

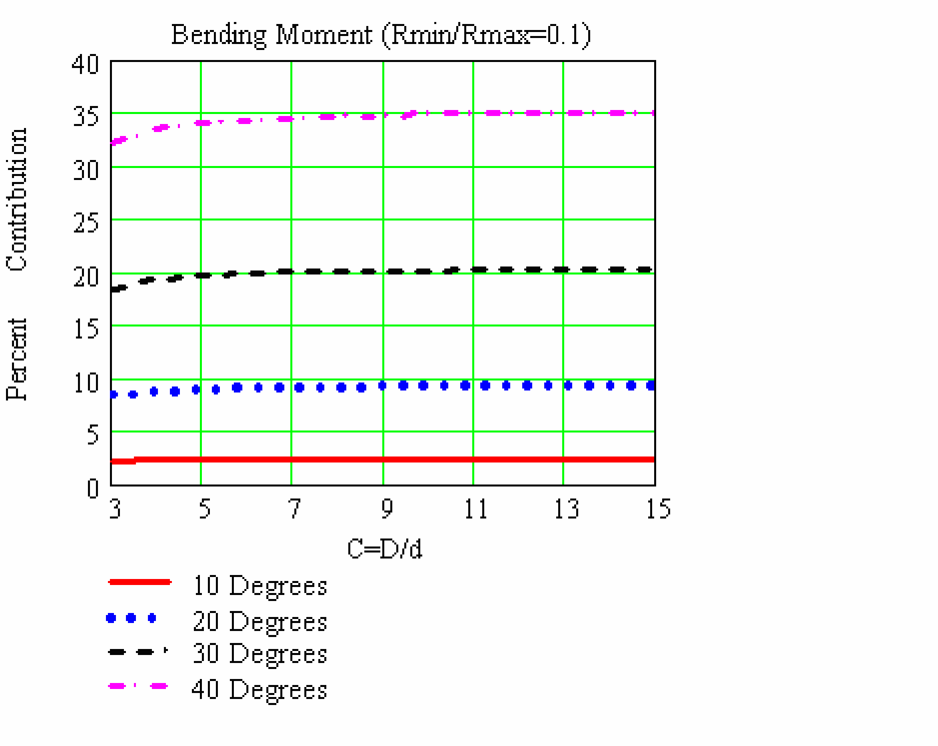

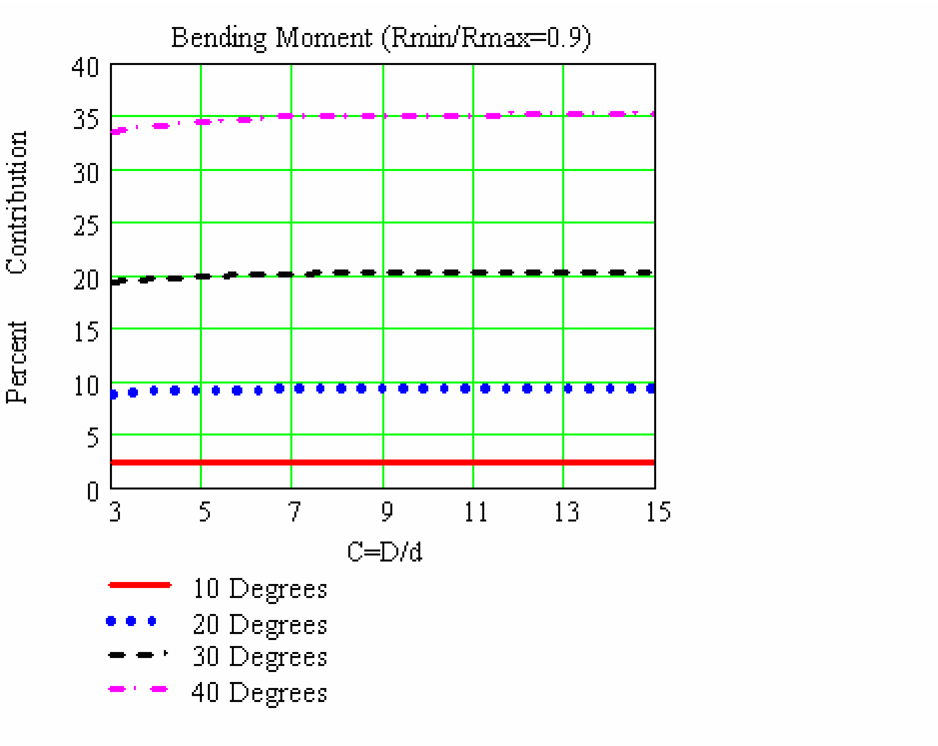

Figure 4.6. Percent contribution of bending moment on the total deflection of conical isotropic spring

The effect of the torsional moment on the tip deflection (Figure 4.7):

- ✓ Increasing the helix angle results a noticeable decrease in the percent contribution of the torsional moment on the tip deflection of the conical spring.
- ✓ Increasing the spring index increases very slowly the percent contribution of the torsional moment on the tip deflection of the conical helical spring. It may be concluded that the value of the spring index almost the same for $C \geq 10$.
- ✓ Increasing the ratio R_{min}/R_{max} increases very slightly those effects especially for small helix indices.
- ✓ For small helix pitch angles $(\alpha=10^o)$, for large ratio R_{min}/R_{max} the effect of the torsional moment on the tip deflection is about 97.5%. For $\alpha=40^o$ this value is about 65%.
- ✓ In general the effect of the torsional moment on the tip deflection is not mainly changed with the types of helices for $C \geq 10$.

4.2.3. Barrel Helical Springs

The percent effect of the stress resultants on the tip deflection of the barrel helical compression spring is shown in Figures (4.8-4.11). From those figures the followings may be stated (See also Appendix D).

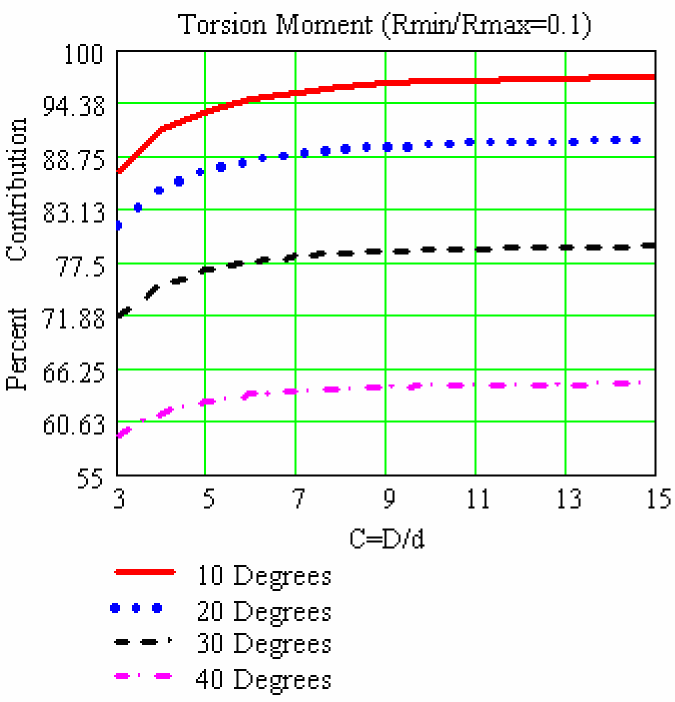

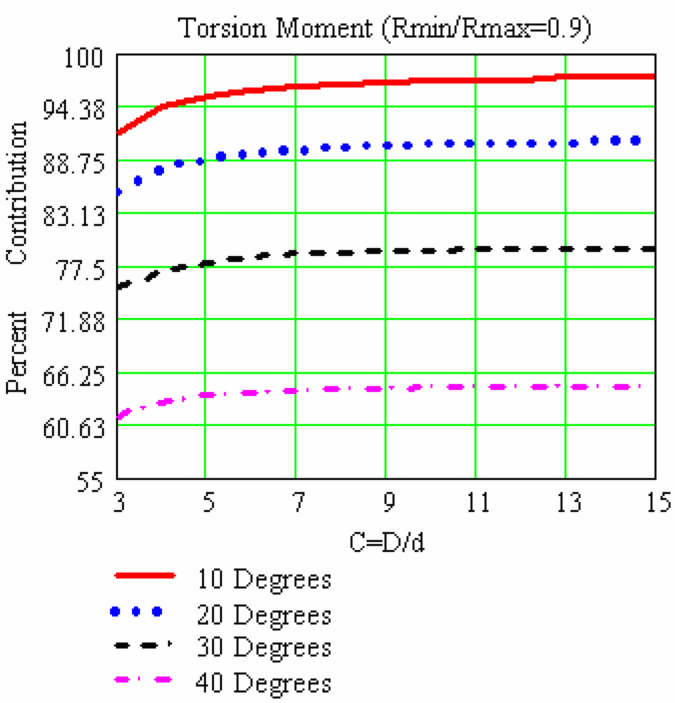

Figure 4.7. Percent contribution of torsional moment on the total deflection of conical isotropic spring

The effect of the axial force on the tip deflection (Figure 4.8):

- ✓ Increasing the helix angle results an obvious increase in the percent contribution of the axial force on the tip deflection of the barrel spring.
- ✓ Increasing the spring index decreases the percent contribution of the axial force on the tip deflection of the barrel spring.
- ✓ Increasing the ratio R_{min}/R_{max} decreases those effects.
- ✓ For small spring indices *(C=3),* for small ratio R_{min}/R_{max} and large helix pitch angles $(\alpha=40^o)$, the effect of the axial force on the tip deflection is about 1.4% while this value is almost 1% for cylindrical helical springs and 1.8% for conical springs.
- ✓ The percent contribution of the axial force acting on the barrel springs is greater than the cylindrical ones and less than the conical springs.

The effect of the shearing force on the tip deflection (Figure 4.9):

- ✓ Increasing the helix angle results a decrease in the percent contribution of the shearing force on the tip deflection of the barrel spring.
- ✓ Increasing the spring index decreases the percent contribution of the shearing force on the tip deflection of the barrel spring. For $C \geq 10$ the percent contribution is less than 1%.
- ✓ Increasing the ratio R_{min}/R_{max} decreases those effects.
- ✓ For small spring indices *(C=3),* for small ratio R_{min}/R_{max} and small helix pitch angles $(\alpha=10^o)$, the effect of the shearing force on the tip deflection is less than 8% while this value is almost 6% for cylindrical helical springs and while this value is almost 11% for conical helical springs.

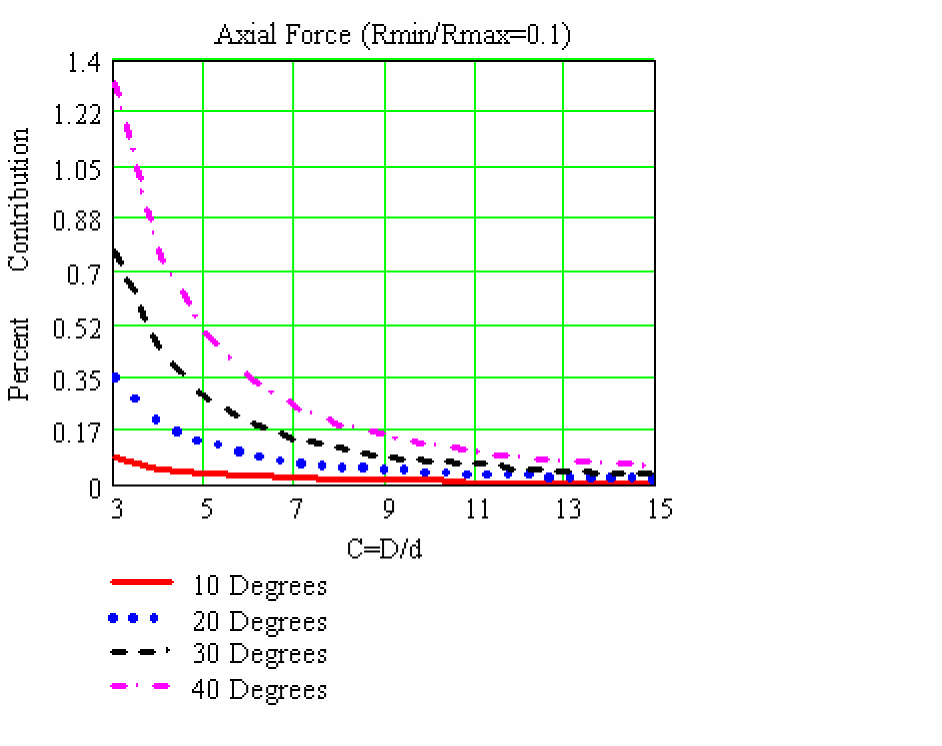

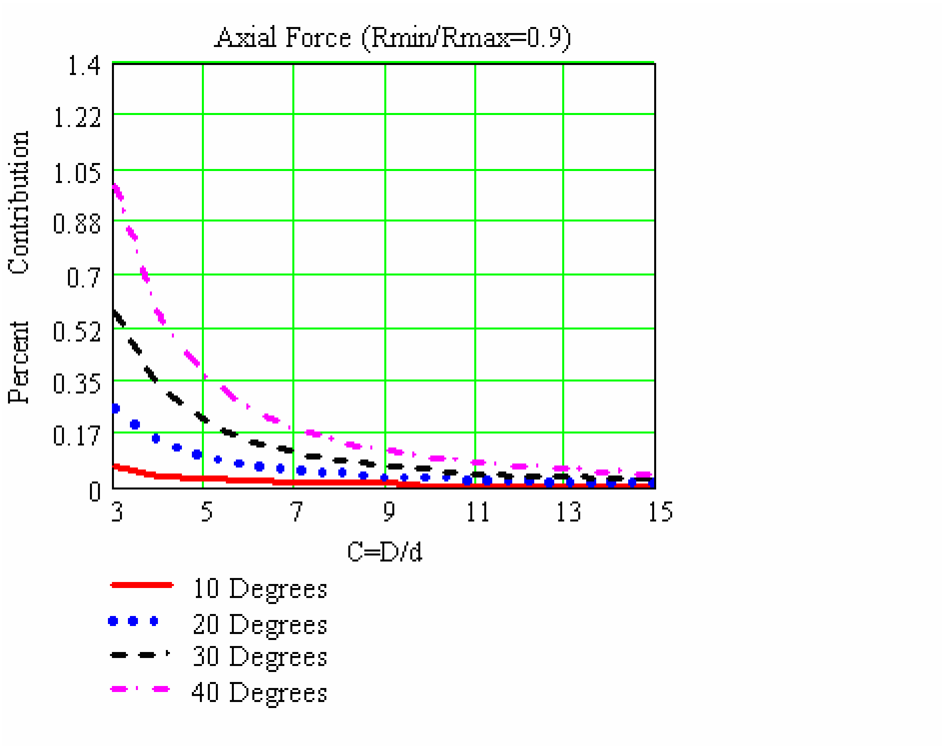

Figure 4.8. Percent contribution of axial force on the total deflection of barrel isotropic spring

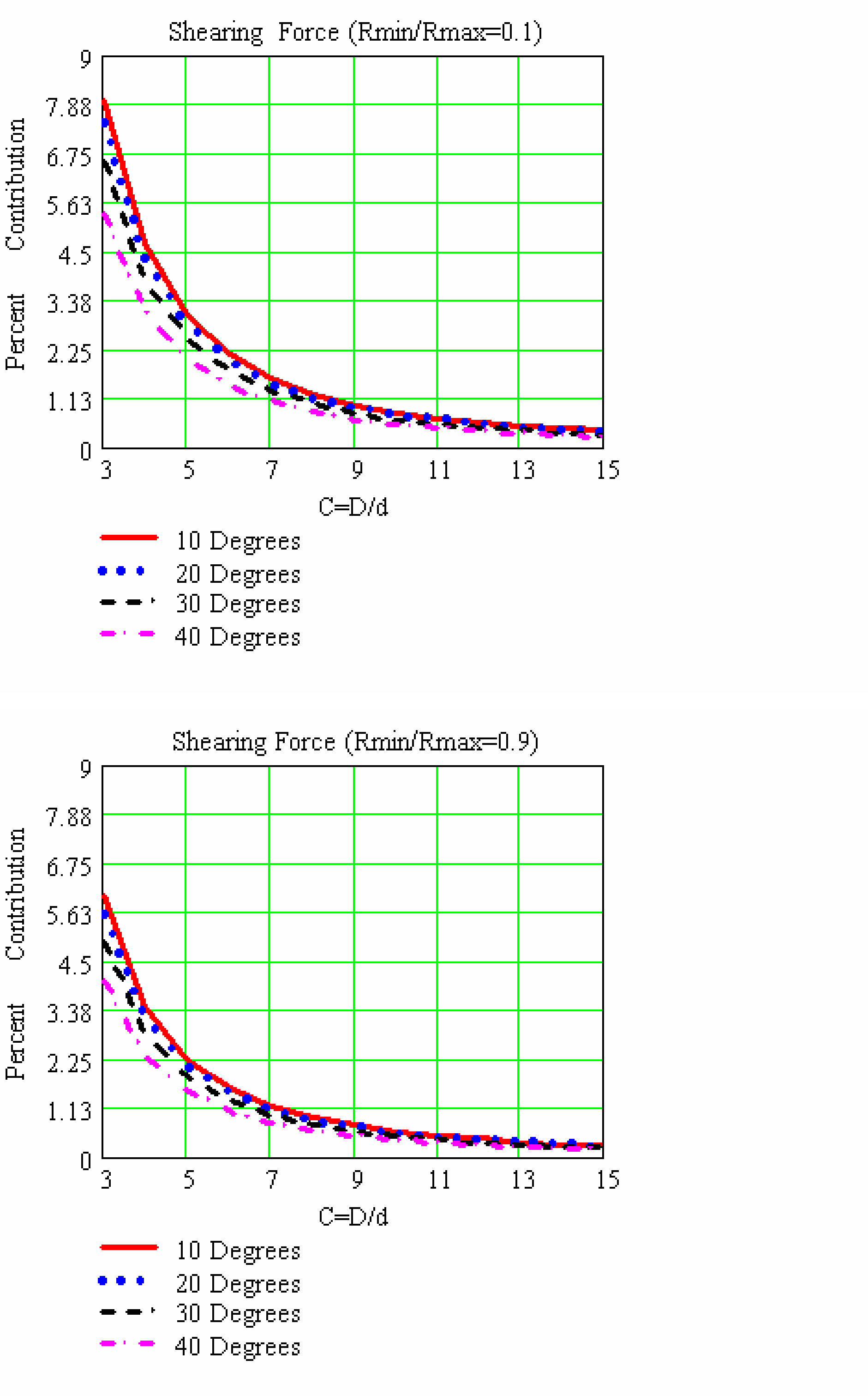

Figure 4.9. Percent contribution of shearing force on the total deflection of barrel isotropic spring

The effect of the bending moment on the tip deflection (Figure 4.10):

- ✓ Increasing the helix angle results a noticeable increase in the percent contribution of the bending moment on the tip deflection of the barrel spring.
- ✓ Increasing the spring index increases very slowly the percent contribution of the bending moment on the tip deflection of the barrel helical spring. It may be concluded that the value of the spring index almost does not affect the numerical value of the tip deflection for $C \geq 7$.
- ✓ Increasing the ratio R_{min}/R_{max} increases very slightly those effects especially for small helix indices.
- ✓ For large helix pitch angles $(\alpha=40^o)$, for large ratio R_{min}/R_{max} the effect of the bending moment on the tip deflection is about 35%. For $\alpha=10^o$ this value is about 2-2.5%.
- ✓ In general the effect of the bending moment on the tip deflection is not very changed with the types of isotropic helices for $C \geq 7$.

The effect of the torsional moment on the tip deflection (Figure 4.11):

- ✓ Increasing the helix angle results a noticeable decrease in the percent contribution of the torsional moment on the tip deflection of the barrel spring.
- ✓ Increasing the spring index increases very slowly the percent contribution of the torsional moment on the tip deflection of the barrel helical spring. It may be concluded that the value of the spring index almost the same for $C \geq 10$.
- ✓ Increasing the ratio R_{min}/R_{max} increases very slightly those effects especially for small helix indices.
- ✓ For small helix pitch angles $(\alpha=10^o)$, for large ratio R_{min}/R_{max} the effect of the torsional moment on the tip deflection is about 97.5%. For $\alpha=40^o$ this value is about 65%.
- ✓ In general the effect of the torsional moment on the tip deflection is not mainly changed with the types of isotropic helices for $C \geq 10$.

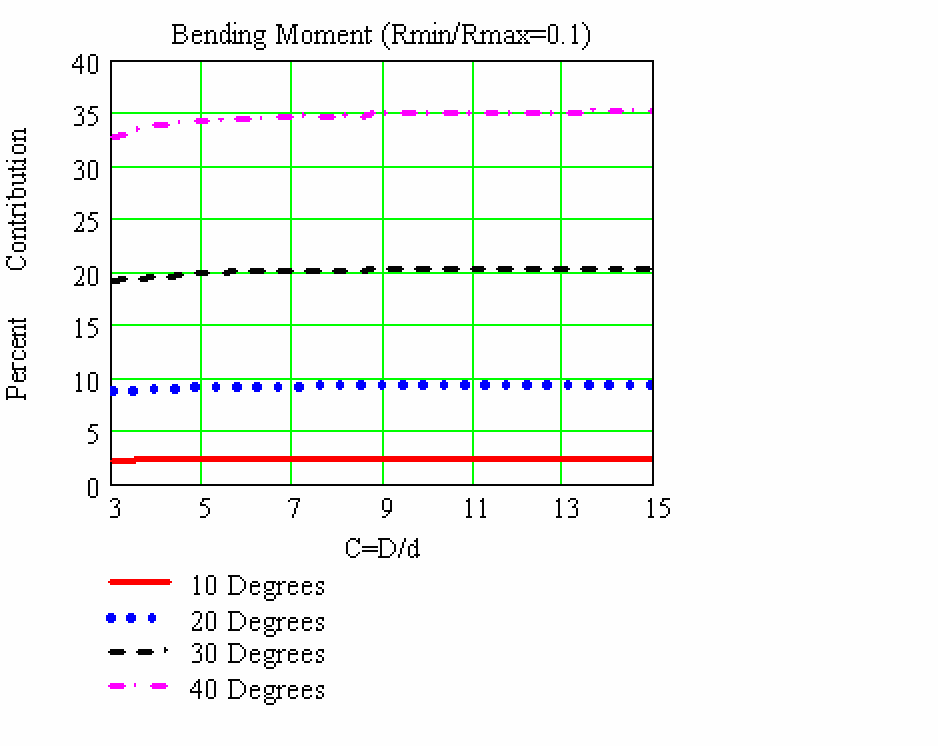

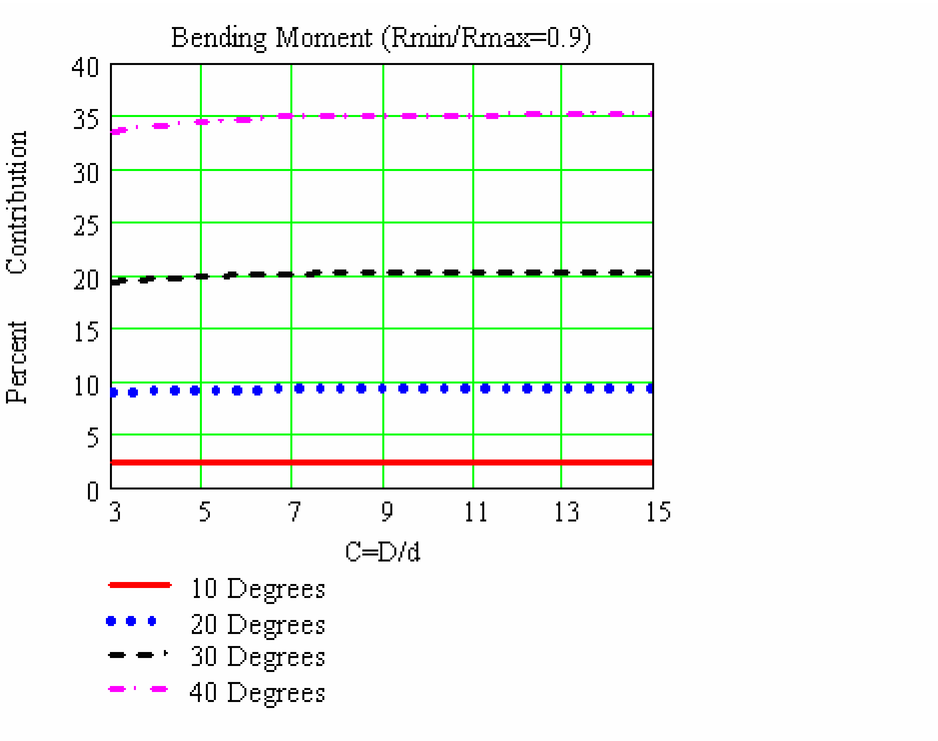

Figure 4.10. Percent contribution of bending moment on the total deflection of barrel isotropic spring

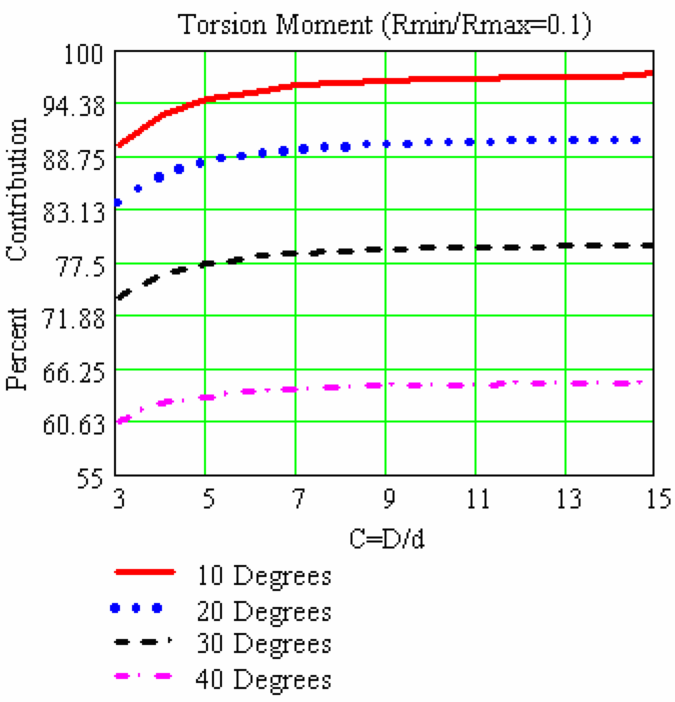

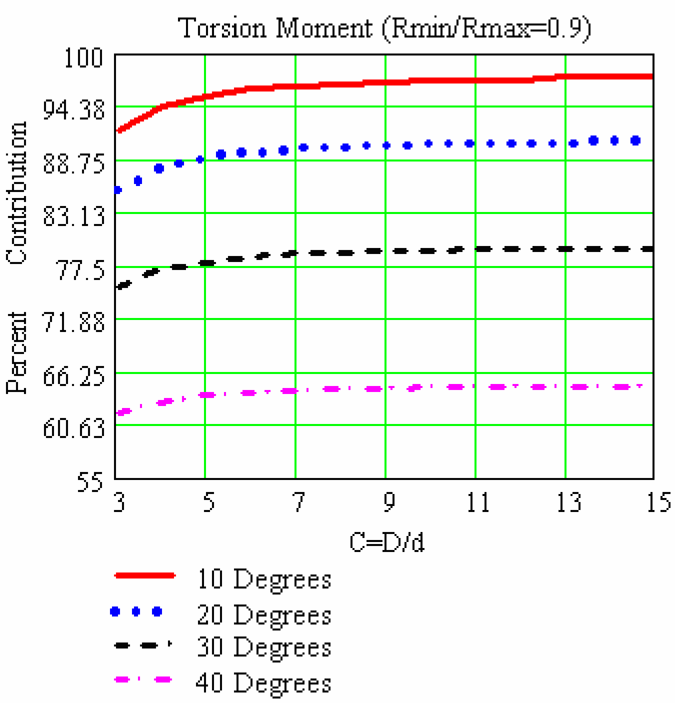

Figure 4.11 Percent contribution of torsional moment on the total deflection of barrel isotropic spring

4.2.4. Hyperboloidal Helical Springs

The percent effect of the stress resultants on the tip deflection of the hyperboloidal helical compression spring is shown in Figures (4.12-4.15). From those figures the followings may be concluded (See also Appendix E).

The effect of the axial force on the tip deflection (Figure 4.12):

- ✓ Increasing the helix angle results an obvious increase in the percent contribution of the axial force on the tip deflection of the hyperboloidal spring.
- ✓ Increasing the spring index decreases the percent contribution of the axial force on the tip deflection of the hyperboloidal spring.
- ✓ Increasing the ratio R_{min}/R_{max} decreases those effects.
- ✓ For small spring indices *(C=3)*, for small ratio R_{min}/R_{max} and large helix pitch angles (α=40^o), the effect of the axial force on the tip deflection is about 2.2% while this value is almost 1% for cylindrical helical springs, and while this value is almost 1.8 for conical helical springs and while this value is almost 1.4% for barrel helical springs.
- ✓ The percent contribution of the axial force acting on the hyperboloidal springs is greater than all other types of helices.

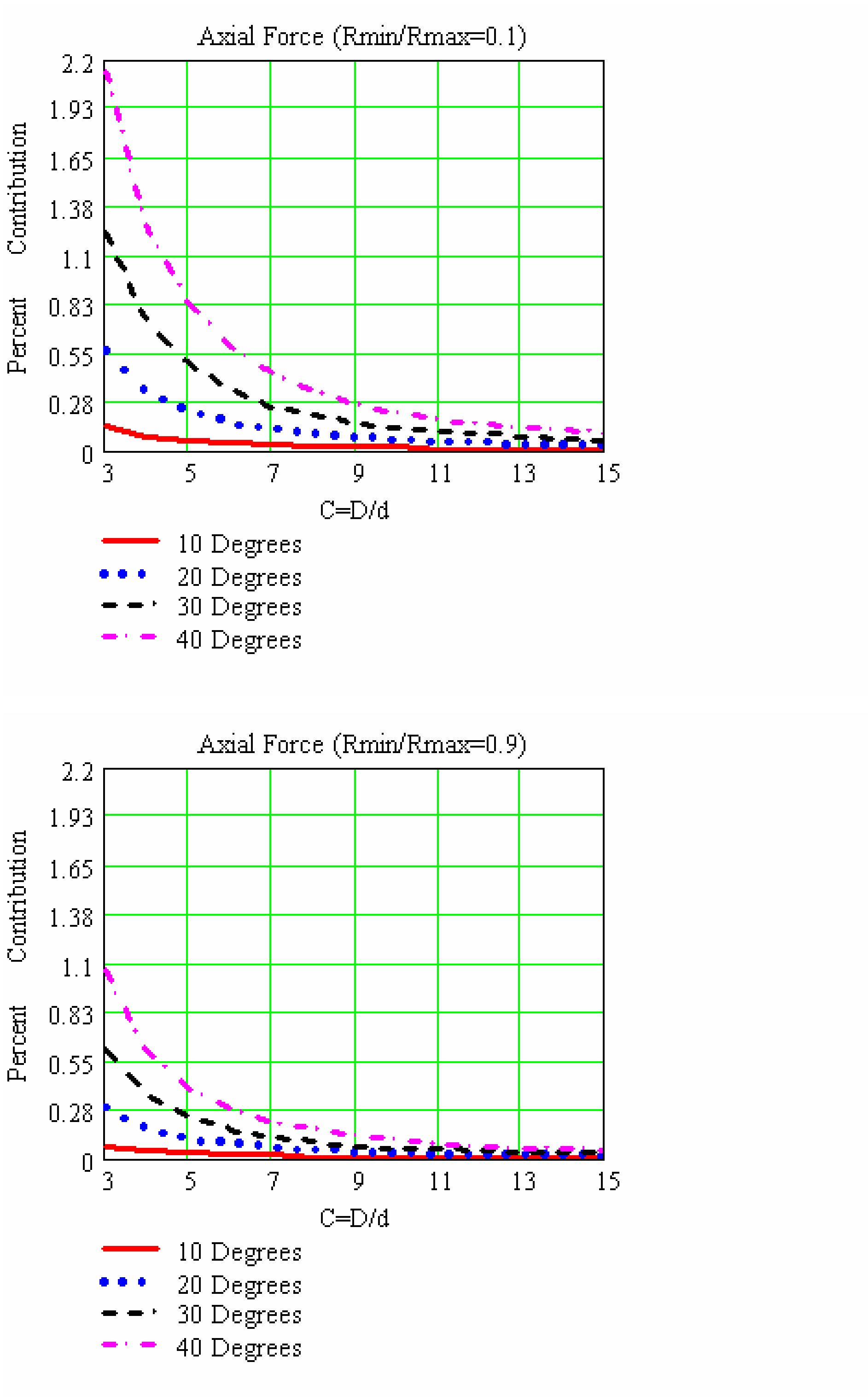

Figure 4.12. Percent contribution of axial force on the total deflection of hyperboloidal isotropic spring

The effect of the shearing force on the tip deflection (Figure 4.13):

- ✓ Increasing the helix angle results a decrease in the percent contribution of the shearing force on the tip deflection of the hyperboloidal spring.
- ✓ Increasing the spring index decreases the percent contribution of the shearing force on the tip deflection of the hyperboloidal spring. For $C \geq 10$ the percent contribution is less than 1%.
- ✓ Increasing the ratio R_{min}/R_{max} decreases those effects.
- ✓ For small spring indices *(C=3),* for small ratio R_{min}/R_{max} and small helix pitch angles ($\alpha=10^o$), the effect of the shearing force on the tip deflection is less than 13% while this value is almost 6% for cylindrical helical springs, while this value is almost 11% for conical helical springs, and while this value is almost 8% for barrel helical springs.
- ✓ The percent contribution of the shearing force acting on the hyperboloidal springs is greater than all other types of helices.

The effect of the bending moment on the tip deflection (Figure 4.14):

- ✓ Increasing the helix angle results a noticeable increase in the percent contribution of the bending moment on the tip deflection.
- ✓ Increasing the spring index increases very slightly the percent contribution of the bending moment on the tip deflection. It may be concluded that the value of the spring index almost does not affect the numerical value of the tip deflection for $C \geq 7$.
- ✓ Increasing the ratio R_{min}/R_{max} increases very slowly those effects especially for small helix indices.
- ✓ For large helix pitch angles ($\alpha=40^o$), for large ratio R_{min}/R_{max} the effect of the bending moment on the tip deflection is about 35%. For $\alpha=10^o$ this value is about 2-2.5%. In general the effect of the bending moment on the tip deflection is not very changed with the types of helices for $C \geq 7$.

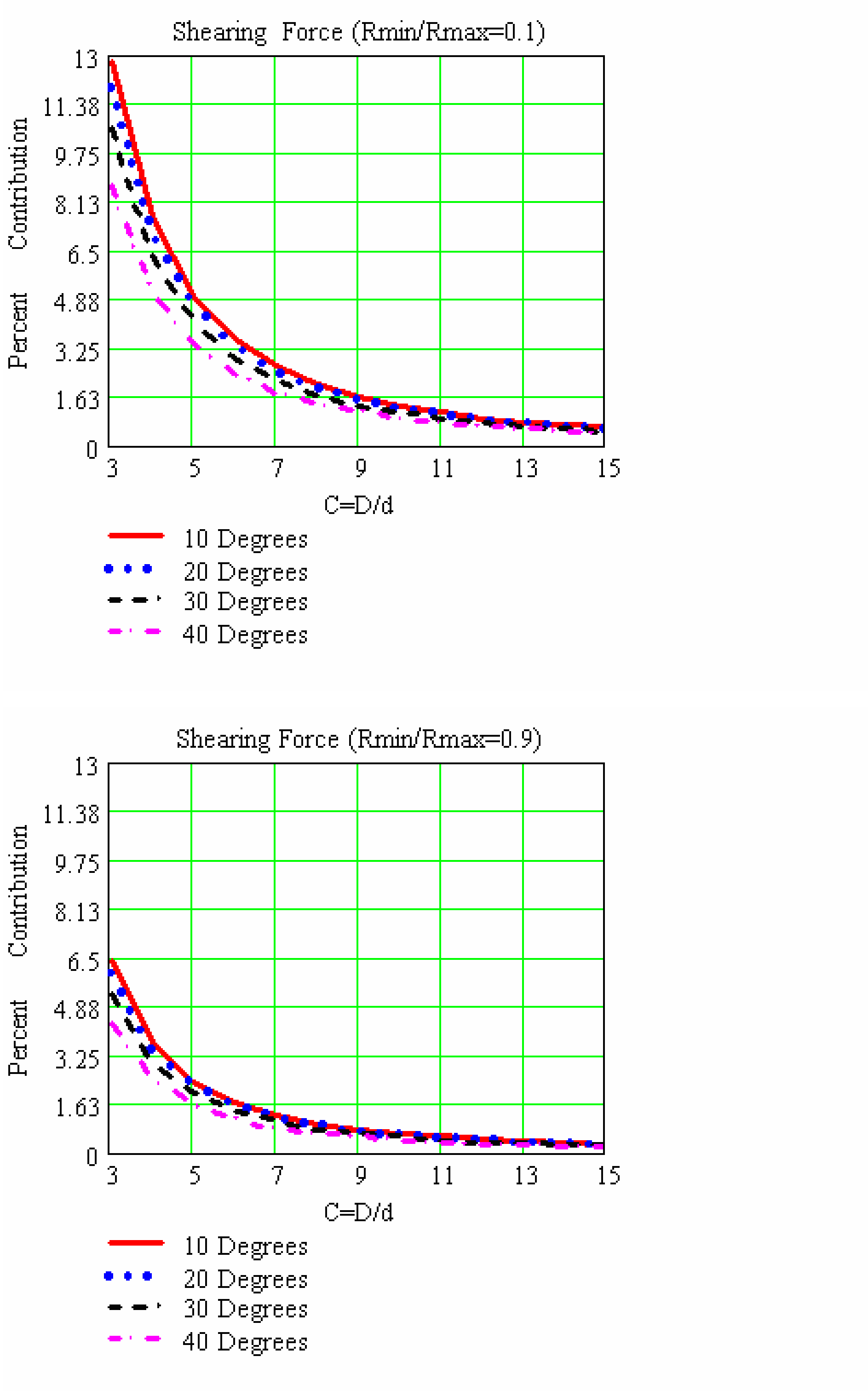

Figure 4.13. Percent contribution of shearing force on the total deflection of hyperboloidal isotropic spring

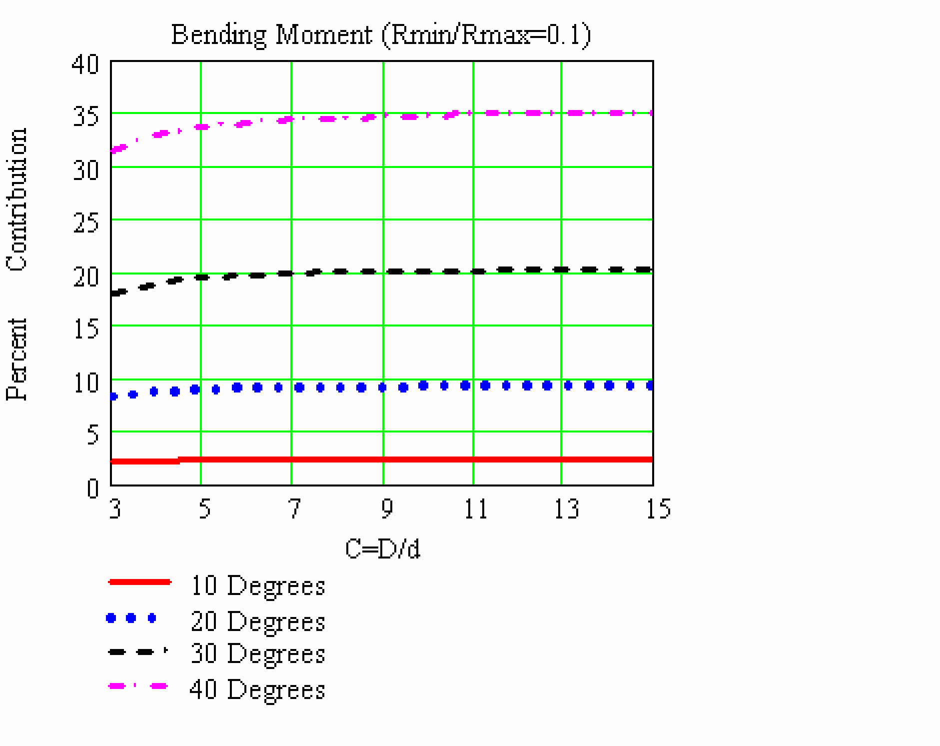

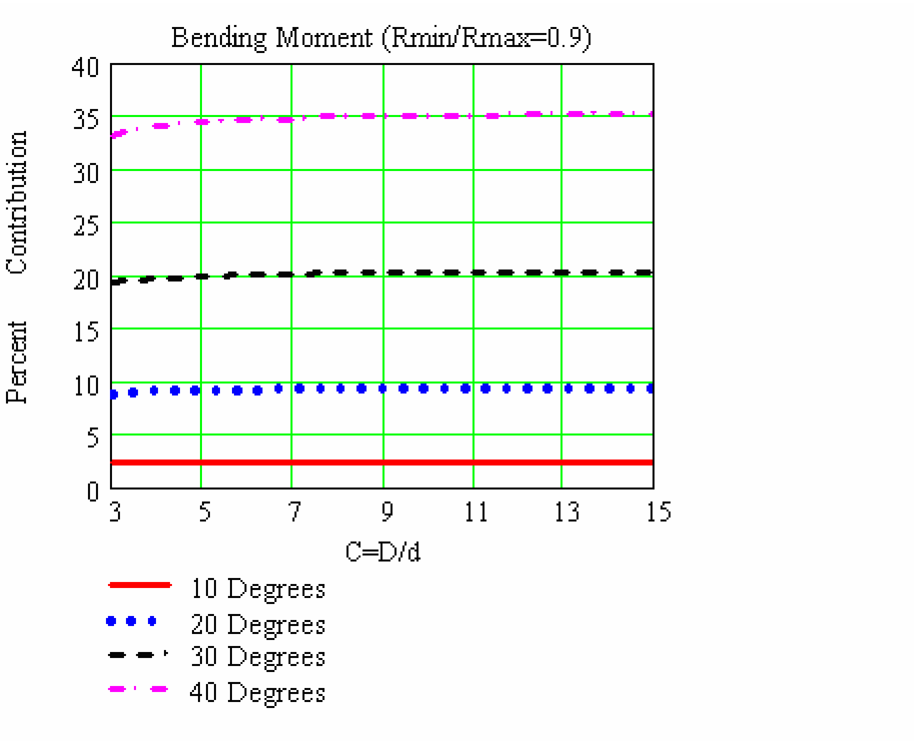

Figure 4.14. Percent contribution of bending moment on the total deflection of hyperboloidal isotropic spring

The effect of the torsional moment on the tip deflection (Figure 4.15):

- ✓ Increasing the helix angle results a noticeable decrease in the percent contribution of the torsional moment on the tip deflection of the hyperboloidal type spring.
- ✓ Increasing the spring index increases slowly the percent contribution of the torsional moment on the tip deflection of the hyperboloidal helical spring. It may be concluded that the value of the spring index almost the same for $C \geq 10$.
- ✓ Increasing the ratio R_{min}/R_{max} increases very slightly those effects especially for small helix indices.
- ✓ For small helix pitch angles $(\alpha=10^o)$, for large ratio R_{min}/R_{max} the effect of the torsional moment on the tip deflection is about 97.5%. For $\alpha=40^o$ this value is about 65%.
- ✓ In general the effect of the torsional moment on the tip deflection is not mainly changed with the types of helices for $C \geq 10$.

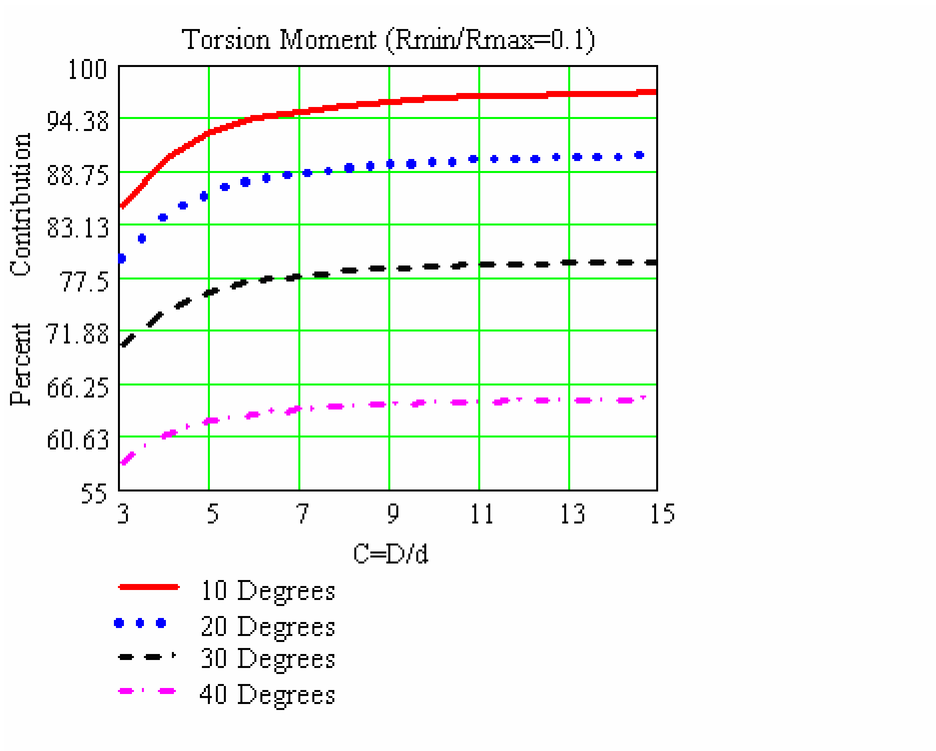

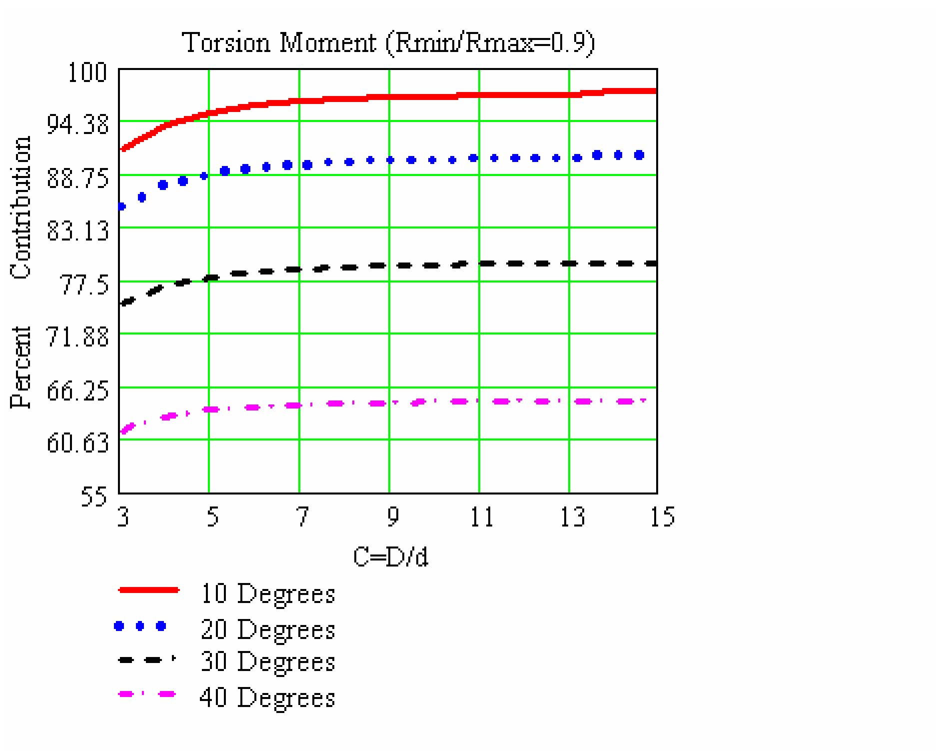

Figure 4.15. Percent contribution of torsional moment on the total deflection of hyperboloidal isotropic spring

4.3. Effect of the Section Types of the Tip Deflection

The spring index of the spring of square section is defined by

$$C = \frac{a}{D_{\max}} \tag{4.7}$$

In this section to compare the results belong to square and circular sections, the undeformed area of the section is taken constant. This means that since *A=constant*, the axial rigidity will be the same for both square and circular sections.

$a = 1.639519812\,cm = const$

$A = a^2$

$k_b = 1.2$

$J_b = 0.141a^4$

$I_b = \frac{a^4}{12}$

$G = 800000\ kg_f / cm^2$

$P = 150\ kg_f$

$n = 18$

$\nu = 0.3$

$R_{\max} = \frac{Ca}{2}$

$C = 3,4,..15$

$\frac{R_{\min}}{R_{\max}} = 0.1 - 0.9$

$\alpha = 10^o - 40^o$

Figures (4.16-4.18) show the percent contribution of shearing force, bending moment and torsional moment on the total deflection of cylindrical isotropic spring having circular and square sections, respectively.

- ✓ For small spring indices *(C=3),* and small helix pitch angles *(α=10^o)*, the effect of the shearing force on the tip deflection of the cylindrical isotropic spring with square section is about 7% while this value is almost 6% for circular section.
- ✓ The effect of the shearing force on the tip deflection of the cylindrical spring with square section is greater than circular section.

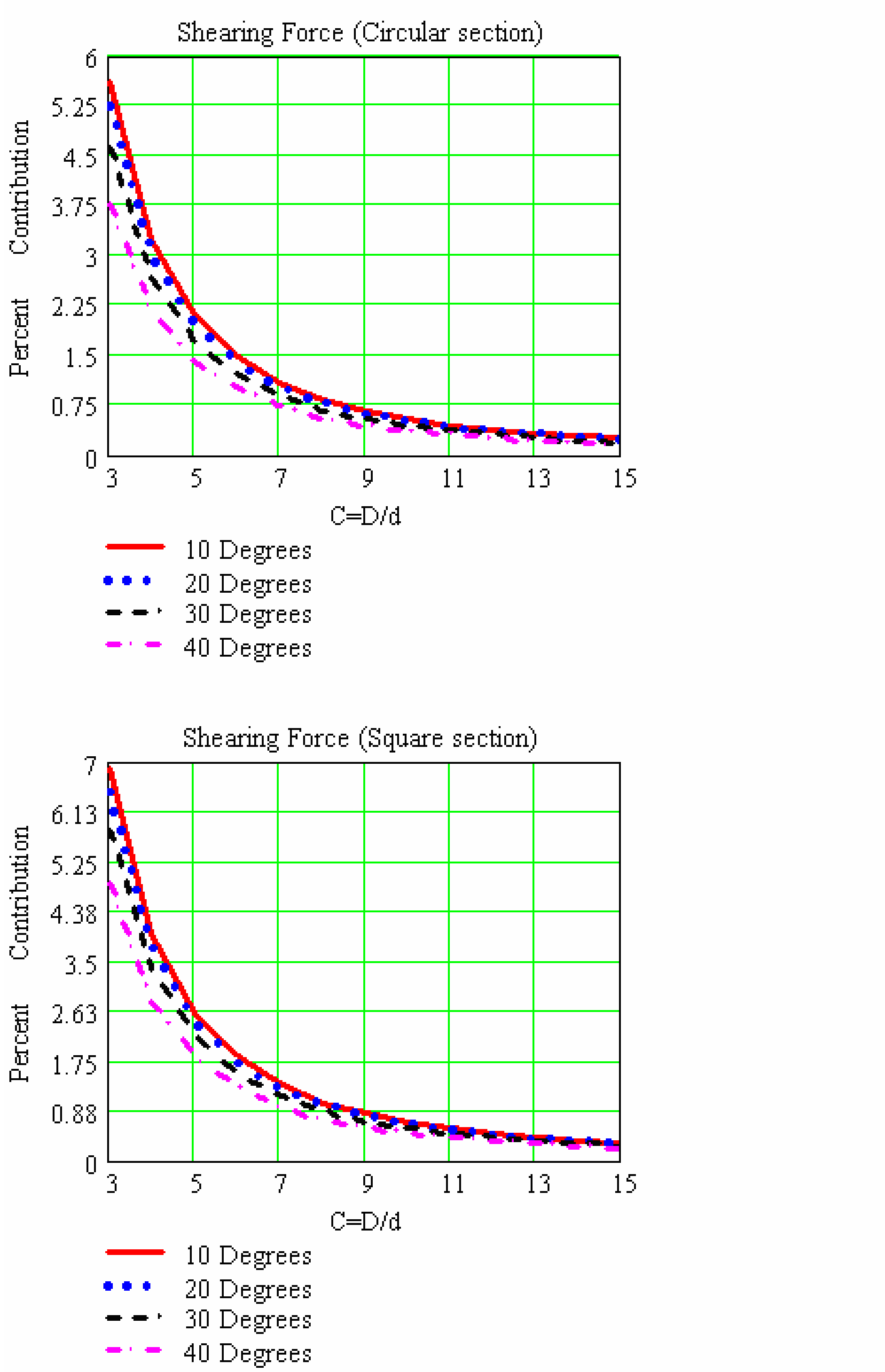

Figure 4.16. Percent contribution of shearing force on the total deflection of cylindrical isotropic spring having circular and square sections

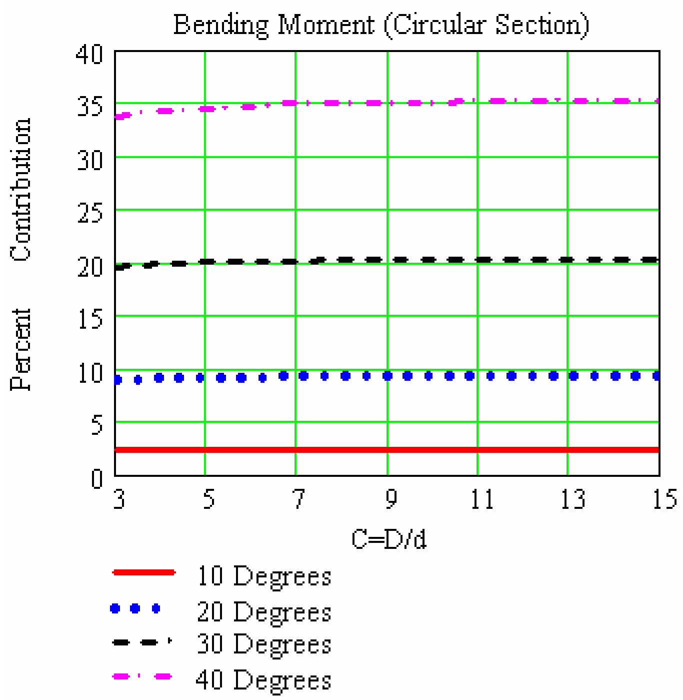

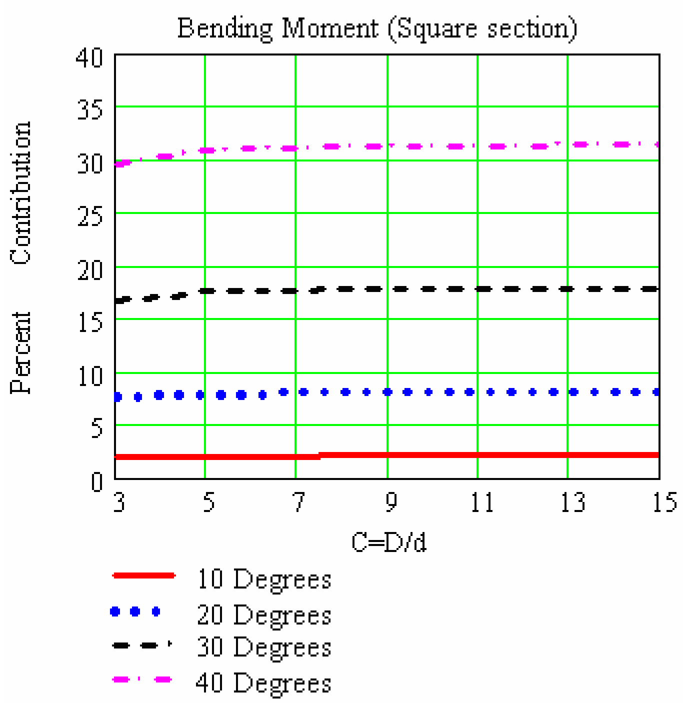

Figure 4.17. Percent contribution of bending moment on the total deflection of cylindrical isotropic spring having circular and square sections

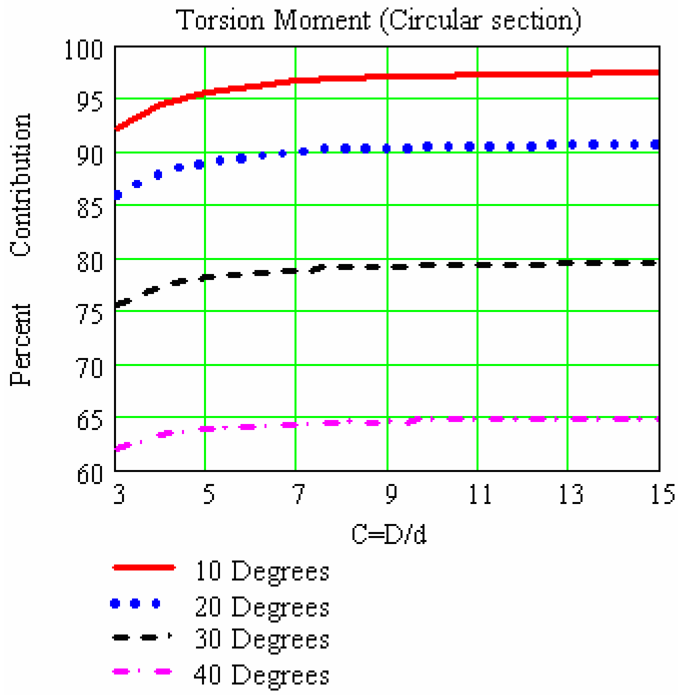

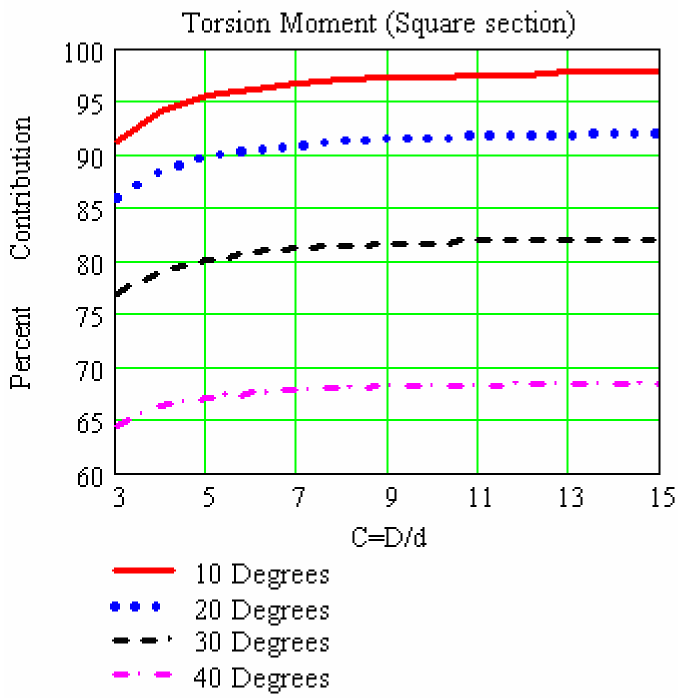

Figure 4.18. Percent contribution of torsional moment on the total deflection of cylindrical isotropic spring having circular and square sections

- ✓ The effect of the bending moment on the tip deflection of the cylindrical spring with square section is less than circular section. The percent effect decreases from 35% to 31% for *C=3* and $\alpha = 40^o$.
- ✓ The effect of the torsional moment on the tip deflection of the cylindrical spring with square section is somewhat greater than circular section. The percent effect increases from 65% to about 68% for large spring indices and $\alpha = 40^o$.

Figures (4.19-4.21) show the percent contribution of shearing force, bending moment and torsional moment on the total deflection of hyperboloidal type isotropic spring having circular and square sections, respectively ($R_{\min} / R_{\max} = 0.1$).

- ✓ For small spring indices *(C=3),* $R_{\min} / R_{\max} = 0.1$ and small helix pitch angles *(*α*=10*^{o}*)*, the effect of the shearing force on the tip deflection of the hyperboloidal isotropic spring with square section is about 16% while this value is almost 13% for circular section.
- ✓ The effect of the shearing force on the tip deflection of the non-cylindrical spring with square section is greater than circular section.
- ✓ For $R_{\min} / R_{\max} = 0.1$, the effect of the bending moment on the tip deflection of hyperboloidal spring with square section is less than circular section. The percent effect decreases from 35% to 31% for *C=3* and $\alpha = 40^o$.
- ✓ For $R_{\min} / R_{\max} = 0.1$, the effect of the torsional moment on the tip deflection of hyperboloidal spring with square section is somewhat greater than circular section. The percent effect increases from 77% to about 83% for large spring indices and $\alpha = 30^o$.

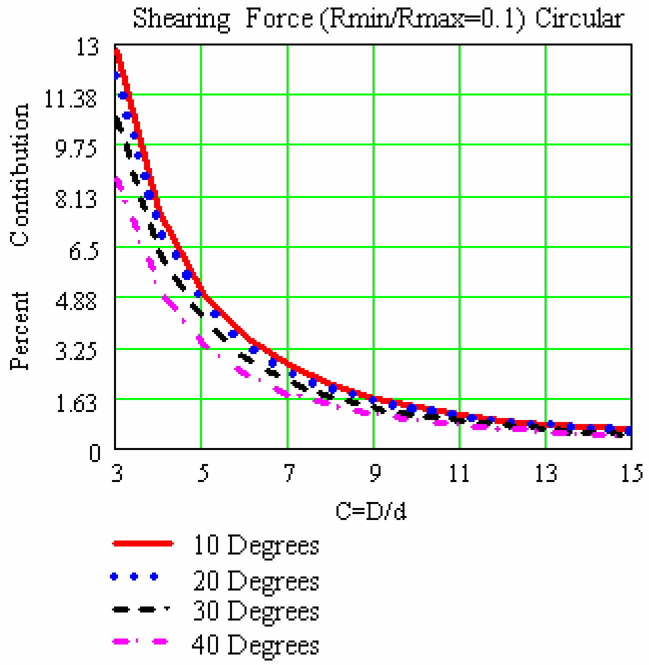

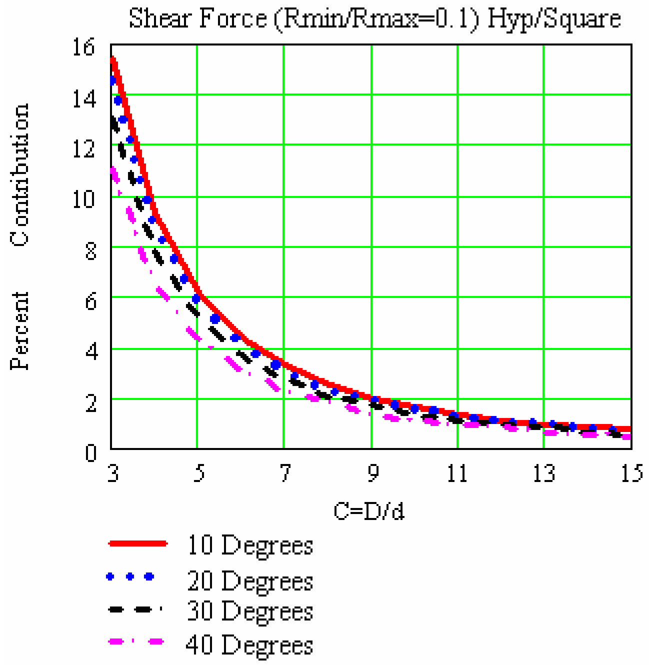

Figure 4.19. Percent contribution of shearing force on the total deflection of hyperboloidal isotropic spring having square and circular sections for $R_{min} / R_{max} = 0.1$

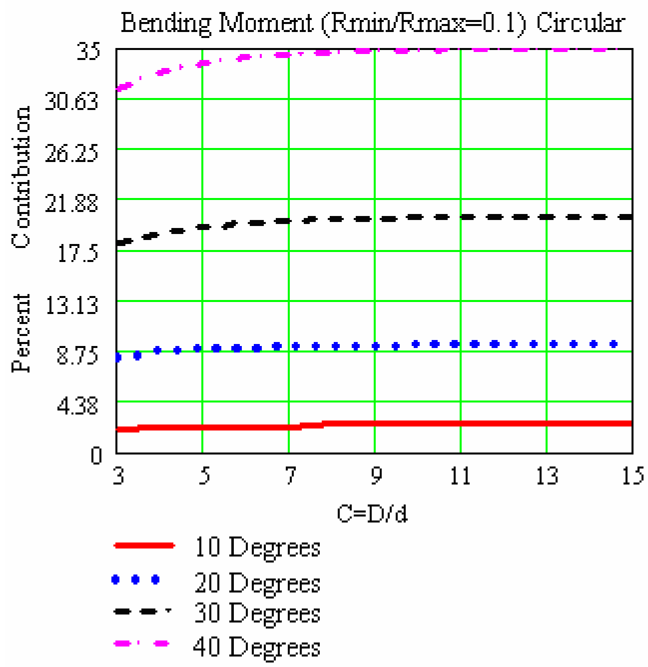

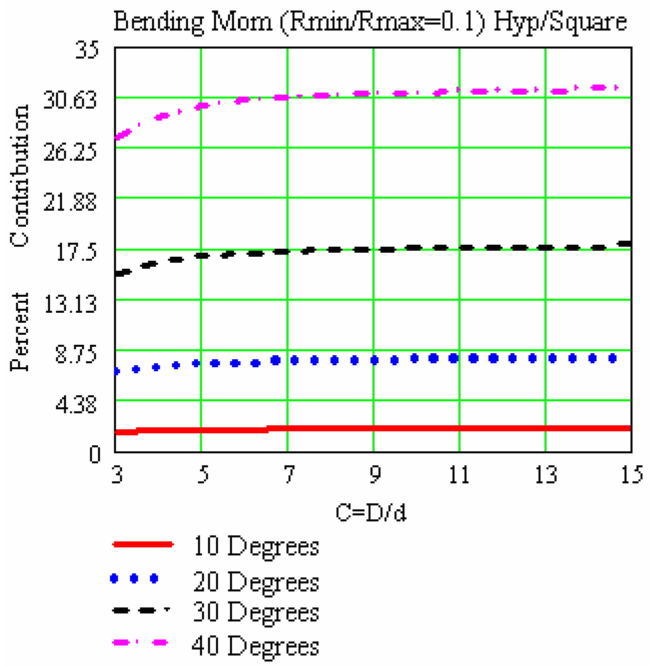

Figure 4.20. Percent contribution of bending moment on the total deflection of hyperboloidal isotropic spring having square and circular sections for $R_{min} / R_{max} = 0.1$

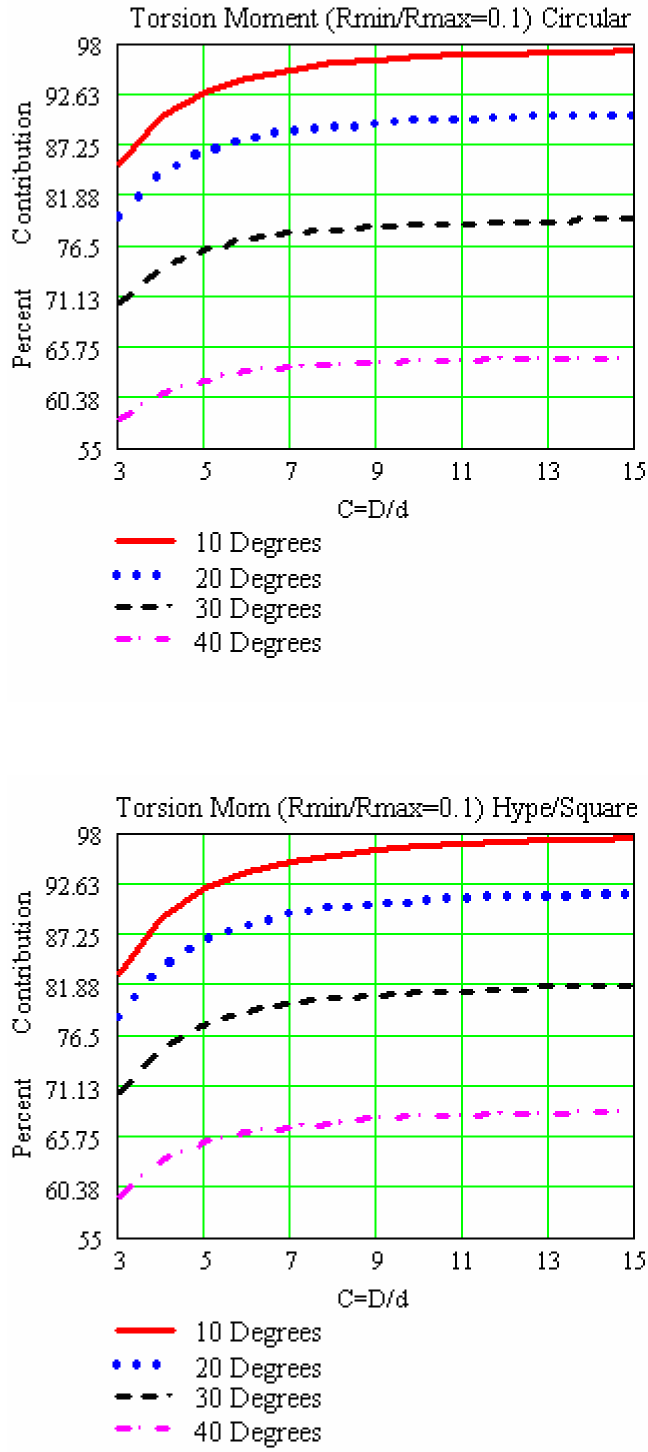

Figure 4.21. Percent contribution of torsional moment on the total deflection of hyperboloidal isotropic spring having square and circular sections for $R_{\min} / R_{\max} = 0.1$

As stated in "Introduction", Wahl (1963) presented the following formula for cylindrical helical springs with square sections.

$$\delta = \frac{5.59PD^3n}{Ga^4} \tag{4.8}$$

Comparison of the present analytical formulas in equations (4.2) and Wahl's formula in equation (4.8) for square sections is shown in Figure (4.22). From the figure we can say that Wahl's formula for valid for small helix pitch angles, $\alpha \leq 10^o$.

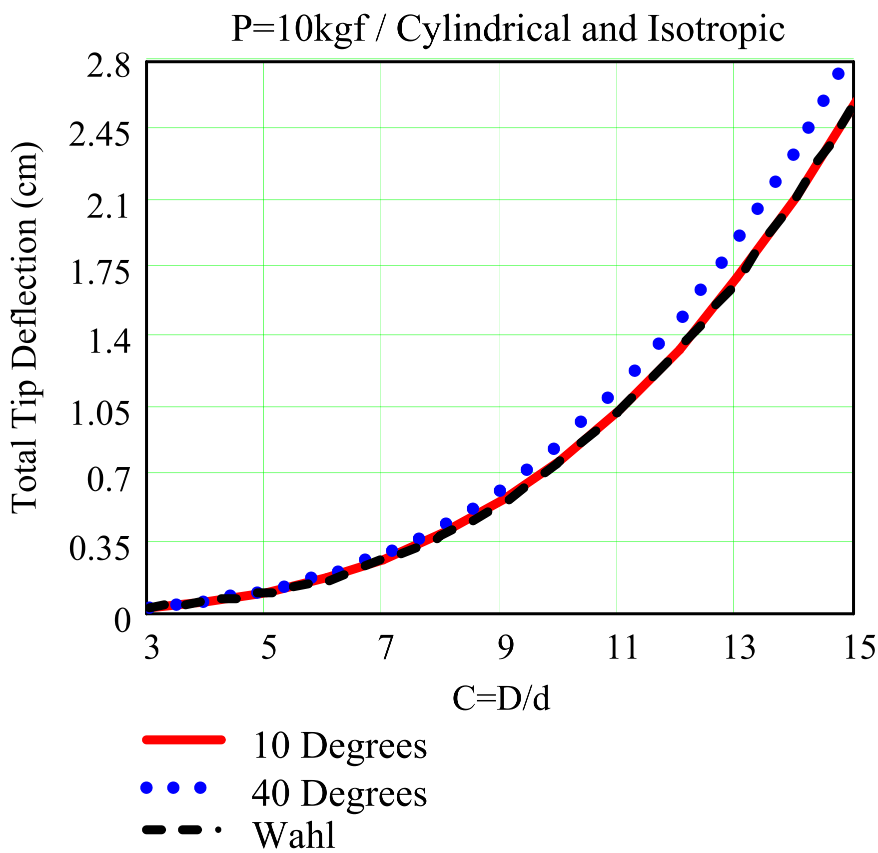

Figure 4.22. Comparison of the present analytical formula and Wahl's formula for square sections

4.4. Numerical Results for Composite Cylindrical Springs

The properties of the composite materials considered in this section are given in Table (4.1).

Table 4.1. The transversely isotropic material properties (Yıldırım and Sancaktar, 2000; Yıldırım, 2001a-2001b, 2004)

	Carbon Epoxy (AS4/3501-6)	Carbon Epoxy (T300/N5208)	Kevlar 49-Epoxy
E_1 (GPa)	144.8	181.0	76.0
E_2 (GPa)	9.65	10.3	5.56
E_3 (GPa)	9.65	10.3	5.56
G_{12} (GPa)	4.14	7.17	2.30
G_{13} (GPa)	3.45	3.433	1.618
ν_{12}	0.3	0.28	0.34
ν_{13}	0.019	0.0159	0.0248
ν_{23}	0.019	0.0159	0.0248
ρ (kg/m^3)	1389.23	1600.0	1460.0

The geometric properties of the composite cylindrical spring with circular section are as follows

$$k_b = 1.1\,(circular) \qquad R_{\max} = \frac{Cd}{2}$$
$$P = 150.9.81\,N$$
$$n = 18 \qquad C = 3,4,..15$$
$$\nu = 0.3 \qquad R_{\min} / R_{\max} = 0.1 - 0.9$$
$$d = 1.85.10^{-3}\,m = const \qquad \alpha = 10^o - 40^o$$

Figures (4.23-4.26) show the percent contribution of axial force, shearing force, bending moment, torsional moment on the total deflection of cylindrical unidirectional composite spring having circular section, respectively (See also Appendix F). From the figures, the followings may be drawn:

- ✓ The effect of the percent contribution of the axial force on the tip deflection of the cylindrical composite spring is considerable less than isotropic ones (maximum 0.11%-0.15%).
- ✓ The effect of the percent contribution of the shearing force on the tip deflection of the cylindrical composite spring is almost independent of the helix pith angle and material types (maximum 6%).
- ✓ The effect of the percent contribution of the bending moment on the tip deflection of the cylindrical composite spring is noticeable less than isotropic ones (maximum 4%).
- ✓ The effect of the percent contribution of the torsional moment on the tip deflection of the cylindrical composite spring is noticeable greater than isotropic ones (minimum 90%).

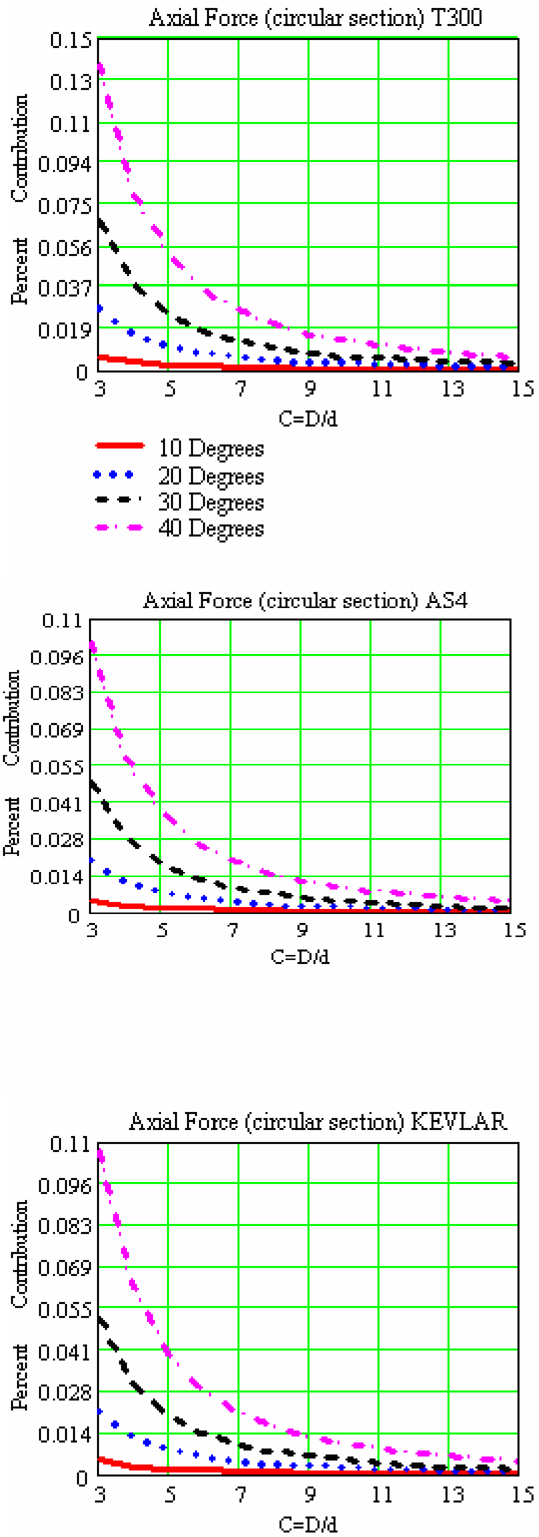

Figure 4.23. Percent contribution of axial force on the total deflection of cylindrical unidirectional composite spring having circular section

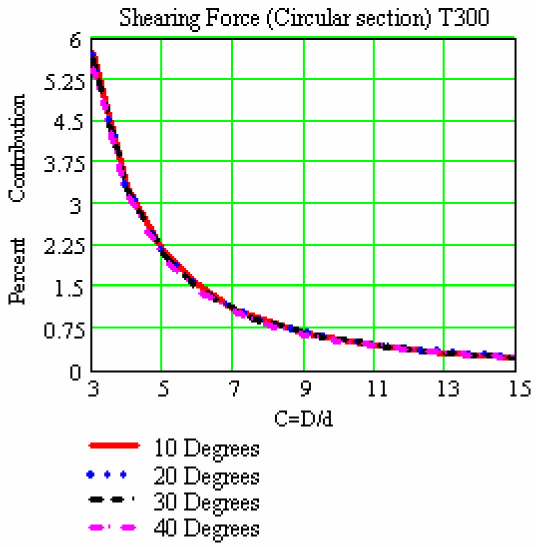

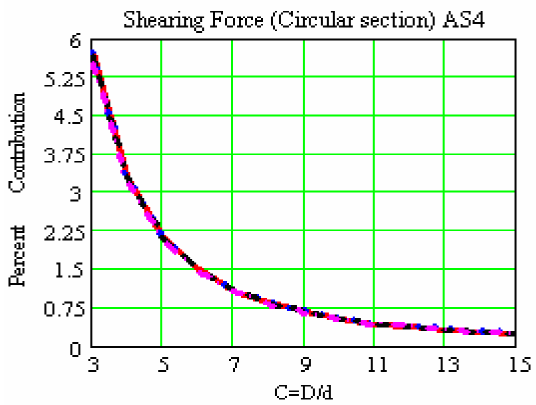

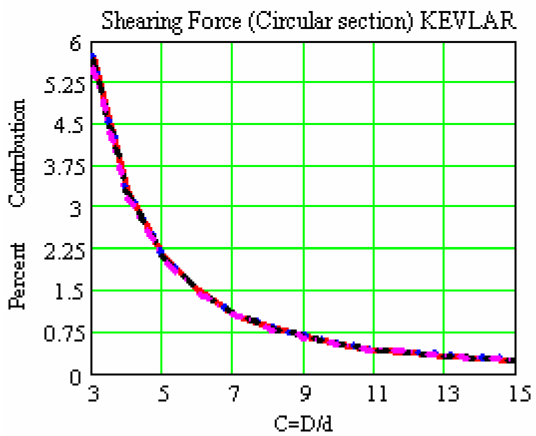

Figure 4.24. Percent contribution of shearing force on the total deflection of cylindrical unidirectional composite spring having circular section

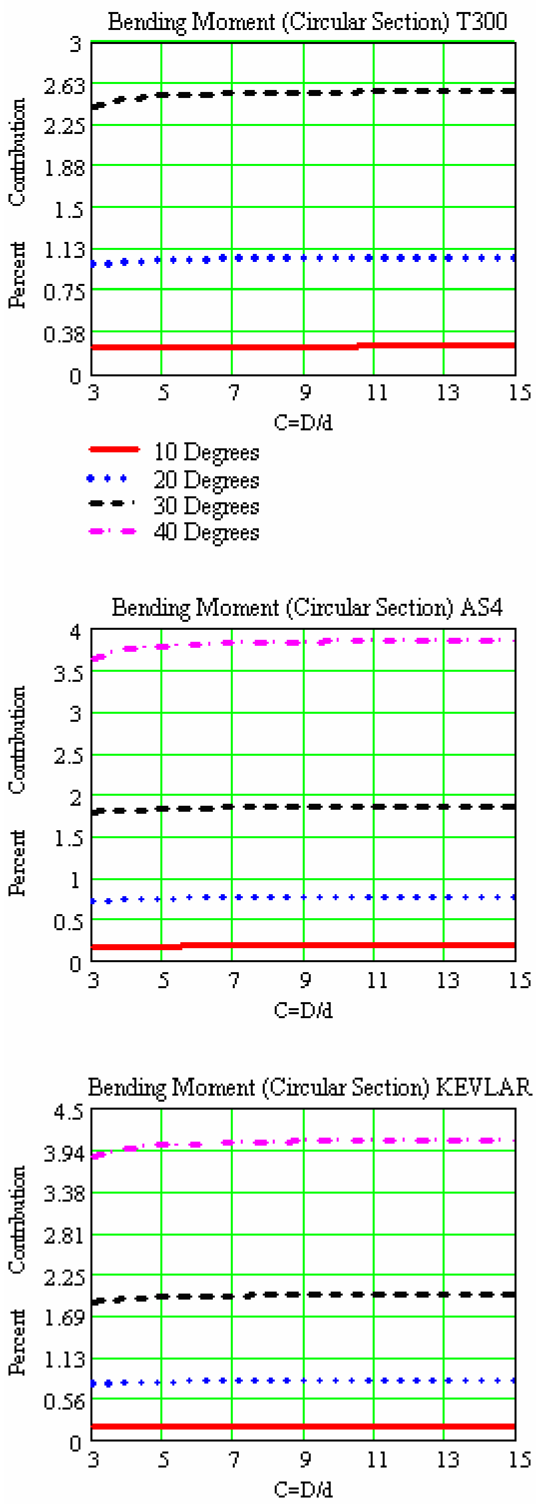

Figure 4.25. Percent contribution of bending moment on the total deflection of cylindrical unidirectional composite spring having circular section

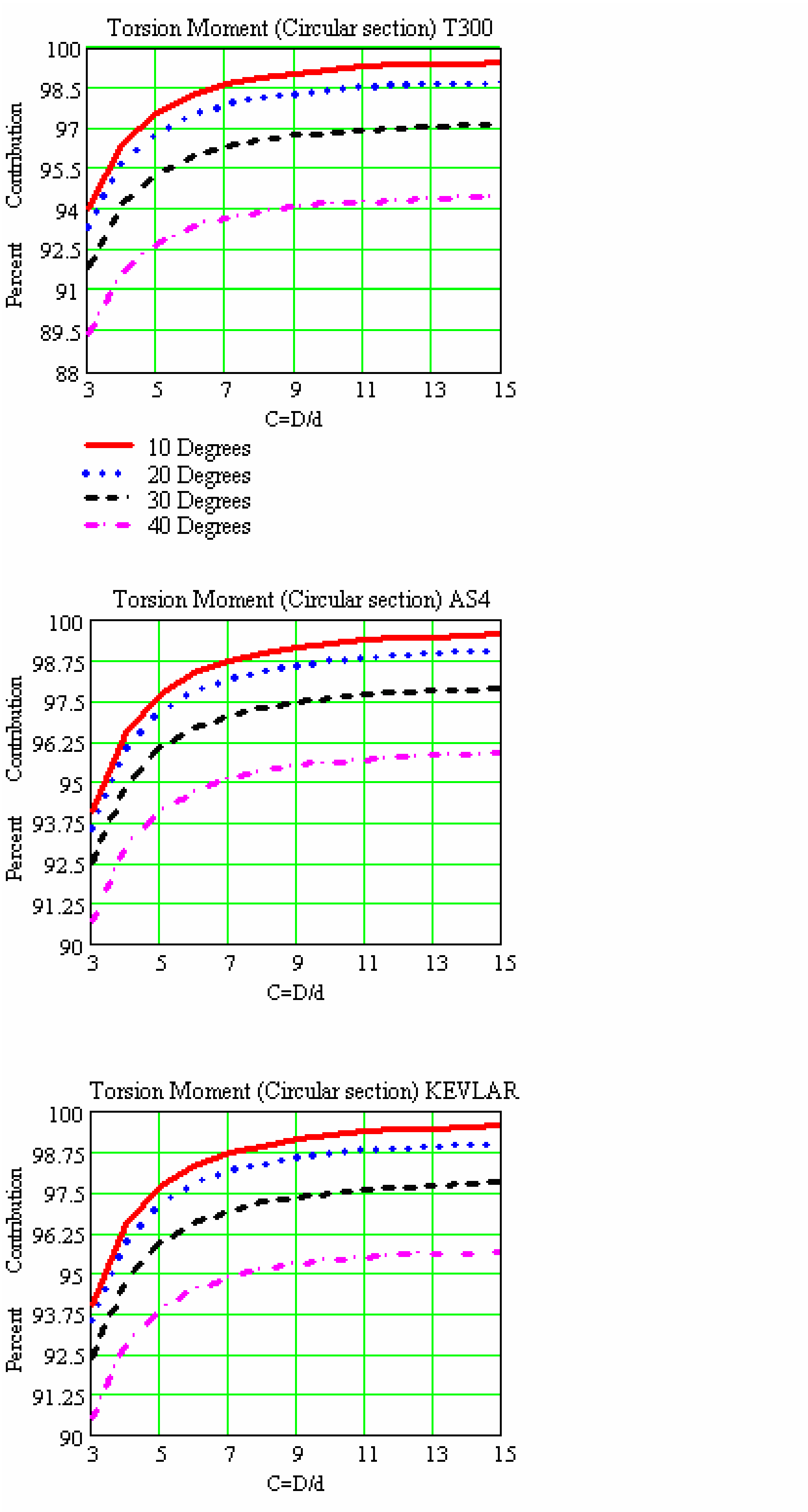

Figure 4.26. Percent contribution of torsional moment on the total deflection of cylindrical unidirectional composite spring having circular section

5. CONCLUSIONS

In this study, analytical expressions for determination of the vertical tip displacement of both isotropic/composite cylindrical and non-cylindrical helices subjected to an axial force acting along the helix cylinder axis are presented by using the Castigliano's first theorem. These formulas comprise the whole effect of the stress resultants such as axial and shearing forces, bending and torsional moments and may be used for

- ✓ constant helix pitch angles
- ✓ homogeneous and linear isotropic and composite materials
- ✓ doubly symmetric cross-sections
- ✓ both small and large pitch angles
- ✓ all types of helices used in practice such as cylindrical, conical, barrel and hyperboloidal springs

Comparison of the present results with the results of the existing formulas given by Wahl (1963) shows that Wahl's formulas are valid for just small helix pitch angles $\alpha \leq 10^o$ and isotropic materials. Apart from this it is shown that, among the springs having the same value of spring index, $C = \frac{D_{\max}}{d} = \frac{2R_{\max}}{d}$, hyperboloidal type helical spring is the most stronger one. The other conclusions obtained from the present work are outlined below:

<u>The effect of the axial force:</u>

- ✓ Increasing the helix angle results an obvious increase in the percent contribution of the axial force on the tip deflection of cylindrical and noncylindrical helical compression spring.
- ✓ Increasing the spring index decreases the percent contribution of the axial force on the tip deflection of cylindrical and noncylindrical helical compression spring.

- ✓ Increasing the ratio R_{min}/R_{max} decreases those effects.
- ✓ For small spring indices *(C=3),* for small ratio R_{min}/R_{max} and large helix pitch angles $(\alpha=40^o)$, the effect of the axial force on the tip deflection is about
  - 1% for cylindrical isotropic spring with circular section
  - 1.4% for barrel isotropic spring with circular section
  - 1.8% for conical isotropic spring with circular section
  - 2.2% for hyperboloidal isotropic spring with circular section
- ✓ The percent contribution of the axial force acting on the hyperboloidal springs is greater than all other types of helices.
- ✓ The effect of the percent contribution of the axial force on the tip deflection of the cylindrical composite spring is considerable less than isotropic ones (maximum 0.11%-0.15%).

The effect of the shearing force:

- ✓ Increasing the helix angle results a decrease in the percent contribution of the shearing force on the tip deflection of cylindrical and noncylindrical spring.
- ✓ Increasing the spring index decreases the percent contribution of the shearing force on the tip deflection of cylindrical and noncylindrical spring. For $C \geq 10$ the percent contribution is less than 1% for springs with circular section.
- ✓ Increasing the ratio R_{min}/R_{max} decreases those effects.
- ✓ For small spring indices *(C=3),* for small ratio R_{min}/R_{max} and small helix pitch angles $(\alpha=10^o)$, the effect of the shearing force on the tip deflection is almost
  - 6% for isotropic cylindrical spring with circular section
  - 8% for isotropic barrel spring with circular section
  - 11% for isotropic conical spring with circular section
  - 13% for isotropic hyperboloidal spring with circular section

- ✓ The percent contribution of the shearing force acting on the hyperboloidal springs is greater than all other types of helices.

- ✓ For small spring indices *(C=3),* and small helix pitch angles *(α=10^o)*, the effect of the shearing force on the tip deflection of the cylindrical isotropic spring with square section is about 7% while this value is almost 6% for circular section.
- ✓ The effect of the shearing force on the tip deflection of the cylindrical spring with square section is greater than circular section.
- ✓ For small spring indices *(C=3),* $R_{\min} / R_{\max} = 0.1$ and small helix pitch angles *(α=10^o)*, the effect of the shearing force on the tip deflection of the hyperboloidal isotropic spring with square section is about 16% while this value is almost 13% for circular section.
- ✓ The effect of the shearing force on the tip deflection of the non-cylindrical spring with square section is greater than circular section.
- ✓ The effect of the percent contribution of the shearing force on the tip deflection of the cylindrical composite spring is almost independent of the helix pith angle and material types (maximum 6%).

The effect of the bending moment:

- ✓ Increasing the helix angle results a noticeable increase in the percent contribution of the bending moment on the tip deflection of cylindrical and noncylindrical helical springs.
- ✓ Increasing the spring index increases very slightly the percent contribution of the bending moment on the tip deflection. It may be concluded that the value of the spring index almost does not affect the numerical value of the tip deflection for $C \geq 7$.
- ✓ Increasing the ratio R_{min}/R_{max} increases very slowly those effects especially for small helix indices.

- For large helix pitch angles *(α=40^o)*, for large ratio R_{min}/R_{max} the effect of the bending moment on the tip deflection is about 35%. For α=10^o this value is about 2-2.5%. In general the effect of the bending moment on the tip deflection is not very changed with the types of isotropic helices for $C \geq 7$.
- The effect of the bending moment on the tip deflection of isotropic cylindrical spring with square section is less than circular section. The percent effect decreases from 35% to 31% for *C=3* and $\alpha = 40^o$.
- For $R_{\min} / R_{\max} = 0.1$, the effect of the bending moment on the tip deflection of isotropic hyperboloidal spring with square section is less than circular section. The percent effect decreases from 35% to 31% for *C=3* and $\alpha = 40^o$.
- The effect of the percent contribution of the bending moment on the tip deflection of the cylindrical composite spring is noticeable less than isotropic ones (maximum 4%).

The effect of the torsional moment:

- Increasing the helix angle results a noticeable decrease in the percent contribution of the torsional moment on the tip deflection of cylindrical and noncylindrical helical springs.
- Increasing the spring index increases slowly the percent contribution of the torsional moment on the tip deflection of cylindrical and noncylindrical helical springs.
- It may be concluded that the value of the isotropic spring index almost the same for $C \geq 10$.
- Increasing the ratio R_{min}/R_{max} increases very slightly those effects especially for small helix indices.

- ✓ For small helix pitch angles *(α=10^o)*, for large ratio R_{min}/R_{max} the effect of the torsional moment on the tip deflection is about 97.5%. For α=40^o this value is about 65% for isotropic springs with circular section.
- ✓ In general the effect of the torsional moment on the tip deflection is not mainly changed with the types of isotropic helices for $C \geq 10$.
- ✓ The effect of the torsional moment on the tip deflection of the cylindrical isotropic spring with square section is somewhat greater than circular section. The percent effect increases from 65% to about 68% for large spring indices and $\alpha = 40^o$.
- ✓ For $R_{\min} / R_{\max} = 0.1$, the effect of the torsional moment on the tip deflection of hyperboloidal spring with square section is somewhat greater than circular section. The percent effect increases from 77% to about 83% for large spring indices and $\alpha = 30^o$.
- ✓ The effect of the percent contribution of the torsional moment on the tip deflection of the cylindrical composite spring is noticeable greater than isotropic ones (minimum 90%).

REFERENCES

BEER F.P., JOHNSTON E.R., 1992, Mechanics of Materials, Second Edition in SI units, McGraw Hill, London.

COWPER, G.R., 1966, “The shear coefficient in Timeshenko’s beam theory”, ASME JAM, 33, 335-340.

HAKTANIR, V., 1992, “Eksenel yüklenmiş konik yaylarda yay rijitliğine etki eden parametrelerin incelenmesi”, Ç.Ü. Müh. Mim. Fak. Dergisi, 7/2, 99-109.

HAKTANIR, V., 1994, “Basmaya çalışan keyfi biçimli helisel yaylarda yay rijitliğine etki eden parametrelerin analitik incelenmesi”, 6. Uluslar Arası Makine Tasarım ve İmalat Kongresi, 21-23 Eylül 1994, OTÜ, 473-482.

HALL A.S., HALOWENKEN, A.R., LAUGHLIN, H.G., 1961, Teori ve Problemlerle Makina Dizaynı, Schaum’s Outline Series, Çeviren: Yaşar Pancar. Bilim Teknik Yayınevi, Istanbul.

İNAN, M., 1967. Cisimlerin Mukavemeti, Birsen Yayınevi.

JONES R.M., 1975. Mechanics of Composite Materials, McGraw-Hill Book Company.

KAYAN, İ., 1987, Cisimlerin Mukavemeti, İTÜ Kütüphanesi, Sayı: 1334.

OMURTAG, M.H., 2005. Mukavemet Cilt II, Birsen Yayınevi.

TIMOSHENKO, S.P., 1921, “On the correction for shear of the differential equation for transverse vibrations of prismatic bars”, Philosophical Magazine, 41, 744-746.

TIMOSHENKO, S.P., 1922, “On the transverse vibrations of bars of uniform cross-section”, Philosophical Magazine, 43, 125-131.

TIMOSHENKO, S.P., 1991, Mechanics of Materials, Chapman & Hall.

TSAI S.W. and HAHN H.T., 1980, Introduction to Composite Materials, Technomic Publishing, U.S.A.

WAHL, A.M., 1963, Mechanical Springs, Second Edition, McGraw-Hill, New York.

YILDIRIM, V., 1999, “Governing equations of initially twisted elastic space rods made of laminated composite materials”, International Journal of Engineering Science, 37, 1007-1035.

YILDIRIM, V., 1999, “An efficient numerical method for predicting the natural frequencies of cylindrical helical springs”, International Journal of Mechanical Sciences, 41/ 8, 919-939.

YILDIRIM, V. and SANCAKTAR, E., 2000, “Linear free vibration analysis of cross-ply laminated cylindrical helical springs”, International Journal of Mechanical Sciences, 42/6, 1153-1169.

YILDIRIM, V., 2001a, “Free vibration of uniaxial composite cylindrical helical springs with circular section”, Journal of Sound and Vibration, 239/2, 321-333.

YILDIRIM,V., 2001b,"Free vibration characteristics of composite barrel and hyperboloidal coil springs", Mechanics of Composite Materials and Structures, 8/3, 205-217.

YILDIRIM, V., 2002, “Expressions for predicting fundamental natural frequencies of non-cylindrical helical springs”, Journal of Sound and Vibration, 252/3, 479-491.

YILDIRIM, V., 2004, “A parametric study on the natural frequencies of unidirectional composite conical springs”, Communications in Numerical Methods in Engineering 20 (3): 207-227.

http://www.efunda.com/designstandards/springs/spring_design.cfm

http://www.engineerstoolbox.com/doc/etb/mod/stat1/spring/spring_help.html

http://www.efunda.com/designstandards/springs/spring_design.cfm

http://www.efunda.com/designstandards/springs/calc_comp_k.cfm

CURRICILUM VITAE

Eylem ZEYDAN was born in Mersin, 1977. After being graduated from Dumlupınar High School, he enrolled in Mechanical Engineering Department of Çukurova University in 1996. He graduated from Çukurova University as a Mechanical Engineer in September 2000. He started his master of science education in the same department in 2001.

Variation of Integrals with respect to the Ratio of R_{min} and R_{max}

$$c := 0.1, 0.2 .. 1 \qquad rm := 1 \qquad int1k(r1,r2) := \pi\cdot(r1 + r2) \qquad int1vh(r1,r2) := \frac{2}{3}\cdot\pi\cdot(2\cdot r1 + r2)$$

$$int2k(r1,r2) := \frac{1}{2}\cdot\pi\cdot(r1 + r2)\cdot\left(r1^2 + r2^2\right)$$

Barrel and conical-> R2=c*R1 (Rmax=Rm=R1)

Hyperboloidal -> R1=c*R2 (Rmax=Rm=R2)

$$int2vh(r1,r2) := \frac{2}{35}\cdot\pi\cdot\left(5\cdot r2^3 + 6\cdot r2^2\cdot r1 + 8\cdot r2\cdot r1^2 + 16\cdot r1^3\right)$$

$$f1k(rm,c) := \pi\cdot(rm + c\cdot rm) \qquad f1v(rm,c) := \frac{2}{3}\cdot\pi\cdot(2\cdot rm + c\cdot rm)$$

$$f1h(rm,c) := \frac{2}{3}\cdot\pi\cdot(2\cdot c\cdot rm + rm) \qquad f2k(rm,c) := \frac{1}{2}\cdot\pi\cdot(rm + c\cdot rm)\cdot\left[rm^2 + (c\cdot rm)^2\right]$$

$$f2v(rm,c) := \frac{2}{35}\cdot\pi\cdot\left[5\cdot(c\cdot rm)^3 + 6\cdot(c\cdot rm)^2\cdot rm + 8\cdot c\cdot rm\cdot rm^2 + 16\cdot rm^3\right]$$

$$f2h(rm,c) := \frac{2}{35}\cdot\pi\cdot\left[5\cdot rm^3 + 6\cdot rm^2\cdot c\cdot rm + 8\cdot rm\cdot(c\cdot rm)^2 + 16\cdot(c\cdot rm)^3\right]$$

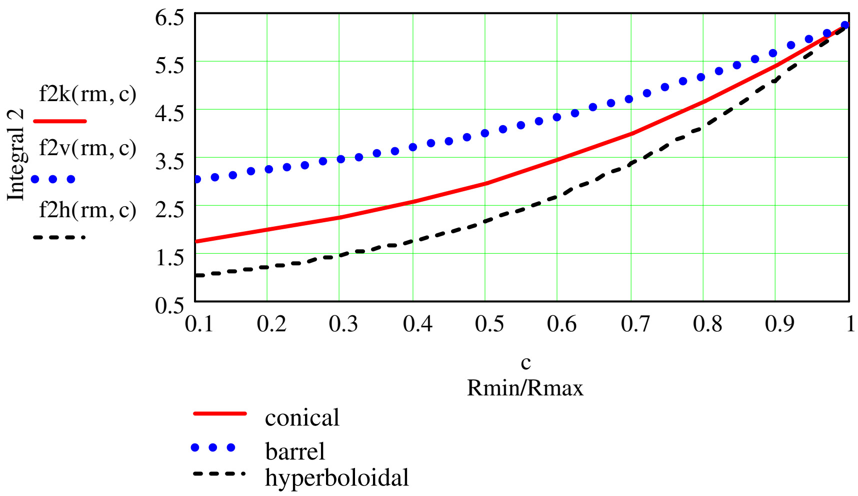

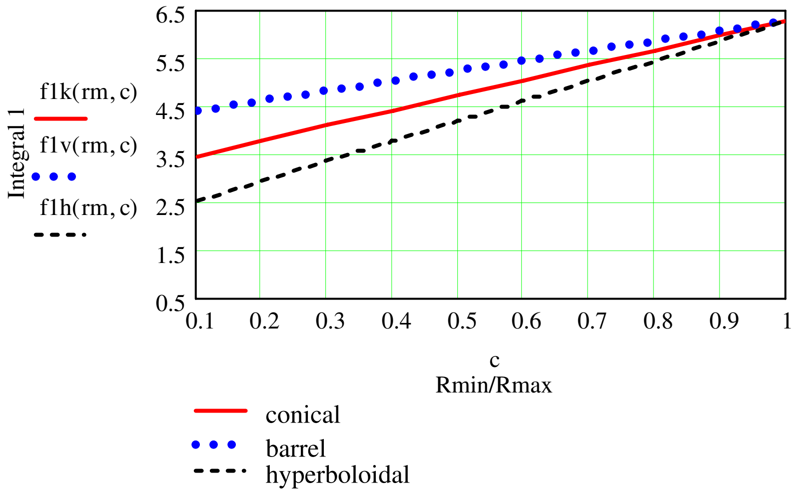

Variation of Integrals with respect to the Ratio of R_{min} and R_{max}

oran1 := f1k(1, 1) oran1 = 6.283

oran2 := f2k(1, 1) oran2 = 6.283

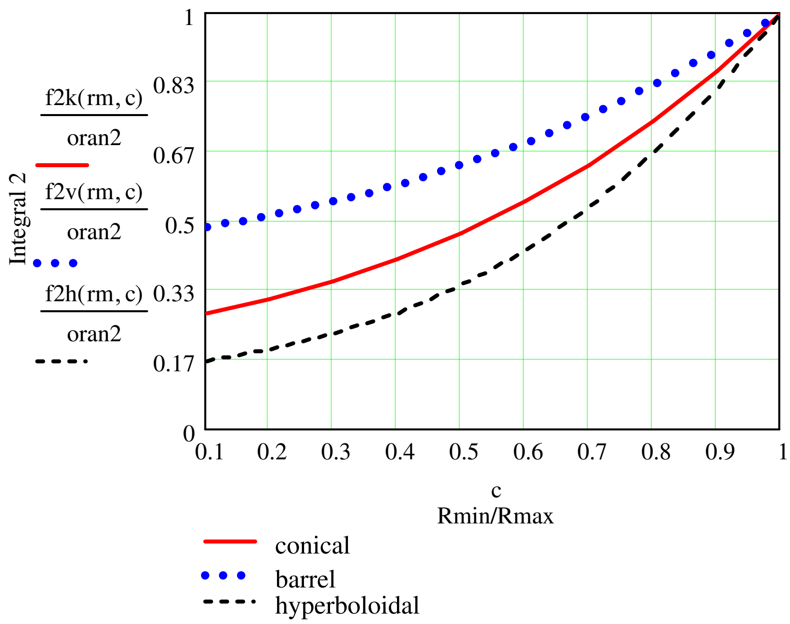

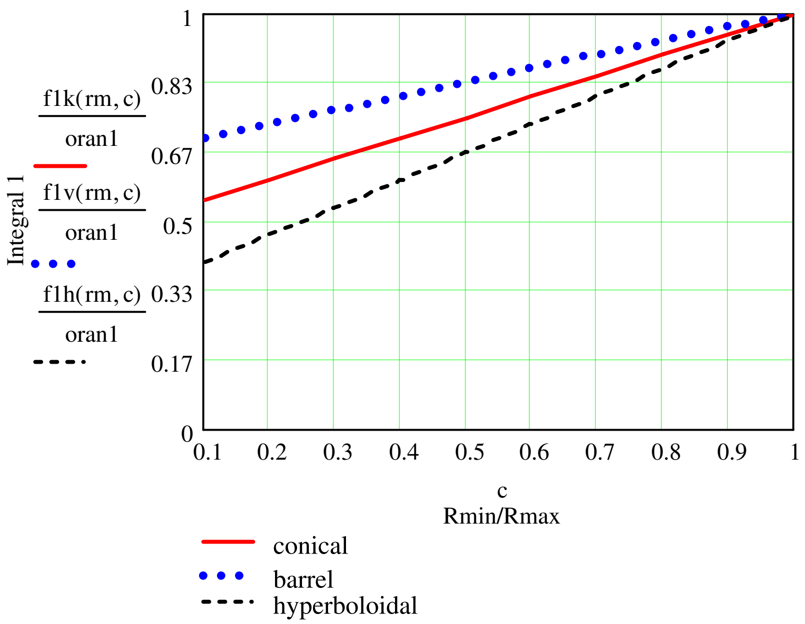

Tip Deflection of Cylindrical Isotropic Helical Springs

C=D/d=2R/d, R=Rmax=rm=Cd/2 d=constant
Note: Angles are radial

$P := 15($ $\quad \alpha b := 1.1$ $\quad G := 8\times 10^{5}$ $\quad d := 1.8\text{5}$ $\quad \upsilon := 0.3$

$n := 18$ $\quad E := 2\cdot(1+\upsilon)\cdot G$ $\quad Rd := \frac{\pi}{180}$ $\quad E = 2.08\times 10^{6}$

$Ib := \frac{\pi\cdot d^{4}}{64}$ $\quad Jb := 2\cdot Ib$ $\quad A := \frac{\pi\cdot d^{2}}{4}$ $\quad C := 3..15$

$CT := \frac{G\cdot A}{\alpha b}$ $\quad CN := E\cdot A$ $\quad De := E\cdot Ib$ $\quad Db := G\cdot Jb$

$$fT(\alpha,C) := \frac{P\cdot\cos(\alpha)}{CT}\cdot 2\cdot\pi\cdot\frac{C\cdot d}{2}\cdot n$$

$$fN(\alpha,C) := \frac{P\cdot\sin(\alpha)\cdot\tan(\alpha)}{CN}\cdot 2\cdot\pi\cdot\frac{C\cdot d}{2}\cdot n$$

$$fMb(\alpha,C) := \frac{P\cdot\cos(\alpha)}{Db}\cdot 2\cdot\pi\cdot\left(\frac{C\cdot d}{2}\right)^{3}\cdot n$$

$$fMe(\alpha,C) := \frac{P\cdot\sin(\alpha)\cdot\tan(\alpha)}{De}\cdot 2\cdot\pi\cdot\left(\frac{C\cdot d}{2}\right)^{3}\cdot n$$

$$fTOT(\alpha,C) := fT(\alpha,C) + fN(\alpha,C) + fMb(\alpha,C) + fMe(\alpha,C)$$

$fT(5\cdot Rd,10) = 0.0799648177$ $\quad fN(5\cdot Rd,10) = 2.1401119043\times 10^{-4}$

$fMb(5\cdot Rd,10) = 14.5390577559$ $\quad fMe(5\cdot Rd,10) = 0.0856044762$

$fTOT(5\cdot Rd,10) = 14.704841061$

$$or1(\alpha,C) := \frac{fN(\alpha,C)}{fTOT(\alpha,C)}\cdot 10(\qquad or2(\alpha,C) := \frac{fT(\alpha,C)}{fTOT(\alpha,C)}\cdot 10($$

$$or3(\alpha,C) := \frac{fMb(\alpha,C)}{fTOT(\alpha,C)}\cdot 10(\qquad or4(\alpha,C) := \frac{fMe(\alpha,C)}{fTOT(\alpha,C)}\cdot 10($$

$or1(5\cdot Rd,10) = 1.4553791472\times 10^{-3}$ $\quad or2(5\cdot Rd,10) = 0.5437992653$

$or3(5\cdot Rd,10) = 98.8725936966$ $\quad or4(5\cdot Rd,10) = 0.5821516589$

Tip Deflection of Cylindrical Isotropic Helical Springs

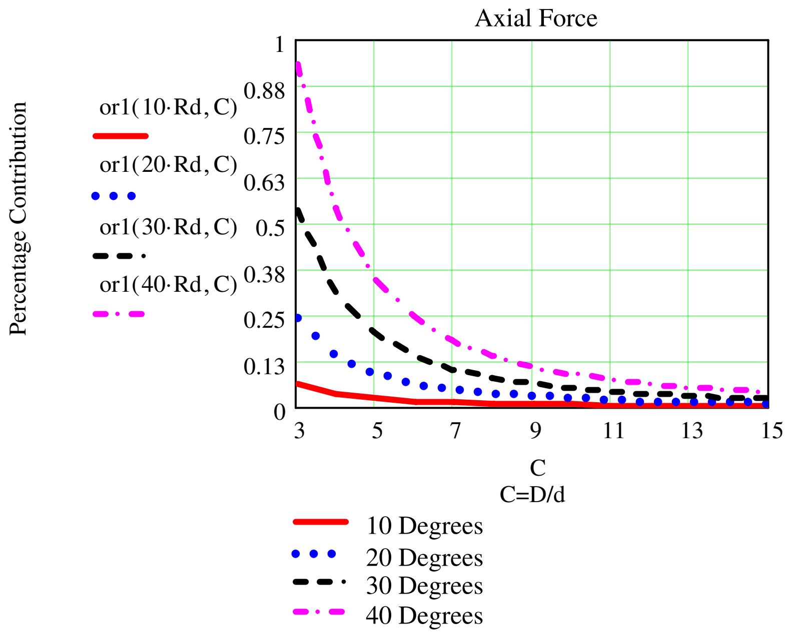

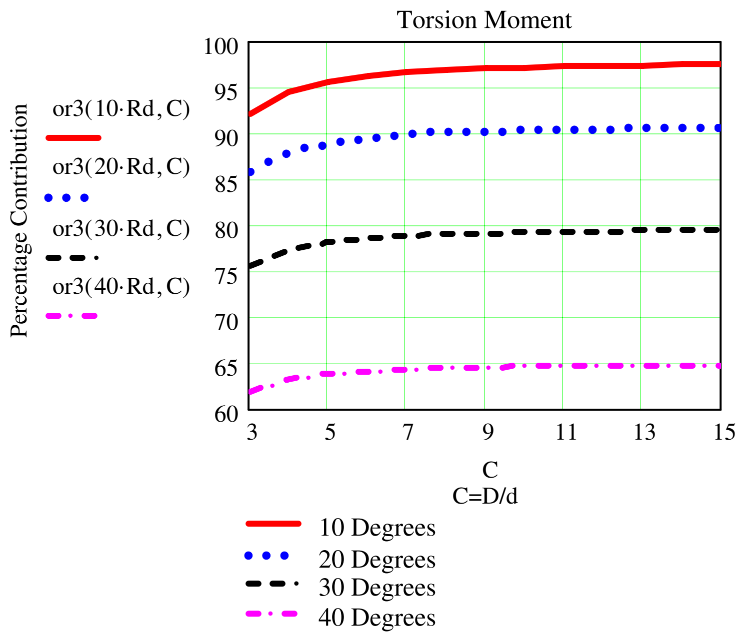

Tip Deflection of Conical Isotropic Helical Springs

C=D/d=2R/d, R=Rmax=rm=Cd/2 d=constant
Note: Angles are radial

$P := 150 \qquad \alpha b := 1.1 \qquad G := 8 \times 10^{5} \qquad d := 1.85 \qquad \upsilon := 0.3 \qquad c := 0.1, 0.2 .. 1$

$n := 18 \qquad E := 2\cdot(1+\upsilon)\cdot G \qquad Rd := \dfrac{\pi}{180} \qquad E = 2.08 \times 10^{6}$

$Ib := \dfrac{\pi\cdot d^{4}}{64} \qquad Jb := 2\cdot Ib \qquad A := \dfrac{\pi\cdot d^{2}}{4} \qquad C := 3 .. 15 \qquad rr_{C} := \dfrac{C\cdot d}{2}$

$CT := \dfrac{G\cdot A}{\alpha b} \qquad CN := E\cdot A \qquad De := E\cdot Ib \qquad Db := G\cdot Jb$

rm

$rm(C) := rr_{C}$

$$f1k(rm, c, C) := \pi\cdot(rm(C) + c\cdot rm(C))$$

$$fTk(\alpha, C, c, rm) := \frac{P\cdot\cos(\alpha)\cdot n}{CT}\cdot f1k(rm, c, C)$$

$$fNk(\alpha, C, c, rm) := \frac{P\cdot n\cdot\sin(\alpha)\cdot\tan(\alpha)}{CN}\cdot f1k(rm, c, C)$$

$$f2k(rm, c, C) := \frac{1}{2}\cdot\pi\cdot(rm(C) + c\cdot rm(C))\cdot\left[rm(C)^{2} + (c\cdot rm(C))^{2}\right]$$

$$fMbk(\alpha, C, c, rm) := \frac{P\cdot n\cdot\cos(\alpha)}{Db}\cdot f2k(rm, c, C)$$

$$fMek(\alpha, C, c, rm) := \frac{P\cdot n\cdot\sin(\alpha)\cdot\tan(\alpha)}{De}\cdot f2k(rm, c, C)$$

$$fTOTk(\alpha, C, c, rm) := fTk(\alpha, C, c, rm) + fNk(\alpha, C, c, rm) + fMbk(\alpha, C, c, rm) + fMek(\alpha, C, c, rm)$$

$$fTk(5\cdot Rd, 10, 0.2, rm) = 0.0479788906$$

$$or1(\alpha, C, c, rm) := \frac{fNk(\alpha, C, c, rm)}{fTOTk(\alpha, C, c, rm)}\cdot 100 \qquad or2(\alpha, C, c, rm) := \frac{fTk(\alpha, C, c, rm)}{fTOTk(\alpha, C, c, rm)}\cdot 100$$

$$or3(\alpha, C, c, rm) := \frac{fMbk(\alpha, C, c, rm)}{fTOTk(\alpha, C, c, rm)}\cdot 100 \qquad or4(\alpha, C, c, rm) := \frac{fMek(\alpha, C, c, rm)}{fTOTk(\alpha, C, c, rm)}\cdot 100$$

Tip Deflection of Conical Isotropic Helical Springs

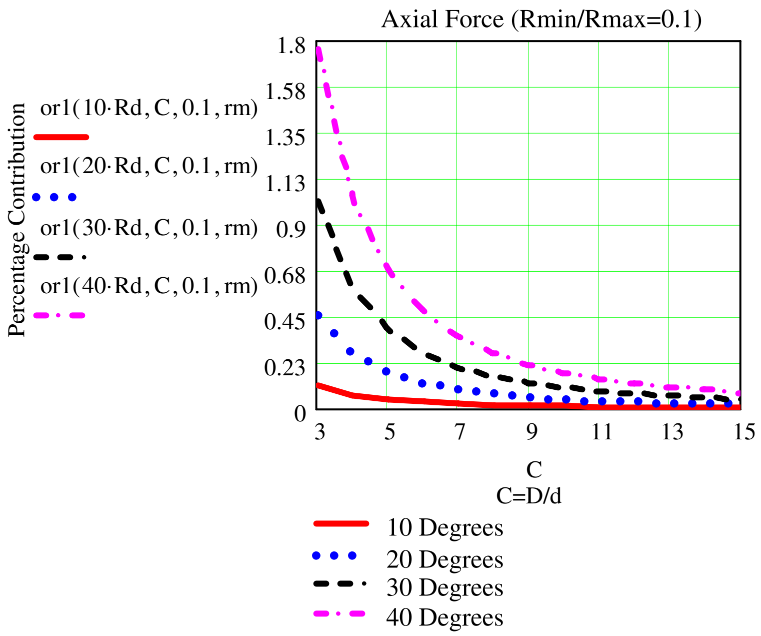

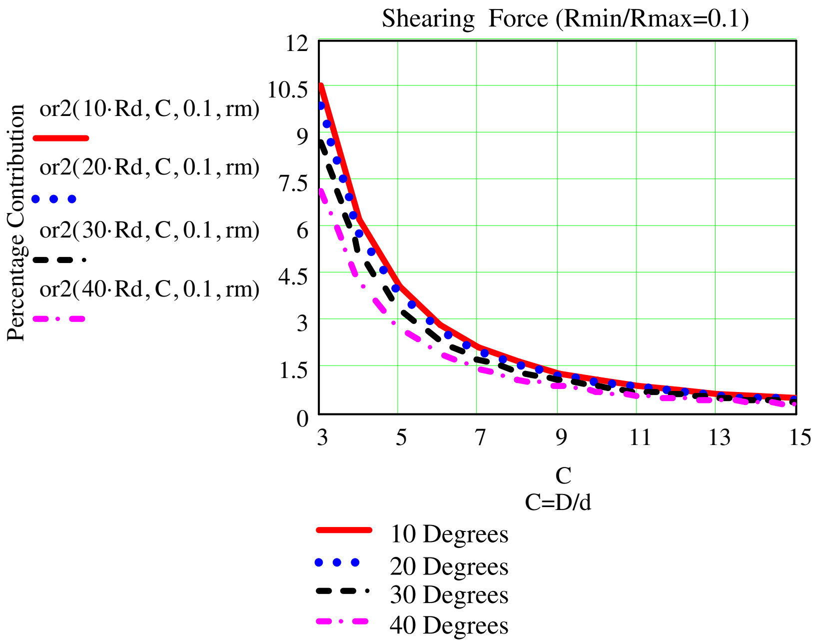

Tip Deflection of Conical Isotropic Helical Springs

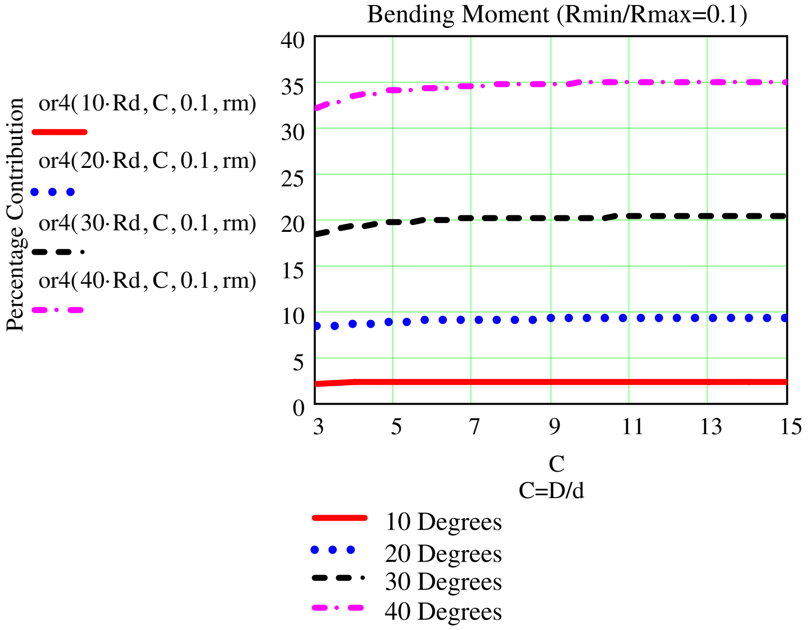

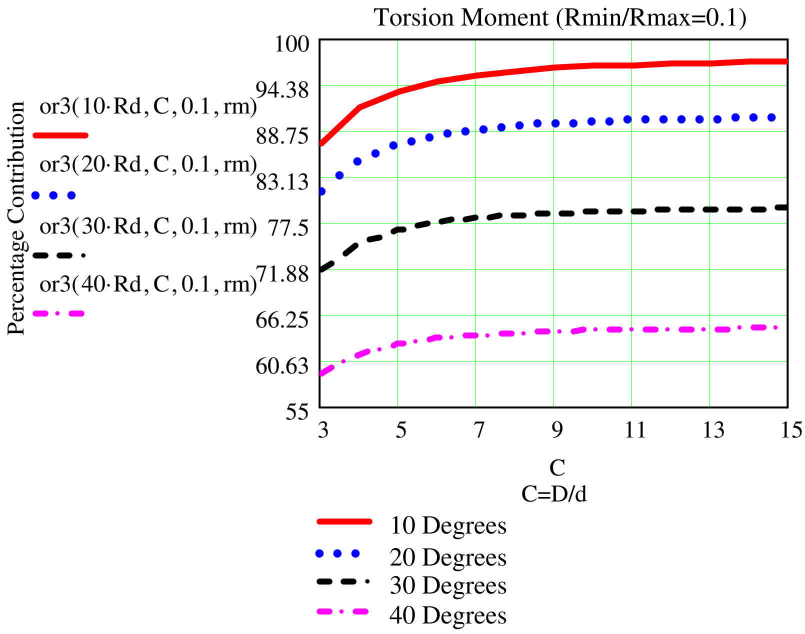

Tip Deflection of Barrel Isotropic Helical Springs

C=D/d=2R/d, R=Rmax=rm=Cd/2 d=constant
Note: Angles are radial

$P := 15($ $\alpha b := 1.1$ $G := 8\times 10^{5}$ $d := 1.8\xi$ $\upsilon := 0.3$ $c := 0.1, 0.2.. 1$

$n := 1\xi$ $E := 2\cdot(1+\upsilon)\cdot G$ $Rd := \frac{\pi}{180}$ $E = 2.08\times 10^{6}$

$Ib := \frac{\pi\cdot d^{4}}{64}$ $Jb := 2\cdot Ib$ $A := \frac{\pi\cdot d^{2}}{4}$ $C := 3.. 15$ $rr_{C} := \frac{C\cdot d}{2}$

$CT := \frac{G\cdot A}{\alpha b}$ $CN := E\cdot A$ $De := \frac{E\cdot Ib}{rm}$ $Db := G\cdot Jb$

$rm(C) := rr_{C}$

$$f1k(rm,c,C) := \frac{2}{3}\cdot\pi\cdot(2\cdot rm(C) + c\cdot rm(C))$$

$$fTk(\alpha,C,c,rm) := \frac{P\cdot\cos(\alpha)\cdot n}{CT}\cdot f1k(rm,c,C)$$

$$fNk(\alpha,C,c,rm) := \frac{P\cdot n\cdot\sin(\alpha)\cdot\tan(\alpha)}{CN}\cdot f1k(rm,c,C)$$

$$f2k(rm,c,C) := \frac{2}{35}\cdot\pi\cdot\left[5\cdot(c\cdot rm(C))^{3} + 6\cdot(c\cdot rm(C))^{2}\cdot rm(C) + 8\cdot c\cdot rm(C)\cdot rm(C)^{2} + 16\cdot rm(C)^{3}\right]$$

$$fMbk(\alpha,C,c,rm) := \frac{P\cdot n\cdot\cos(\alpha)}{Db}\cdot f2k(rm,c,C)$$

$$fMek(\alpha,C,c,rm) := \frac{P\cdot n\cdot\sin(\alpha)\cdot\tan(\alpha)}{De}\cdot f2k(rm,c,C)$$

$$fTOTk(\alpha,C,c,rm) := fTk(\alpha,C,c,rm) + fNk(\alpha,C,c,rm) + fMbk(\alpha,C,c,rm) + fMek(\alpha,C,c,rm)$$

$$fTk(5\cdot Rd, 10, 0.2, rm) = 0.0586408663$$

$$or1(\alpha,C,c,rm) := \frac{fNk(\alpha,C,c,rm)}{fTOTk(\alpha,C,c,rm)}\cdot 10($$ $$or2(\alpha,C,c,rm) := \frac{fTk(\alpha,C,c,rm)}{fTOTk(\alpha,C,c,rm)}\cdot 10($$

$$or3(\alpha,C,c,rm) := \frac{fMbk(\alpha,C,c,rm)}{fTOTk(\alpha,C,c,rm)}\cdot 10($$ $$or4(\alpha,C,c,rm) := \frac{fMek(\alpha,C,c,rm)}{fTOTk(\alpha,C,c,rm)}\cdot 10($$

Tip Deflection of Barrel Isotropic Helical Springs

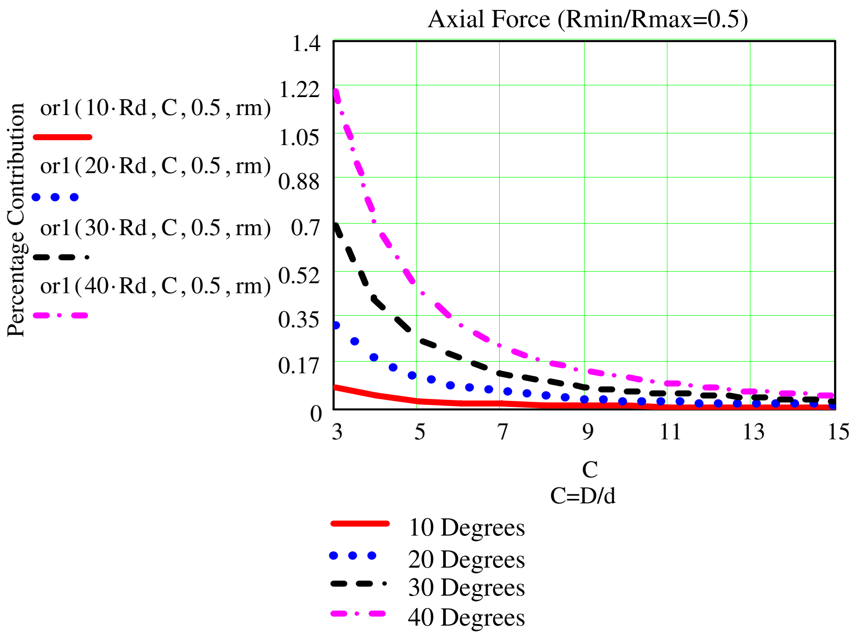

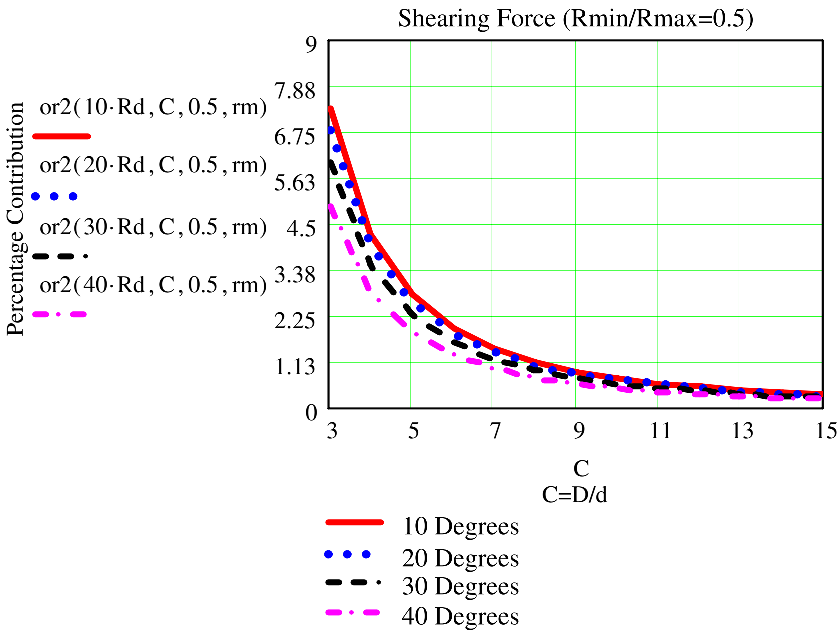

Tip Deflection of Barrel Isotropic Helical Springs

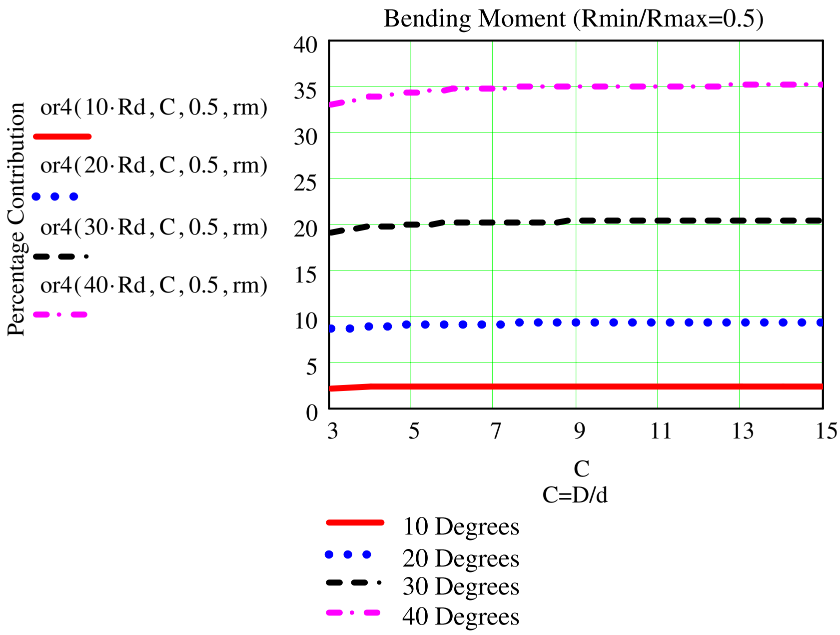

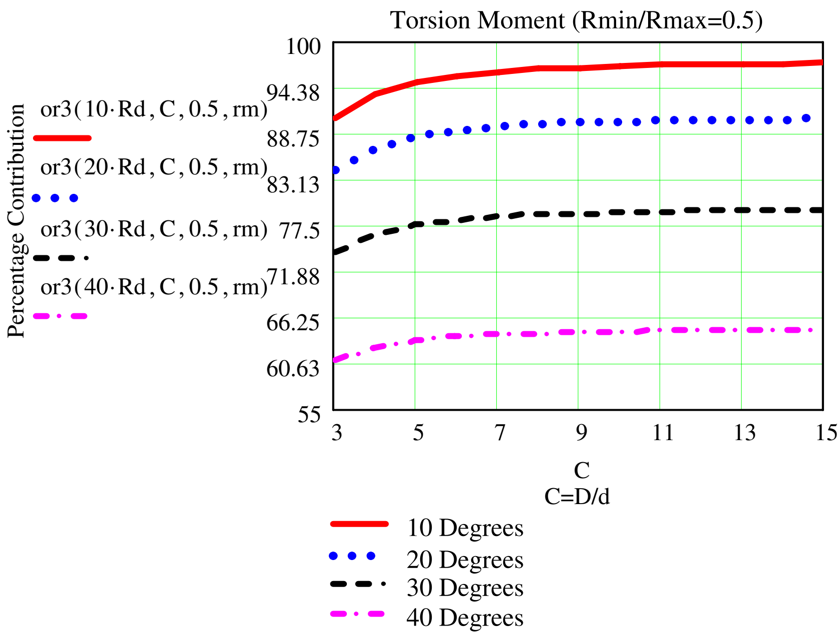

Tip Deflection of Hyperboloidal Isotropic Helical Springs

C=D/d=2R/d, R=Rmax=rm=Cd/2 d=constant
Note: Angles are radial

$P := 15($ $\alpha b := 1.1$ $G := 8\times 10^{5}$ $d := 1.8$ $\upsilon := 0.3$ $c := 0.1, 0.2..1$

$n := 1\varepsilon$ $E := 2\cdot(1+\upsilon)\cdot G$ $Rd := \dfrac{\pi}{180}$ $E = 2.08\times 10^{6}$

$Ib := \dfrac{\pi\cdot d^{4}}{64}$ $Jb := 2\cdot Ib$ $A := \dfrac{\pi\cdot d^{2}}{4}$ $C := 3..15$ $rr_{C} := \dfrac{C\cdot d}{2}$

$CT := \dfrac{G\cdot A}{\alpha b}$ $CN := E\cdot A$ $De := \dfrac{E\cdot Ib}{rm}$ $Db := G\cdot Jb$

$rm(C) := rr_{C}$

$$f1k(rm,c,C) := \frac{2}{3}\cdot\pi\cdot(2\cdot c\cdot rm(C) + rm(C))$$

$$fTk(\alpha,C,c,rm) := \frac{P\cdot\cos(\alpha)\cdot n}{CT}\cdot f1k(rm,c,C)$$

$$fNk(\alpha,C,c,rm) := \frac{P\cdot n\cdot\sin(\alpha)\cdot\tan(\alpha)}{CN}\cdot f1k(rm,c,C)$$

$$f2k(rm,c,C) := \frac{2}{35}\cdot\pi\cdot\left[5\cdot rm(C)^{3} + 6\cdot rm(C)^{2}\cdot c\cdot rm(C) + 8\cdot rm(C)\cdot(c\cdot rm(C))^{2} + 16\cdot(c\cdot rm(C))^{3}\right]$$

$$fMbk(\alpha,C,c,rm) := \frac{P\cdot n\cdot\cos(\alpha)}{Db}\cdot f2k(rm,c,C)$$

$$fMek(\alpha,C,c,rm) := \frac{P\cdot n\cdot\sin(\alpha)\cdot\tan(\alpha)}{De}\cdot f2k(rm,c,C)$$

$$fTOTk(\alpha,C,c,rm) := fTk(\alpha,C,c,rm) + fNk(\alpha,C,c,rm) + fMbk(\alpha,C,c,rm) + fMek(\alpha,C,c,rm)$$

$$or1(\alpha,C,c,rm) := \frac{fNk(\alpha,C,c,rm)}{fTOTk(\alpha,C,c,rm)}\cdot 10($$ $$or2(\alpha,C,c,rm) := \frac{fTk(\alpha,C,c,rm)}{fTOTk(\alpha,C,c,rm)}\cdot 10($$

$$or3(\alpha,C,c,rm) := \frac{fMbk(\alpha,C,c,rm)}{fTOTk(\alpha,C,c,rm)}\cdot 10($$ $$or4(\alpha,C,c,rm) := \frac{fMek(\alpha,C,c,rm)}{fTOTk(\alpha,C,c,rm)}\cdot 10($$

Tip Deflection of Hyperboloidal Isotropic Helical Springs

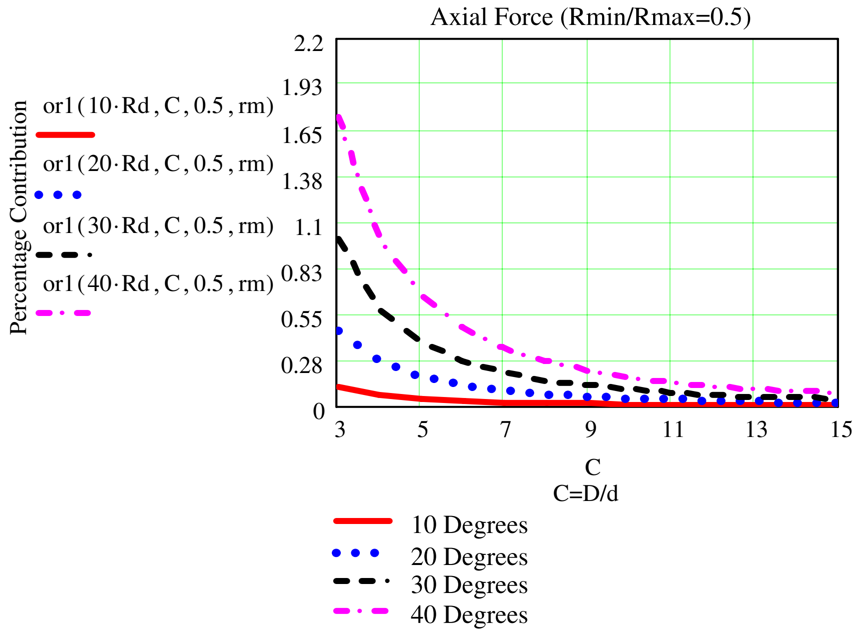

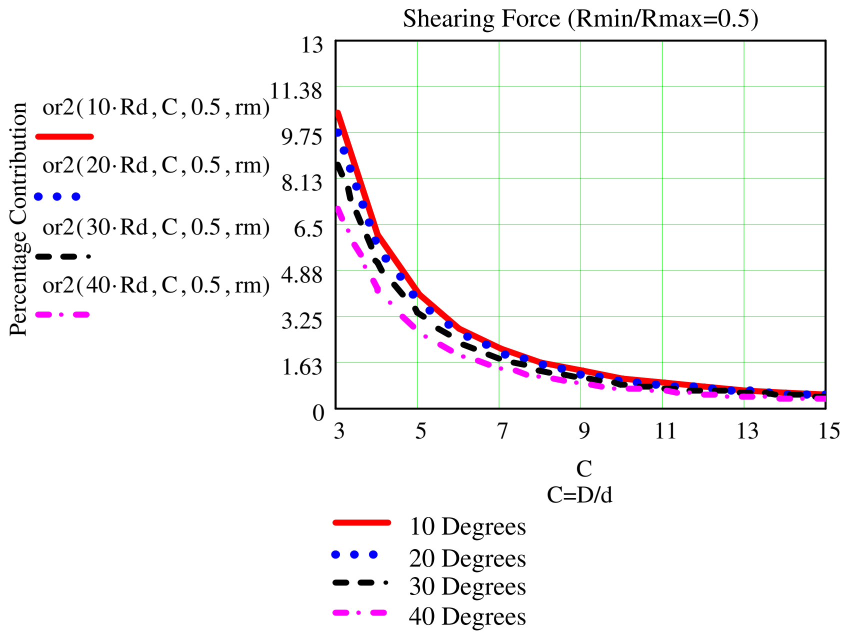

Tip Deflection of Hyperboloidal Isotropic Helical Springs

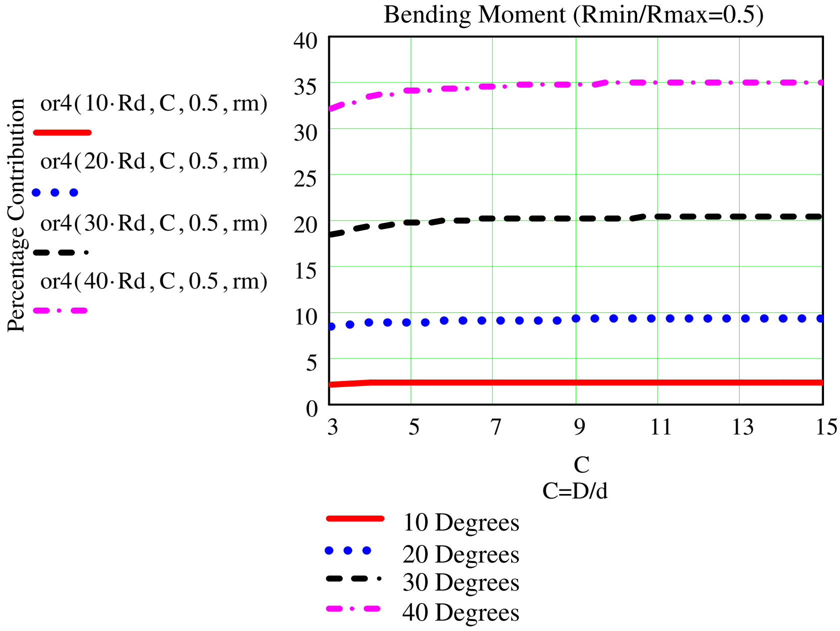

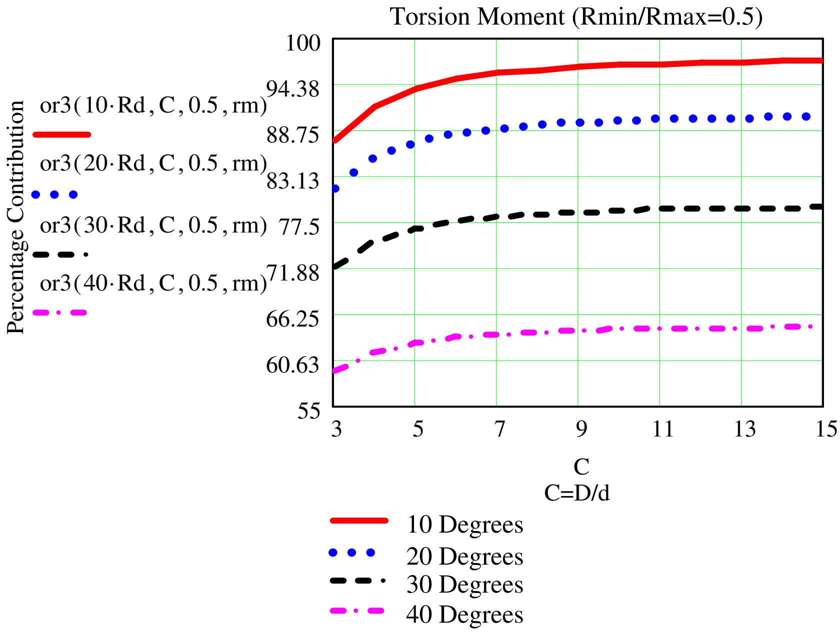

Tip Deflection of Cylindrical Composite Helical Springs

C=D/d=2R/d, R=Rmax=rm=Cd/2 d=constant Carbon Epoxy T300/N5208

$K := 1 \times 10^{9}$ $E1 := 181.0 \cdot K$ $E2 := 10.3 \cdot K$ $E3 := E2$ $\frac{E1}{E2} = 17.572815534$

$G12 := 7.17 \cdot K$ $G13 := G12$ $G23 := 3.433 \cdot K$ $\frac{E1}{G12} = 25.2440725244$

$\nu12 := 0.28$ $\nu13 := 0.0159$ $\nu23 := 0.0159$

$S11 := \frac{1}{E1}$ $S22 := \frac{1}{E2}$ $S33 := \frac{1}{E3}$ $S55 := \frac{1}{G13}$ $S66 := \frac{1}{G12}$

$S12 := \frac{-\nu12}{E1}$ $S13 := \frac{-\nu13}{E1}$ $S23 := \frac{-\nu23}{E2}$

$S := S11 \cdot S22 \cdot S33 - S11 \cdot S23^2 - S22 \cdot S13^2 - S33 \cdot S12^2 + 2 \cdot S12 \cdot S23 \cdot S13$

$C11 := \frac{\left(S22 \cdot S33 - S23^2\right)}{S}$ $C12 := \frac{(S13 \cdot S23 - S12 \cdot S33)}{S}$

$C13 := \frac{(S12 \cdot S23 - S13 \cdot S22)}{S}$ $C55 := \frac{1}{S55}$ $C66 := \frac{1}{S66}$

$Q11 := C11 + \frac{(C12 \cdot S12 + C13 \cdot S13)}{S11}$ $Q22 := C66$ $Q33 := C55$

$E := Q11$ $G := Q22$

$P := 150 \cdot 9.81$ $n := 18$ $d := 0.0185$ $\alpha b := 1.1$ $Rd := \frac{\pi}{180}$

$Ib := \frac{\pi \cdot d^4}{64}$ $Jb := 2 \cdot Ib$ $A := \frac{\pi \cdot d^2}{4}$ $C := 3 .. 15$

$CT := \frac{G \cdot A}{\alpha b}$ $CN := E \cdot A$ $De := E \cdot Ib$ $Db := G \cdot Jb$

$$fT(\alpha, C) := \frac{P \cdot \cos(\alpha)}{CT} \cdot 2 \cdot \pi \cdot \frac{C \cdot d}{2} \cdot n$$

$$fN(\alpha, C) := \frac{P \cdot \sin(\alpha) \cdot \tan(\alpha)}{CN} \cdot 2 \cdot \pi \cdot \frac{C \cdot d}{2} \cdot n$$

Tip Deflection of Cylindrical Composite Helical Springs

$$fMb(\alpha, C) := \frac{P \cdot \cos(\alpha)}{Db} \cdot 2 \cdot \pi \cdot \left(\frac{C \cdot d}{2}\right)^3 \cdot n$$

$$fMe(\alpha, C) := \frac{P \cdot \sin(\alpha) \cdot \tan(\alpha)}{De} \cdot 2 \cdot \pi \cdot \left(\frac{C \cdot d}{2}\right)^3 \cdot n$$

$$fTOT(\alpha, C) := fT(\alpha, C) + fN(\alpha, C) + fMb(\alpha, C) + fMe(\alpha, C)$$

$fT(5 \cdot Rd, 10) = 8.7526344348 \times 10^{-3}$ $\quad$ $fN(5 \cdot Rd, 10) = 2.4126273693 \times 10^{-6}$

$fMb(5 \cdot Rd, 10) = 1.5913880791$ $\quad$ $fMe(5 \cdot Rd, 10) = 9.6505094773 \times 10^{-4}$

$fTOT(5 \cdot Rd, 10) = 1.6011081771$

$$or1(\alpha, C) := \frac{fN(\alpha, C)}{fTOT(\alpha, C)} \cdot 100 \qquad or2(\alpha, C) := \frac{fT(\alpha, C)}{fTOT(\alpha, C)} \cdot 100$$

$$or3(\alpha, C) := \frac{fMb(\alpha, C)}{fTOT(\alpha, C)} \cdot 100 \qquad or4(\alpha, C) := \frac{fMe(\alpha, C)}{fTOT(\alpha, C)} \cdot 100$$

$or1(5 \cdot Rd, 10) = 1.5068484465 \times 10^{-4}$ $\quad$ $or2(5 \cdot Rd, 10) = 0.5466610289$

$or3(5 \cdot Rd, 10) = 99.3929143484$ $\quad$ $or4(5 \cdot Rd, 10) = 0.0602739379$

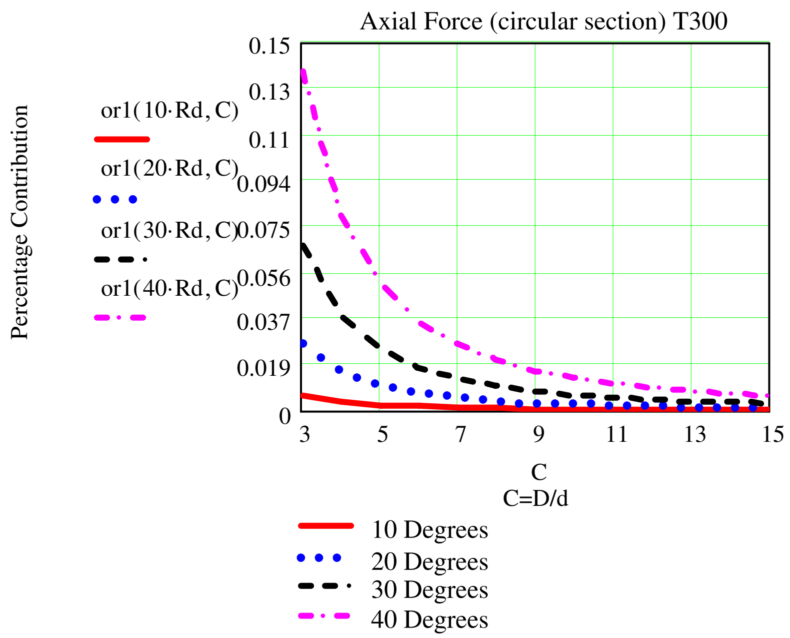

Tip Deflection of Cylindrical Composite Helical Springs

$$S_{11} = \frac{1}{E_1} \quad S_{22} = \frac{1}{E_2} \quad S_{33} = \frac{1}{E_3} \quad S_{55} = \frac{1}{G_{13}} \quad S_{66} = \frac{1}{G_{12}}$$

$$S_{12} = -\frac{\vartheta_{12}}{E_1} \quad S_{13} = -\frac{\vartheta_{13}}{E_1} \quad S_{23} = -\frac{\vartheta_{23}}{E_2}$$

$$S = S_{11}S_{22}S_{33} - S_{11}S_{23}^2 - S_{22}S_{13}^2 - S_{33}S_{12}^2 + 2S_{12}S_{23}S_{13}$$

$$C_{11} = \frac{S_{22}S_{33} - S_{23}^2}{S} \quad C_{12} = \frac{S_{13}S_{23} - S_{12}S_{33}}{S}$$

$$C_{13} = \frac{S_{12}S_{23} - S_{13}S_{22}}{S} \quad C_{55} = \frac{1}{S_{55}} \quad C_{66} = \frac{1}{S_{66}}$$

$$Q_{11} = C_{11} + (C_{12}S_{12} + C_{13}S_{13})/S_{11} \quad Q_{22} = C_{66} \quad Q_{33} = C_{55}$$

Composite Material Constants

	E_1 (GPa)	E_2 (GPa)	$G_{12}=G_{13}$ (GPa)	G_{23} (GPa)	ρ (kg/m^3)	ν_{12}	$\nu_{13}=\nu_{23}$
Graphite-epoxy[1] (AS4/3501-6)	144.8	9.65	4.14	3.45	1389.23	0.3	0.019
Graphite-epoxy[2] (T300/N5208)	181.0	10.3	7.17	3.433	1600.0	0.28	0.0159
Kevlar 49-epoxy	76.0	5.56	2.30	1.618	1460.0	0.34	0.0248